INHIBITION OF MOBILE GENETIC ELEMENTS WITH SMALL MOLECULES

DEVELOPMENT OF HIGH THROUGHPUT SCREENING APPROACHES TO TARGET Tn*1549* and F PLASMID MOVEMENT

BY: DREW HANSEN, B.Sc.

A Thesis Submitted to the School of Graduate Studies in Partial Fulfilment of the Requirements for the Degree Master of Science

McMaster University

Department of Chemistry and Chemical Biology

Hamilton, Ontario, Canada

MASTER OF SCIENCE (2019)

TITLE: Development of high throughput screening approaches to target Tn*1549* and F plasmid movement

AUTHOR: Drew Hansen, B. Sc. (McMaster University)

SUPERVISOR: Dr. Gerard D. Wright

NUMBER OF PAGES: xii, 121

Lay Abstract

Antibiotics are small molecules that cure bacterial infections. However, their efficacy is fading as a result of the ability of mobile genetic elements (MGEs) to spread antimicrobial resistance genes between bacteria. Conjugative plasmids (CPs) and conjugative transposons (CTns) are two of the major types of MGEs that contribute to the dissemination of antimicrobial resistance in pathogens. The goal of this research is to search for inhibitors of CTns and CPs in order to prevent the emergence of multi-drug resistant bacteria. High throughput assays were designed to model both a CTn (Tn*1549*) and a CP (F plasmid) to find small molecules targeting their movement. A screen of the Tn*1549* excision assay identified fluoroquinolone antibiotics that inhibit excision in a dose-dependent manner and indirectly inhibit the integrase used to excise the CTn. Ciprofloxacin, a fluoroquinolone, inhibited the conjugation frequency of Tn*1549*. Future work will focus on identifying new inhibitors of these MGEs and their characterization.

Abstract

The antimicrobial resistance (AMR) crisis, where new antibiotic discovery is not keeping pace with the emergence of resistant pathogens, is driven by mobile genetic elements (MGEs). MGEs can autonomously transfer between bacteria, along with AMR genes. The widespread use of antibiotics in the clinic, in agriculture, and animal husbandry, has accelerated the MGE-mediated transfer of AMR genes in the environment. However, despite playing such an important role in the AMR crisis, the dynamics and mechanisms behind the transmission of genes are poorly understood. Furthermore, which natural and man-made compounds inhibit or promote their movement in these environments is unknown.

One method to combat the rise in AMR is to identify small molecules as probes to understand the molecular basis of transmission and apply this information to prevent MGE-mediated resistance dissemination. Since conjugation is the main mechanism for AMR gene transfer, targeting MGEs that use conjugation, such as conjugative plasmids (e.g. Tn*1549*) and conjugative transposons (e.g. F plasmid), has the potential to prevent the emergence of multi-drug resistant pathogens. In this work, a high throughput assay modeled after Tn*1549* excision was screened against a library of known bioactive compounds to find modulators of the integrase and excisionase activity. Several fluoroquinolone antibiotics including ciprofloxacin were identified as dose-dependent inhibitors of excision, which acted by changing supercoiling levels in the cell. Ciprofloxacin enhanced conjugation frequency of Tn*1549* at sub-MIC concentrations relative to an untreated control and inhibited conjugation frequency at higher concentrations. A second project was focused on a high throughput conjugation assay based on the separation of the *lux* operon between a donor and recipient cell, such that only transconjugants produce luminescence to reflect active gene transfer. This work furthers our understanding of the development of assays to target MGEs and screening for inhibitors of their movement.

Acknowledgments

Reflecting on my past two years of graduate school, I have been unbelievably lucky. I could not have asked for a better supervisor, lab members, and work environment. Without Dr. Gerry Wright accepting me into his lab none of these memories and experiences would have been possible. Thank you for mentoring me and showing me what it takes to be a scientist. Your work ethic, principles, and character inspire us all to do better. I also want to thank my supervisory committee, Dr. Lori Burrows and Dr. Michael Surette, for their involvement in my project. I enjoyed our committee meetings together and appreciated your input.

I would like to specifically thank the following individuals who made an impact on my daily life in the lab. Special thanks to Matt who helped me get started in the lab and for always willing to help solve problems with me. I would also like to thank Caitlyn who was always around to cheer me on and support me at any hour of the day. To Min, thank you for sharing your wisdom, answering every question I had, and talking about basketball with me. To Allison, thank you for your encouragement to go deeper into my science and ask meaningful questions. To Beth, thank you for inspiring me to work harder, become more disciplined, and baking amazing birthday cakes for everyone in the lab. To Haley, thank you for your willingness to help me and for the laughs we have shared along the way. To Emily, thank you for showing me your dedication to your work and the importance of treating yourself. To Vishwas, thank you for reminding me of being methodical about each experiment and for talking through my experiments with me. To Adam, thank you for inspiring me to ask more questions, sharing your knowledge, and for making me laugh nonstop. To Dave, thank you for sharing your passion for science each day and for introducing me to Kan Jam. Thank you all for making these past two years so memorable and for your friendship.

Thank you to my brothers from 28 Kingsmount where I lived for 5 years – Brandon, Cal, Dean, Ben, Cam, and George. Thank you for the laughs and for the great memories we have shared throughout undergrad and my time in graduate school. You all made our home in Hamilton a wonderful place to live in.

Lastly, I need to thank my parents, Alan and Eden, for their love and support throughout my Master's degree. Special thanks to my Mom who answered every call, for cheering me on, and for your constant encouragement. Thank you both for taking care of me whenever I came home.

Table of Contents

List of Figures

List of Tables

List of Abbreviations

AMR	Antimicrobial resistance
BHI	Brain heart infusion
Bp	base pair
CAMHB	cation adjusted Mueller-Hinton II broth
CAMHA	cation adjusted Mueller-Hinton II agar
CI	Conjugative intermediate
CLSI	Clinical and Laboratory Standards Institute
CFU	Colony forming unit
CTn	Conjugative Transposon
DMSO	Dimethylsulfoxide
DNA	deoxyribonucleic acid
dNTP	deoxyribonucleotide phosphate
DP	Donor plasmid
HTS	high throughput screening
ICE	Integrative and Conjugative Element
IR_L	Inverted repeat left
IR_R	Inverted repeat right
Int	Integrase
IPTG	Isopropyl β-D-1thiogalactopyranoside
Kb	kilobase
LB	lysogeny broth
MGE	mobile genetic elements
MDR	multi-drug resistant
MOB	Mobility genes
MOPS	3-(*N*-morpholino)propanesulfonic acid
MPF	Mating pair formation
MRSA	methicillin resistant *Staphylococcus aureus*
MIC	minimum inhibitory concentration
OD_{600}	optical density measured at a wavelength of 600 nanometers
PCR	Polymerase chain reaction
PFL	Prefractionated Library
RDP	Recombinant donor plasmid
Rpm	revolutions per minute
TfBI	Transformation buffer I
TfBII	Transformation buffer II
T4CP	Type 4 coupling protein
T4SS	Type 4 secretion system
VRE	vancomycin resistant *Enterococci*
Xis	Excisionase
Z’	Z prime

Declaration of Academic Achievement

Drew Hansen performed the majority of the experiments, data collection, and analyses presented in this thesis.

Supervisor Dr. Gerry Wright and committee members Dr. Lori Burrows and Dr. Michael Surette provided guidance and direction throughout the project.

High throughput screening was accomplished with the help of Dr. Susan McCusker and Cecilia Murphy. HTS analysis was done by Fazmin Nizam and Dr. Tracey Campbell.

Cloning of TPEP and TEMP and initial Tn*1549* assay development was done by Dr. Lotte Lambertsen, in collaboration with Dr. Orsolya Barabas.

Matthew Surette thought of the idea behind the high throughput conjugation assay in Chapter 3 and illustrated Figures 3-1 and 3-2.

Chapter 1.

Introduction

1.1 Introduction: Mobile Genetic Elements are key players in the Antimicrobial Resistance Crisis

Antibiotics are powerful medicines that can cure bacterial infections. Their efficacy is deteriorating as a result of antimicrobial resistance (AMR) emerging from resistance genes and associated mutations in regulatory elements that reduce the efficacy of these compounds. Mobile genetic elements (MGEs) autonomously transfer themselves between bacteria, often carrying AMR genes as cargo, and are partially responsible for the rapid spread of resistance that is observed globally. The widespread use of antibiotics in the clinic, agriculture, and animal husbandry over the past 70 years confounds this problem, as it selects for the transfer of these genetic elements. It is widely recognized that environmental organisms are the original source of many of these resistance genes, and the use of antibiotics in the environment and their subsequent transfer to pathogens is an acute issue.[1–3] The discovery of new antibiotics and the investigation of ways to prevent or inhibit resistance dissemination are necessary in order to preserve antibiotics for future generations.

With new drug resistant pathogens emerging and antimicrobial discovery stalling, targeting the root cause of gene transfer provides an alternative approach to combating the AMR crisis. This approach could prolong the shelf-life of current antibiotics, prevent the emergence of multi-drug resistant (MDR) pathogens, and provide more opportunity to find

new antibiotics. Despite playing such an important role in the AMR crisis, the dynamics and mechanisms behind the transmission of genes are poorly understood. The activity of MGEs containing AMR genes is especially high in certain environments, such as wastewater treatment plants, agriculture, farming, and the intestinal microbiome of humans and animals. Furthermore, we don't understand which natural and man-made compounds inhibit or promote their movement in these environments. To tackle this underlying cause of the AMR crisis, research aimed at understanding the molecular basis of transmission to find targets that prevent gene transfer is critical. Chemical probes of MGEs can be used to study the molecular mechanisms of the components of gene transfer and testing of lead compounds will inform whether limiting transfer beyond the laboratory is realistic.

The approach described in this thesis aims to develop small molecule screens that target MGEs such as conjugative plasmids (CPs) and conjugative transposons (CTns) that play a significant role in resistance dissemination. By targeting these elements, we have the potential to prevent the formation of MDR pathogens. First, it is necessary to understand the molecular mechanisms involved in the transmission of MGEs in order to target essential steps in their transmission. Next, we need robust assays to discover molecules that can inhibit or enhance resistance gene transfer. This thesis focuses on finding small molecules using high throughput screening to target MGEs that use conjugation to transfer AMR genes.

1.2 Mobilization Strategies That Spread Antimicrobial Resistance

To tackle AMR transfer, we must understand how bacteria acquire and transmit resistance genes. One means of acquiring AMR is through vertical gene transfer (VGT),

where genetic information is passed down from a parental organism to its offspring. An example is a point mutation in *rpoB*, a subunit in RNA polymerase, that confers resistance to rifampin.[4] Another mechanism of gene mobilization is horizontal gene transfer (HGT), which refers to the movement of genetic information from a donor to a recipient organism that is not its offspring. Genes responsible for AMR are transferred through three main mechanisms of HGT: transduction, transformation, and conjugation.

Transduction uses bacteriophages to transfer bacterial genes (**Figure 1-1a**). During infection, bacterial DNA (e.g. an AMR gene) is sometimes accidentally packaged into a bacteriophage capsid. This bacteriophage is then capable of targeting a recipient cell and injecting the foreign DNA. Transduction is achieved when the phage-associated bacterial DNA is recombined into the recipient's genome.[5] Transduction is a highly specific process as phages need to bind to a specific marker/receptor on the target bacteria, thus this process typically occurs between members of the same species.[6–8] Transduction of extended spectrum β-lactamase (ESBL) genes from the pathogen *Kluyvera* is hypothesized to have resulted in widespread dissemination of CTX-M alleles among clinically relevant *E. coli* and *Klebsiella* spp. [9,10]

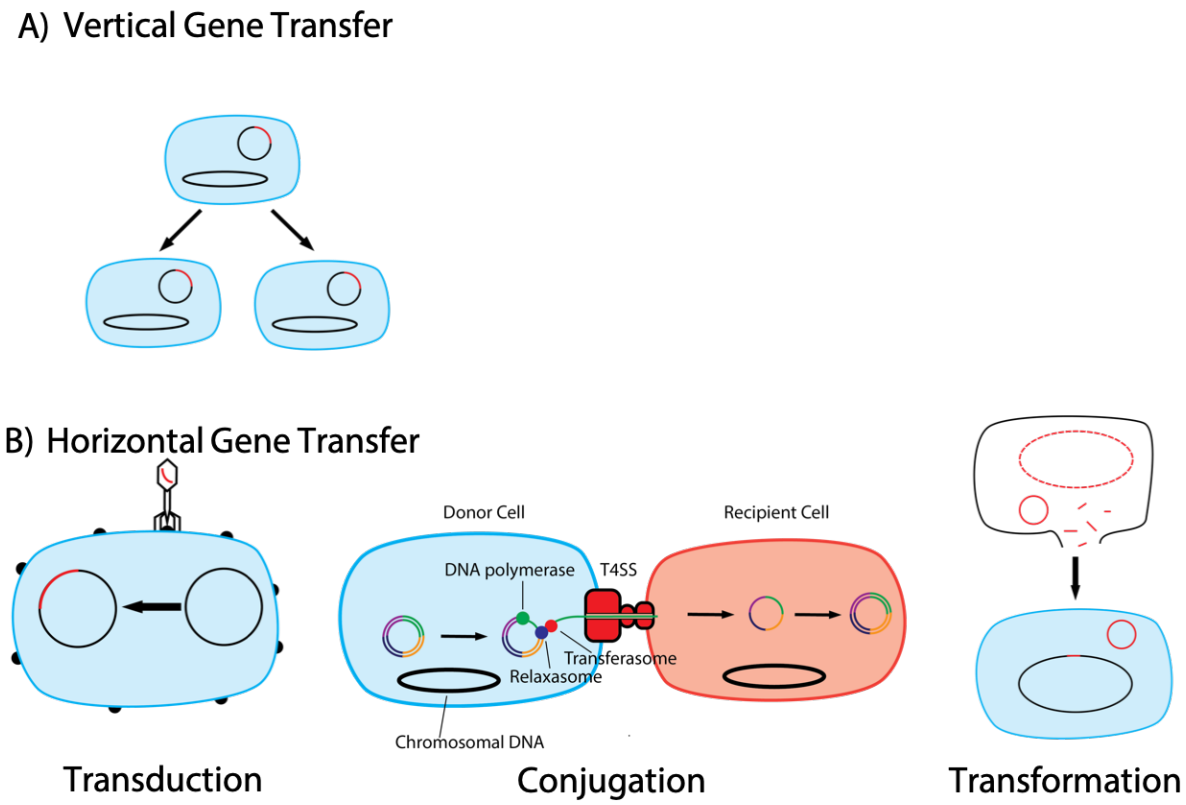

Figure 1-1: Overview of Vertical Gene Transfer and Horizontal Gene Transfer (HGT).
a)VGT is when genetic information is passed down from a parental organism to its offspring. b) HGT is the movement of genetic information from a donor to a recipient organism that is not its offspring. HGT has three main mechanisms (left to right): Transduction, Conjugation, and Transformation.

Transformation occurs when naturally competent bacteria take up extracellular DNA from the environment and an imported gene(s) is integrated into the host genome (**Figure 1-1c**).[11] Transformation may play a more significant role in AMR gene transmission to pathogens than empirical evidence provides. Several clinically relevant antibiotic-resistant pathogens including *Acinetobacter, Haemophilus, Neisseria, Pseudomonas, Staphylococcus*, and *Streptococcus* are capable of DNA uptake and natural transformation.[11,12] Also, environmental *Escherichia* and *Klebsiella* are predicted to be naturally competent.[5] Despite the potential of pathogens to acquire genetic information

through transformation, there is yet no direct evidence that natural transformation contributes to ARG transmission between bacteria in clinical environments.

Conjugation is the process in which bacteria transfer DNA through direct cell-to-cell contact (**Figure 1-1b**). In the context of AMR gene transfer, conjugation is regarded as the most prevalent HGT mechanism.[13] Compared to transduction, which is limited in the amount of DNA transferred and has a narrow host range, conjugation has a broad host range and can transfer large amounts of DNA at once.[14] In addition, since conjugation is a controlled process where DNA is transferred through a conjugative pilus, DNA is not exposed to environmental conditions like in transformation. Conjugation systems are encoded in autonomously replicating CPs and in CTns inserted in the bacterial chromosome. CPs and CTns are two of the major MGEs that contribute to AMR dissemination via conjugation (**Figure 1-2**).[15]

Conjugative systems have two sets of genetic components: mobility (MOB) genes for DNA processing, and mating-pair formation (MPF) genes for DNA delivery between donor and recipient bacteria.[16] The MOB component includes three essential components: an origin of transfer (*oriT*), a relaxase, and a type IV coupling protein (T4CP). MPF genes encode an array of proteins that construct the type IV secretion system (T4SS).

MPF genes are initially expressed in the donor cell to initiate conjugation. MPF genes encode the T4SS complex comprised of the pilus, the core channel complex, the inner membrane platform, and the cytoplasmic ATPases. [16] ATPases are molecular motors driving pilus biogenesis and substrate transport in conjugation.[17] The pilus connects the donor to the recipient cell and retracts to facilitate cell-to-cell contact.[18] Once contact is

established, the relaxase and auxiliary factors form a nucleoprotein complex on the *oriT* called the relaxosome. At this point, the relaxase cleaves the phosphodiester bond at the *nic* site within the *oriT*. This transesterification reaction covalently links the relaxase to the 5`-end of *oriT*. DNA replication starts on the 3`-end of the cleaved strand to repair the template, while the relaxase unwinds DNA for transfer. The relaxase then cleaves the *nic* site to release the transfer stand from the newly formed strand. The T4SS protein machinery then recruits the relaxosome with the T4CP that catalyzes the translocation of the relaxosome across the T4SS. In the recipient cell, now called a transconjugant, the relaxase catalyzes the reverse-nicking reaction to make circular ssDNA. In both the donor and transconjugant, the ssDNA is restored to dsDNA (**Figure 1-1b**). Overall, the main components for conjugation are the relaxase and ATPases of the T4SS.

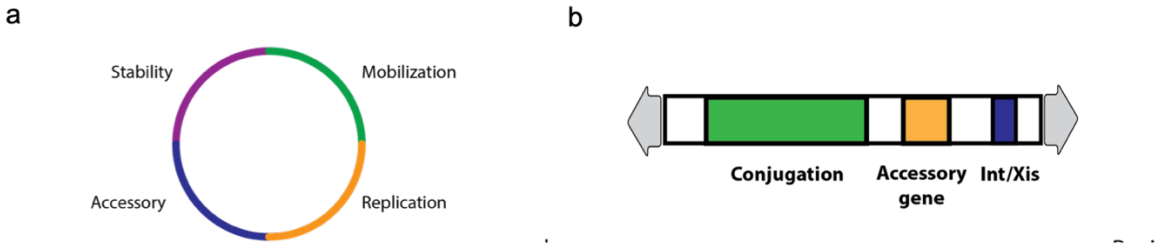

Figure 1-2: Conjugative Plasmids (CPs) and Conjugative Transposons (CTns).
a) CPs usually have a mobilization section containing the genes for conjugation, origin of replication, plasmid stability system (e.g. a toxin-anti-toxin system), and an accessory gene (e.g. antibiotic resistance). b) CTns consist of three modules: a conjugation and mobilization domain, a Xis/Int required for excision and integration, and an accessory gene (e.g. antibiotic resistance).

CTns are a type of integrative and conjugative element (ICE) that combines features of phages and plasmids because they can both integrate into genomes and disseminate by conjugative transfer.[19] They usually reside in the host chromosome, excise using an integrase (Int) and excisionase (Xis), transfer via conjugation with mobilization genes, and

integrate into a recipient bacterium chromosome using an integrase (Int) (**Figure 1-3**). CTns are flanked by inverted repeats (IR_L and IR_R) and composed of three domains that are used to maintain, disseminate, and regulate the element (**Figure 1-3**). Excision in the donor cell creates the CI, with IR_L and IR_R joined by 5-7 nt heteroduplex. A single CI strand is transferred to a recipient bacterium by conjugation and replication re-creates the double-stranded CI, now with homoduplex at the cross-over region. Integration in the recipient genome generates a transconjugant, commonly with a new resistant phenotype (e.g. tetracycline resistance).[20]

All ICEs encode an integrase that enables their integration into the host chromosome and is sometimes also required for excision. Integrases determine the location and the frequency at which an ICE inserts into the host chromosome. The location at which an ICE is integrated is linked to the potential host range of a particular ICE. Furthermore, intricate regulatory systems exist to control ICE transmission.[21]

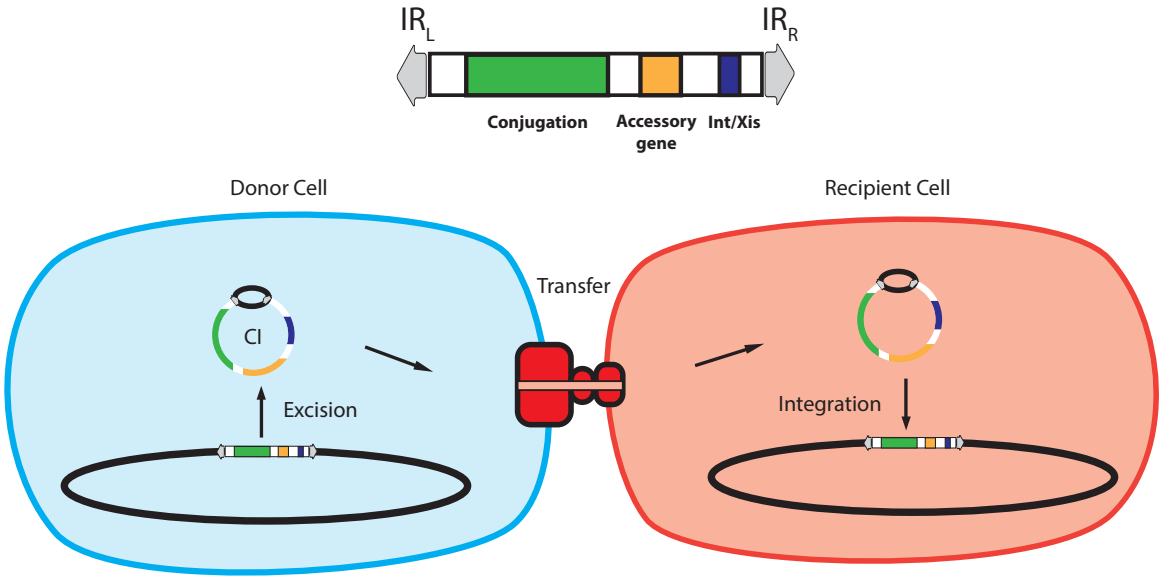

Figure 1-3: Conjugative transposition.
Conjugative transposons reside in the bacterial chromosome and excise themselves in the donor cell (Blue) using Int and Xis. Excision forms a conjugative intermediate (CI) joined by a 5-7 nt heteroduplex (Black bubble in CI) and the donor DNA site is resealed. This CI is a substrate for a relaxase encoded in the conjugation module to initiate conjugation and transfers the CI into a recipient cell through a T4SS. Finally, Int integrates the CI into the recipient cell (Red) chromosome, which becomes a transconjugant. The example of a CTn has the conjugation and mobilization genes in green, the accessory genes in orange, and the Int/Xis genes in purple, flanked by left and right inverted repeats that are recognized by Int/Xis during integration and excision (IR_L and IR_R).

Tyrosine recombinases (TRs) are the primary type of Int found in ICEs which use a catalytic histidine residue in the active site to catalyze its movement. However, there are also serine recombinases and DDE transposases that use the triad of Aspartate-Aspartate-Glutamate in the active site to catalyze the movement of the transposon.[21] TRs perform site-specific recombination in bacteria and archaea. In addition to mobilizing transposons, they drive dissemination of genetic traits and AMR through phages and integrons. TRs are also responsible for capturing AMR genes through insertion into integrons.[22] Consequently, TRs contribute to the emergence and spread of antibiotic resistance. In addition to the relaxase and ATPases discussed above, TRs are ideal targets to prevent the transmission of AMR through ICEs.

While many MGEs confer a selective advantage, bacteria are not always willing to accept foreign DNA. Restriction endonucleases target foreign DNA, such as plasmid or phage DNA, for digestion.[16] Similarly, clustered regularly interspaced short palindromic repeats (CRISPR) cas systems may be employed as a host-defense mechanism against viral DNA.[16] Some conjugative elements contain surface exclusion systems, which create an effective barrier to inhibit transfer into a cell already harbouring a related element.[23] Restriction endonucleases, CRISPR, and surface exclusion are examples of how the

recipient bacteria limits the entry or establishment of DNA, thus deciding the fate of the conjugative element.

ICEs employ several regulation mechanisms to ensure their survival and transmission. Conjugative plasmids regulate their own transfer, block the entry of related plasmids into the same cell, or inhibit conjugative transfer of plasmids present in the same donor bacteria. [16] ICEs are commonly under active repression of transcription because constitutive expression of excision and conjugation genes can be harmful to the host and to the maintenance of the ICE.[24] ICE transfer can be activated or repressed by various environmental stimuli. Even when ICEs are induced, only a small portion appear to excise from the chromosome.[24] Although bacteria have developed several strategies to prevent foreign DNA, the following section will focus on the use of small molecules for targeting these MGEs.

1.3 Targeting Conjugative Transposons and Conjugative Plasmids

1.3.1 Criteria for Targeting MGEs

The goal of this thesis is to find inhibitors of MGEs carrying AMR genes that prevent or reduce the frequency of transfer and emergence of pathogens. The ideal inhibitor of resistance transfer would be specific to a protein, effective at reducing the frequency of transfer, and not put undue selective pressure on bacteria. ICEs and CPs are diverse in nature, which makes finding a ubiquitous target difficult. As discussed in the previous section, the main targets of conjugation are relaxases and ATPases in the T4SS. As for ICEs, in addition to the conjugation machinery components, a TR is essential for integration into a new host, and sometimes excision. Do we want an abundant target that is found in a

wide range of MGEs and widespread in different organisms or should we focus on MGEs with high clinical priority? The former question aims to find broad inhibitors, whereas the latter is narrowly focused on inhibitors of clinically relevant MGEs.

To approach the former question, we can use phylogenetic analysis to identify the most abundant MGEs carrying AMR genes. Recently, Smyshlyaev *et al.* mapped phylogenetically-related TRs.[25] This approach can be used to study and target TRs that are most widespread in bacterial species to prevent future dissemination of AMR genes. For example, from currently available sequences, the Xer and Tn*916* TRs are the most abundant.[25] On the other hand, focusing on MGEs with high clinical priority may help directly prevent the emergence of MDR organisms. For example, CTns are connected to the emergence of vancomycin-resistant *Enterococci* (VRE), methicillin-resistant *Staphylococcus aureus* (MRSA), and ESBL carrying *Enterobacteriaceae*.[26–28] Therefore, we can focus on MGEs with a history of spreading to pathogens or MGEs with the potential to transfer a new resistance element to a pathogen.

1.3.2 Targeting Conjugative Transposons

The literature surrounding the inhibition of CTns is limited. The closest related research involved targeting the phage λ Integrase.[29–31] λ Integrase is a part of the tyrosine recombinase superfamily, similar to Int found in CTns. Both peptide antagonists and a small molecule have been found to inhibit λ Integrase-mediated recombination (**Table 1-1**). The peptide WKHYNY is effective at trapping Holliday junctions in bent-L recombination and integration, but less potent for excisive recombination.[29] Furthermore, WRWYCR is a more potent peptide that stably traps Holliday complexes in all

recombination pathways mediated by λ Integrase.[29] The small molecule, *N*-methyl aminocyclic thiourea, traps Holliday junctions *in vitro* and can inhibit Holliday junction resolution by RecG helicase.[29] These inhibitors have not been tested against other MGE integrases. In addition, there have been no studies focused on finding small molecules targeting Int of CTns. To tackle this problem, we modelled the excision step in conjugative transposition. This high throughput assay is the first of its kind and uses a luciferase reporter to quantify the rate of excision. This research is discussed in Chapter 2.

Table 1-1: λ Integrase-mediated Recombination Inhibitors

Compound	Structure	Reference
N-methyl aminocyclic thiourea	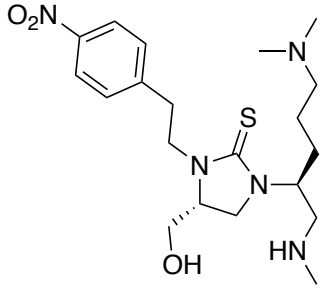	[29]
WKHYNY	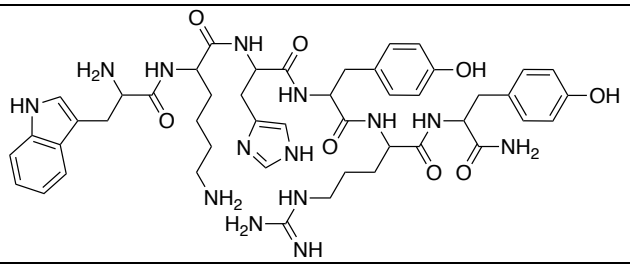	[29]

WRWYCR	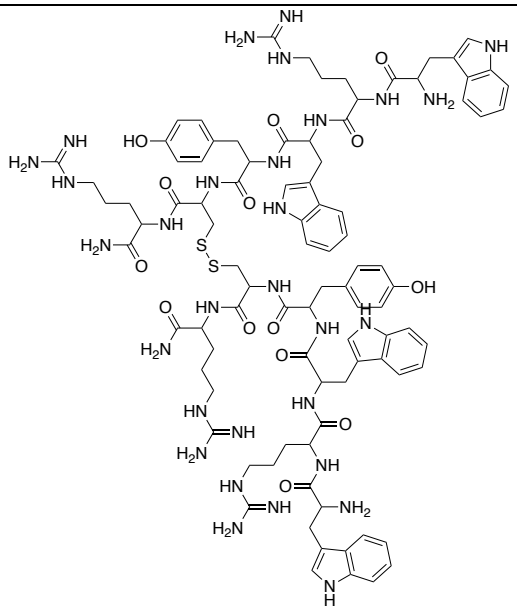	29

1.3.3 Targeting Conjugation

Compared to CTns, many conjugation inhibitors (COINs) have been reported in the literature. COINs aim to target specific components of the conjugation machinery, such as a conjugative relaxase or an ATPase found in a T4SS. This section will review the specific targets and compounds influencing conjugation.

1.3.4 Relaxase Inhibitors

In vitro screens against the relaxase (TraI) from the F plasmid have been fruitless thus far. Initial findings reported that bisphosphonates specifically inhibited TraI and reduced *in vivo* conjugation frequency.[32] However, further analysis reported that these compounds were non-specific chelators of magnesium, which is essential for enzyme function.[33]

1.3.5 TraE Inhibitors

Another targeted approach, led by Baron and colleagues, identified small molecules that bind to TraE and inhibit dimerization. TraE is an ATPase found in the T4SS, and essential for pKM101 conjugation. Structural studies of TraE uncovered four molecules (B8I-16, BAR-072, BAR-073, and UM-024) that specifically inhibited pKM101 transmission (**Table 1-2**).[34] Building on this research, TraE was screened against a fragment library, which led to the development of compounds, 105055 and 239852 (**Table 1-2**).[35] These compounds also bound with high affinity to TraE and reduce the transmission of pKM101.[34,35] Overall, this work demonstrates the feasibility of using structure based design in the pursuit of finding COINs.

1.3.6 TrwD Inhibitors

Fernando de la Cruz and colleagues conducted the first systematic search for COINs using an *E. coli* model conjugative plasmid R388. They used a luminescence-based high throughput conjugation assay of R388 to screen microbial extracts. This screen yielded unsaturated fatty acids, linoleic and oleic acid, from a pilot screen of known compounds, and dehydrocrepenynic acid (DHCA) from a fungal extract (**Table 1-2**). Linoleic acid and DHCA reduced transfer of R388 and pOX38, but not RP4 or R6K. Using the same assay, Tanzawaic acids, fungal polyketides, were found by screening marine microbial extracts (**Table 1-2**).

Based on DHCA and other shared chemically properties of hits, de la Cruz's group synthesized a series of 2-alkynoic fatty acids (2-AFAs) and screened them using a GFP reporter high throughput conjugation assay to identify inhibitors. 2-Hexadecynoic acid (2-

HDA) was the COIN most effective at reducing transfer frequency (**Table 1-2**). In addition, 50% inhibition of R388 conjugation by 2-HDA was sufficient to prevent plasmid spread in the absence of selective pressure.[16]

Every COIN found using this approach non-competitively inhibits TrwD.[36] TrwD acts as a traffic ATPase, regulating the transition between pilus biogenesis and DNA translocation through the conjugation machinery.[36] Based on the lipophilic properties of these COINs, it is unclear whether they are true inhibitors of the enzyme, or are non-specifically impacting conjugation by interfering with the bacterial membrane**.**

Table 1-2: Various Conjugation Inhibitors

Compound Name	Structure	Reference
Oleic acid	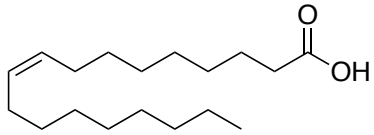	[37]
Linoleic acid	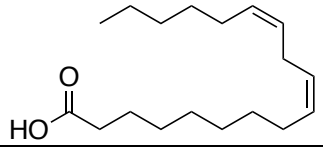	[37]
Dehydrocrepenynic acid (DHCA)	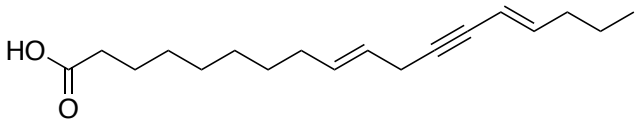	[37]
Tanzawaic acid A	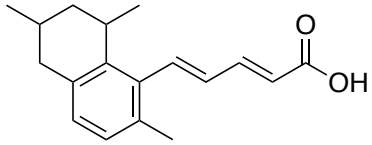	[38]
Tanzawaic acid B	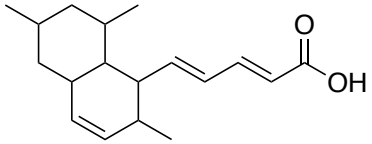	[38]
2-Hexadecanoic acid (2-HDA)	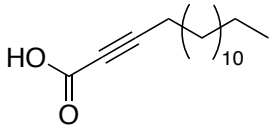	[39]

BAR-072	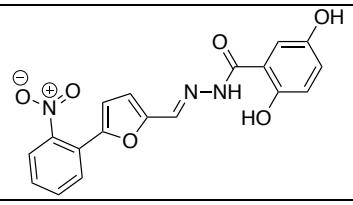	34
BAR-073	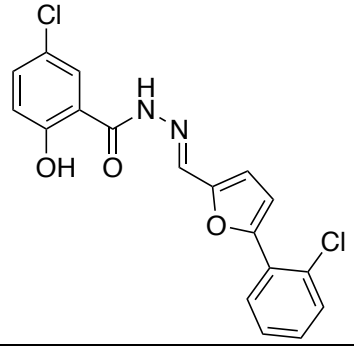	34
B8I-16	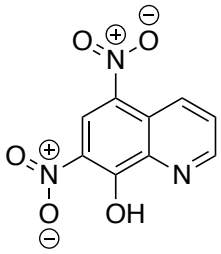	34
UM-024	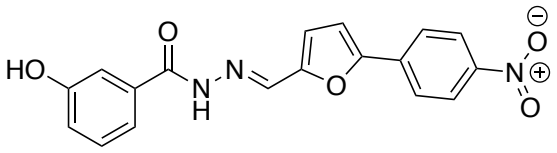	34
239852	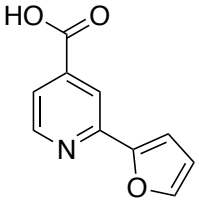	35
4-(1H-pyrrol-1-yl) pyridine-2-carboxylic acid (105055)	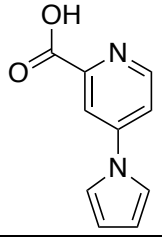	35

1.4 Project Objectives

Horizontal gene transfer of AMR genes will lead to the emergence of new MDR pathogens. Specifically targeting MGEs carrying AMR directly with small molecules is an avenue of research with the potential to prolong the effectiveness of current antibiotics. Developing strategies to find small molecules specific to MGEs is the first step in this approach.

This thesis presents two complementary approaches to preventing AMR dissemination through the discovery of small molecules using cell-based high throughput screening. The first part discusses my progress in designing and developing a high throughput conjugation assay (F conjugative plasmid) to find novel conjugation inhibitors. The second part of this report will discuss my progress in the development and screening of a conjugative transposon assay (Tn*1549*) to find inhibitors of transposition. This project also aims to establish secondary assays to exclude off-target compounds, as well as *in vivo* and *in vitro* assays to determine specific hits. Together, the main objective is to search for inhibitors to target both of the main MGEs that spread AMR horizontally.

Chapter 2.

Tn*1549* Excision Assay

2.1 Introduction

Conjugative transposons (CTn) are one of the mobile genetic elements (MGE) responsible for AMR dissemination. They reside in bacterial chromosomes and are capable of independent self-excision, conjugation, and integration into a new target site.[40] From what is currently understood about the distribution of environmental CTns, the Tn*916* family constitutes the largest and most abundant group.[41] They have spread across 6 different phyla and over 35 genera of bacteria.[42] Their broad host range is due to low sequence specificity for insertion.[43] In collaboration with Dr. Barabas's group, we designed an assay modeling Tn*1549,* a member of the Tn*916* family~~, in order~~ to find chemical probes that influence its movement at the molecular level.[44] Tn*1549* is composed of three modules: one providing the functions for conjugation and mobilization, another for conferring resistance to the antibiotic vancomycin, and a module encoding the integrase (Int) and excisionase (Xis) proteins. Int is the major target of the excision assay because it is essential for excision and integration of Tn*1549,* whereas Xis is vital for efficient and accurate excision by switching Int from its default integration function to excise. Int has an absolute minimum homology requirement for insertion, which explains the broad host-range of Tn*916* family of CTns. Int is part of the tyrosine-recombinase superfamily, sharing similarity with other site-specific recombinases in MGEs. We are interested in studying Tn*1549* because of its broad host range and involvement in the development of MDR enterococci. Our main objective is to find small molecules that enhance or inhibit the

activity of Tn*1549* using our excision assay. Small molecule modulators of MGEs will be used as molecular probes to give a richer understanding of the dynamics and mechanisms underlying the movement of MGEs in the environment. In the future, these molecules may be used as inhibitors to prevent MGE-mediated AMR transfer in environmental hotspots.

2.2 Materials and Methods

2.2.1 Plasmids and Strains for Tn*1549* Assay

This assay uses a dual plasmid expression system that is based on the production of visible light. The first plasmid (TPEP) encodes the Xis and Int proteins (Tn*1549* transposon proteins) expressed from a P_{BAD} promoter. Their expression is induced by arabinose and repressed by glucose. A beta-lactamase encoded by the plasmid provides resistance to 100 µg/ml of ampicillin. The origin of replication is oriA. The second plasmid (TEMP) features the mini-Tn*1549* transposon located upstream of a luciferase reporter, which reduces luciferase expression from a *tac* promoter. The mini-transposon carries resistance to 33 µg/ml of chloramphenicol and the plasmid provides resistance to 10 µg/ml of gentamicin. Chloramphenicol resistance is a result of a chloramphenicol acetyl transferase (*cat*) located within the mini-Tn*1549* in place of the conjugation and mobilization genes, Xis/Int, and the *vanB* operon (**Figure 2-3**). Gentamicin resistance is conferred in the form of an aminoglycoside-(3')-N-acetyltransferase. The origin of replication is constituted by CoEL1.

Plasmids were transformed into electrocompetent *E. coli* BW25113 Δ*bamB* Δ*tolC* cells, a cell line that is significantly more permeable to small molecules, generating the

assay (TEMP and TPEP) and the control (TEMP) strains. Assay and control strains were also prepared with *E. coli* BW25113 Δ*bamB* Δ*tolC gyrA* D87Y cells.

2.2.2 Chemically Competent *E. coli* cells

Psi Broth, TfBI (Transformation Buffer I), and TfBII solutions (Transformation Buffer II) are required to make rubidium chloride chemically competent cells (**Appendix 1**). An overnight *E. coli* culture grown in LB was used to inoculate 100 ml of Psi broth with 1 ml and incubated at 37°C with aeration (250 rpm) to an OD_{550} of 0.48. Cells were placed on ice for 15 min before centrifugation in a 250 ml sterile chilled centrifuge bottle and centrifuged using a JLA 16.250 rotor for 5-min at 5000*g* (Avanti J-25, Beckman Coulter). The supernatant was discarded, and the cells were gently resuspended in 40 ml of TfBI and put in ice for an additional 15 min. Cells were split between two chilled sterile 50 ml Falcon Tubes (Thermo Fisher Scientific) and centrifuged for 5 mins at 5000*g* at 4°C (Thermo Scientific Sorvall ST16R). The supernatant was discarded, and each cell pellet was resuspended in 2 ml of TfBII. After chilling the cells on ice for 15 min, 50-200 µl aliquots of cells were pipetted into chilled 1.5 ml Eppendorf tubes. Samples were flash frozen with liquid nitrogen, and stored at -80°C.

2.2.3 Chemically Competent *E. coli* Transformation

Chemically competent cells were thawed on ice for 30 min. Followed by an addition 30 min incubation of ice with the addition of 1-2 µl of DNA (or entire ligation) into a 50 µl aliquot of cells in a 1.5 ml Eppendorf tube. Eppendorf tubes were heat shocked for 45 s at 42°C using a heating block (Eppendorf Thermomixer® A**)** and placed on ice for 2 min.

To each transformation reaction, 250 µl of LB was added to the Eppendorf tube and incubated for 1 hr at 37°C with shaking (250 rpm). Each transformation was plated on selective media and grown overnight in a 37°C stationary incubator.

2.2.4 Preparation of Electrocompetent *E. coli* cells

An overnight *E. coli* (5 ml) culture was used to inoculate 500 ml of LB with 1/100th volume and grown at 37°C with shaking (250 rpm) to an OD_{600} between 0.4-0.6. Cells were chilled on ice for 20 mins before being transferred into a cold sterile centrifuge bottle. Cells were centrifuged at 4000*g* for 15 min at 4°C, and the supernatant was discarded. The cell pellet was gently resuspended in 500 ml of ice-cold glycerol (10%) and centrifuged at 4000*g* for 15 min at 4°C. The cell pellet was then resuspended in 250 ml of 10% glycerol and centrifuged at 4000*g* for 15 min at 4°C. Next, the cell pellet was resuspended in 20 ml of 10% glycerol and centrifuged at 4000*g* for 15 min at 4°C (Thermo Scientific Sorvall ST16R). Finally, the cell pellet was resuspended in 1-2 ml of 10% glycerol. 50-200 µl aliquots were transferred into chilled 1.5 ml Eppendorf tubes, flash frozen with liquid nitrogen, and stored at -80°C.

2.2.5 Electrocompetent *E. coli* Transformation

Electrocompetent *E. coli* cells were thawed on ice for 30 min. In a cold 1.5 ml tube, 40 µl electrocompetent cells and 1-2 µl of DNA dissolved in water were mixed. The micropulser (BioRad Micropulser) was set to EC1, the mixture was added to a chilled 0.1 mm cuvette and pulsed once. The pulsing parameter was ~5 ms. The cuvette was removed from the micropulser and 1 ml of LB (LBL405; BioShop) was used to gently recover the

cells. Cells were transferred to a 1.5 ml Eppendorf tube and recovered for 1 hr at 37°C with shaking (250 rpm). After 1 hr, each Eppendorf tube was spun at 10 000*g* for 3-4 min. Samples were concentrated by taking out ~700 µl of LB media and the cell pellet was resuspended in the remaining media. Transformation reactions were pipetted onto appropriate plates and glass beads were used to spread cells. Each transformation was plated on selective media and grown overnight in a 37°C stationary incubator (Fisher Scientific Isotemp Incubator).

2.2.6 Gel extraction protocol

GeneJET Gel Extraction Kit was used to purify DNA from agarose gels.[45] DNA samples were precisely excised from 0.8-1% agarose gels and the weight was recorded. An equal amount of binding buffer was added to each sample by weight and incubated at 55°C for 10 min or until fully dissolved (Eppendorf Thermomixer A). Samples were then placed on ice for 2 min and up to 800 µl was added to a DNA column. The column was centrifuged for 5 min at 10000*g* in a 4°C centrifuge (Fisher Scientific accuSpin Micro17R). The flowthrough was discarded and 700 µl of wash buffer was added, and the column was centrifuged for 1 min at 14000*g* at room temperature (Fisher Scientific accuSpin Micro17). This step was repeated once. After the second wash, the column was centrifuged at maximum speed for 1 min and the column air dried at room temperature for 5 min to evaporate excess wash buffer. 20-30 µl of slightly heated nuclease free water was added to the column and incubated for 1 min before the column was centrifuged at maximum speed for 2 min to recover DNA. Finally, the DNA concentration was measured using the Nanodrop 2000 instrument (Nanodrop 2000 Spectrophotometer, Thermo Scientific).

2.2.7 Colony PCR protocol

Each colony PCR reaction contains 5 µl of Thermo Scientific DreamTaq Green PCR Master Mix (2X)[46], 0.5 µl of Forward primer, 0.5 µl of Reverse primer, a colony of interest or 1 µl of control plasmid (1 ng/uL) that replaces 1 µl of water, and 4 µl of Nuclease-free Water. The PCR instrument was to an initial denaturation of 95°C for 5 min, followed by 30 cycles of denaturation at 95°C for 30 s, annealing at 55°C for 30 s, extension for 2 min (1 min/kb) at 72°C, and ended with a 10 min final extension at 72°C (Applied Biosystems by Thermo Fisher Sci Veriti 96 well Thermocycler). After PCR, DNA fragments were added to a 1% agarose gel (AGA001; BioShop) with GelRed® (Biotium) and were run for 1 hr at 110 V (BioRad POWER PAC 300 power supply with Thermo Scientific Owl™ EasyCast™ B3 Gel System).

2.2.8 PCR purification protocol

A Thermo Scientific Kit, GeneJET PCR Purification Kit was used according to the manual.[47]

2.2.9 Miniprep Protocol

An *E. coli* strain with a plasmid of interest was streaked on a plate containing appropriate antibiotics and incubated overnight at 37°C in a stationary incubator. A single colony was used to inoculate 5 ml of LB supplemented with appropriate antibiotics and grown overnight at 37°C with aeration (250 rpm) (Fisher Scientific Isotemp Incubator). Minipreps were conducted using the Invitrogen Purelink™ Quick Plasmid Miniprep Kit

according to the kit instructions.[48] The DNA concentration was measured using the Nanodrop 2000 instrument (Nanodrop 2000 Spectrophotometer, Thermo Scientific).

2.2.10 Generation of fluoroquinolone resistant mutant strains

E. coli BW25113 Δ*bamB* Δ*tolC* cells were streaked onto fresh LB agar plates and grown overnight at 37°C. *E. coli* BW25113 Δ*bamB* Δ*tolC* cells were then tested against ciprofloxacin to determine the agar MIC (**see protocol for agar MICs**). From fresh plates, cultures of various cell densities (10^7, 10^8, and 10^9 cells) were added to each of the following ciprofloxacin plates (2X MIC, 4X MIC, and 8X MIC). Plates were placed in an incubator and grown overnight at 37°C (Fisher Scientific Isotemp Incubator). Ciprofloxacin resistant colonies were isolated after 24-36 hrs of incubation. For each colony, they were restreaked on the same concentration of ciprofloxacin to confirm the resistance phenotype. Colony PCR was used to amplify the quinolone resistance determining regions (QRDR) in *gyrA* and *parC* for each colony. The annealing temperature was 70.2°C for *gyrA* product (607 bp) and 70.7°C for *parC* (477 bp). The forward and reverse primers for *gyrA* amplification are as follows*:*5'CTTCCACTTCTGCGCGAGCGC 3' and 5' CCGAGATGGCCTGAAGCCGG 3' (**Appendix 2)**. The forward and reverse primers for *parC* amplification are as follows: 5` GTTTGGCAGACGGGCAGGTAGC 3` and 5`CGATATGGCAGAGCGCCTTGCG 3` (**Appendix 2**). Phusion polymerase was used and the reactions were run at 98°C for 2 min followed by 30 cycles of 98°C at 10 s, 58°C at 10 s and 72°C at 30 s, and cycles were finalized at 72°C for 2 min (Applied Biosystems™, Veriti™ 96-Well Thermal Cycler). Next, these amplicons were run on a 1% agarose gel for 1 hr at 110 V. Fragments were isolated using gel extraction (see Gel

extraction protocol). After isolation, 5 µl of each reaction was given to a sanger sequencing facility for testing (MOBIX Lab, McMaster University). The *gyrA* sequencing primer is 5' GGATATACACCTTGCCGC 3' and the *parC* sequencing primer is 5' CGAAGTTTGGCACCCAGTC 3' (**Appendix 2**). Colonies with a mutation in the QRDR were then made into electrocompetent cells to be made into the assay and control strains (MOBIX Lab, McMaster University).

2.2.11 Tn*1549* Excision Assay Protocol

The day before the assay, 20 ml of LB with 0.4% glucose was inoculated with assay or control bacteria from a -80°C frozen stock and appropriate antibiotics were added. Cultures were incubated overnight at 37°C with shaking at 250 rpm. Overnight cultures were added to 100 ml LB with appropriate antibiotics and 0.4% glucose to reach a final OD_{600} of 0.05. Cultures were incubated for two hr at 37°C with shaking at 250 rpm to reach log phase. Cultures were centrifuged for 15 min at 3000 rpm at room temperature using a TX-400 rotor (Thermo Scientific Sorvall ST16R), the supernatant was removed, and the cell pellet was resuspended in LB for a final OD_{600} of 0.769. To each well of a 384-well clear bottom white assay plates (Greiner) 30 µL of LB induction media (**Appendix 2**) (containing IPTG and arabinose for a final concentration of 0.1mM and 0.4% in assay plates), 0.5 µl of DMSO, and 19.5 µl of assay or control inoculum (final OD_{600} of 0.3) was added. After all assay components were dispensed, plates were shaken and incubated at 25°C for 4 hr. The OD_{600} was measured after the incubation step using the Synergy (BioTek). Next, 20 µL of Britelite Plus was added and the plates were centrifuged at 300*g* for 2 min at room temperature to remove bubbles (Sorvall LEGEND RT+ with a 75006445

R rotor). Finally, the luminescence signal was read using the Synergy (BioTek) after 60 min from the addition Britelite Plus. Data was analyzed using Gen5 software.

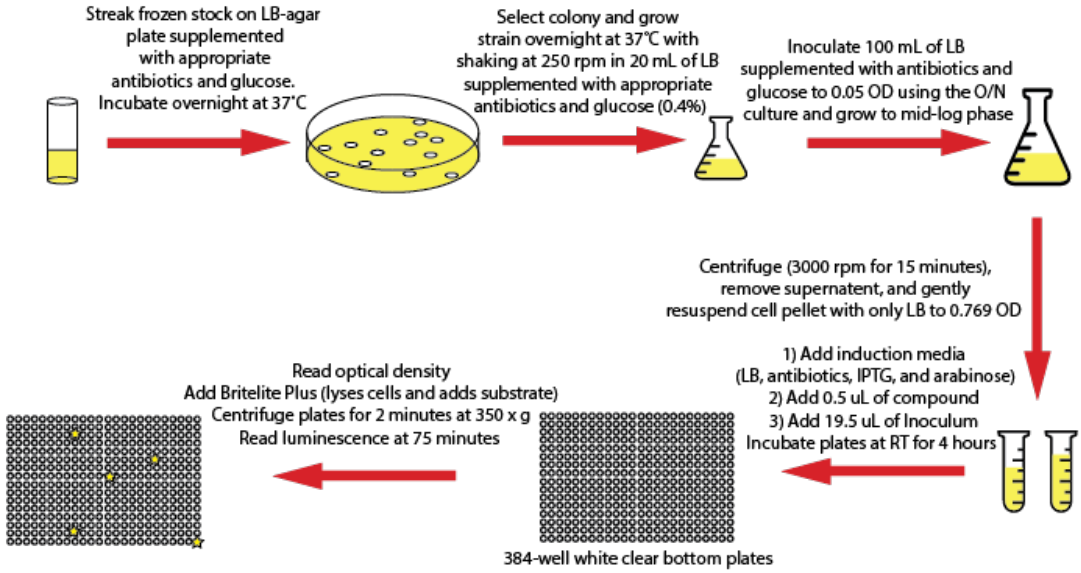

Figure 2-1: Overview of Tn*1549* excision assay.

2.2.12 *gyrA* Mutant Assay Protocol

The assay protocol to test both the wildtype assay and *gyrA* mutant assay strain was the same as described in the previous section. A 10 mg/ml stock of ciprofloxacin (Sigma) was prepared in ddH_2O, a 10 mg/ml stock of ofloxacin (Fisher Scientific) was prepared in water and 0.1 M NaOH (EMD), and a 20 mg/ml stock of levofloxacin (Fisher Scientific) was prepared in DMSO.

2.2.13 High Throughput Screening of Tn*1549* assay

High throughput screening of the Tn*1549* assay tested compounds from the bioactives library and the prefractionated library. The bioactives library consists of 3921 compounds from four libraries. The first library (Prestwick Chemical Library) contains 539

compounds with an average molecular weight of 372 g/mol (Prestwick Chemical; Illkrich, France). This set of small molecules consists of 100% FDA approved drugs with high chemical and pharmacological diversity and known bioavailability and safety in humans. The second library component is the BIOMOL2865 Natural Products Library from Enzo Life Sciences, Inc (Farmingdale, NY, USA). This set of small molecules contains 501 compounds with an average molecular weight of 401 g/mol. These compounds are highly purified natural products with known structures. The third library component is Lopac1280 (International Version) from Sigma-Aldrich Canada Ltd. (Oakville, ON, Canada). This set of small molecules contains 1240 compounds with an average molecular weight of 337 g/mol. These compounds are active in cell signaling and neuroscience assays. The fourth library component is called the Spectrum Collection from MicroSource Discovery Systems, Inc. (Gaylordsville, CT, USA). This set of small molecules contains 1641 compounds with an average molecular weight of 354 g/mol. This collection is comprised of drugs (60%) with defined pharmacological and toxicological profiles, natural products (25%) with unknown biological properties that cover a wide range of chemical classes and structural diversities, and other bioactive components (15%) which include non-drug enzyme inhibitor, receptor blockers, membrane active compounds, and cellular toxins.

The Prefractionated Library (PFL) is a collection of fractionated methanolic extracts of solid media and conditioned media. The samples have been prepared from the Wright Actinomycete Collection, a collection of environmental strains, predominantly actinomycetes with some non-actinomycetes and fungi, that have been isolated from soil. The library consists of 48 96-well plates (**Figure 2-2**). Each PFL plate contains 8 strains

that are separated into 10 fractions, for a total of 80 samples per plate (**Figure 2-2**). Columns 1 and 12 are left empty to allow for controls (**Figure 2-2**). Column 2 contains crude extract in DMSO, column 3 contains conditioned media, and columns 4-11 contain fractions from flash chromatography fractionation of crude extracts in DMSO (8 per strain) (**Figure 2-2**).

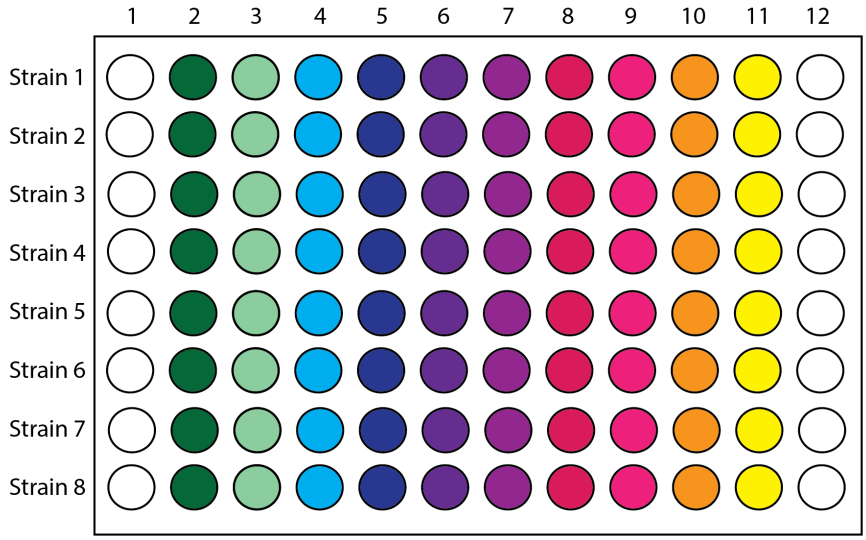

Figure 2-2: Prefractionated Library (PFL) plate schematic.
Each PFL plate consists of 8 strains on a 96-well plate. Columns 1 and 12 are empty for controls, column 2 contains the crude extract, columns 3 contains conditioned media and columns 4-10 contain 8 fractions from flash chromatography fractionation of crude extracts in DMSO.

The day before the assay, 20 ml of LB with 0.4% glucose was inoculated with assay or control bacteria from a -80°C frozen stock and appropriate antibiotics were added. Cultures were incubated overnight at 37°C with shaking at 250 rpm. Overnight cultures were added to 100 ml LB with appropriate antibiotics and 0.4% glucose to reach a final OD_{600} of 0.05. Cultures were incubated for two hrs at 37°C with shaking at 250 rpm to reach log phase. Cultures were centrifuged for 15 min at 3000 rpm at room temperature

using a TX-400 rotor (Thermo Scientific Sorvall ST16R), the supernatant was removed, and the cell pellet was resuspended in LB for a final OD_{600} of 0.769. To each well of a 384-well clear bottom white assay plates (Greiner) 30 µL of LB induction media (**Appendix 2**) (containing IPTG and arabinose for a final concentration of 0.1mM and 0.4% in assay plates), 0.5 µl of compound in DMSO (Bioactives Library) or extract (Prefractionated Library), and 19.5 µl of assay or control inoculum (final OD_{600} of 0.3) was added. These plates were shaken and incubated the plates at room temperature for 4 hr. Before adding luciferase substrate, the optical density was measured using the Perkin Elmer Envision plate reader. Next, 20 µl of Britelite Plus was added and the plates were centrifuged for 1 min at 300*g*. Finally, 20 µl of Britelite Plus was added and the plates were centrifuged at 300*g* for 2 min at room temperature to remove bubbles (Sorvall LEGEND RT+ with a 75006445 R rotor). The luminescence signal was read after 1 hr using the Perkin Elmer Envision plate reader. Luminescence data was collected between 79-94 min after adding Britelite Plus and analyzed using Spot Fire. Compounds were added using pin tools, while the inoculum, induction media, and Britelite Plus were added using the Multi Combi nL dispenser.

A second screen was performed for the Bioactives library. From the primary screen, 90 hits were identified based on compounds below 2SD of the mean normalized luminescence over optical density of both replicates for all compounds screened (see section 2.2.14). These compounds were 'cherry-picked' from the Bioactives library and tested in duplicate. Compound concentrations were diluted in half-log steps from 50 µM to 0.5 nM final concentrations. The purpose of this method was to validate the hits that

specifically showed a dose-dependent relationship with luminescence activity over optical density.

2.2.14 Analysis of Screening Data

Data was normalized using the interquartile method (IQM) with TIBCO Spotfire (v 10.4).[49] Quartiles refer to the division of a rank-ordered data set into four equal parts. The interquartile mean is the mean of the middle two quartiles or the middle 50% of rank-ordered data. Sample data were normalized on a per plate basis by dividing every well of the plate by the interquartile mean of the plate according to the following equation:

$$\text{IQM Normalization activity} = \left(\frac{S}{\mu_{iq}}\right)$$

Where S represents the measured sample value and μ_{iq} represents the mean (μ) of the interquartile (*iq*) data of the plate. The value of μ_{iq} was found for each plate by sorting the data in ascending order and finding the mean of the interquartile (middle 50%) data. The interquartile method has the advantage of not being influenced by outliers on a plate as only the middle 50% of the data is used for normalization. Prior to IQM normalization, the luminescence data was divided by the absorbance 600 nm data to eliminate differences in luminescence signal as a result of growth variation. Prism 8 (Version 8.1.2) was used to make replica plots and IC_{50} curves.

2.2.15 Agar MIC Testing

Agar MIC testing followed the protocol from Weigand et al.[50] Two days before an agar MIC test, the desired bacteria was streaked out on an cation-adjusted Mueller Hinton

Agar (CAMHA) plate containing appropriate antibiotics and grown overnight at 37°C (Fisher Scientific Isotemp Incubator). Using the overnight plate, the strain was restreaked onto another CAMHA-antibiotic plate and grown overnight at 37°C.

CAMHA was prepared with 11 g of cation-adjusted Mueller Hinton II Broth (CAMHB) and 7.5 g of agar (1.5%). CAMHA was autoclaved and cooled to 50°C. Ten 2-fold serial dilutions of each compound were made with water at 100X concentration in a 96-well plate. With a multi-channel pipette, 1 μL of each compound dilution and 99 μL of CAMHA were carefully added to a 96-well U-bottom MIC plate (Sarstedt) in triplicate. For each 96-well plate, one column was reserved as a sterility control (no inoculum or antibiotic) and another for a growth control (inoculum without antibiotic), with the same amount of compound solvent as the test wells. Plates were left at room temperature for 30 min to solidify the agar.

The inoculum was prepared by suspending colonies from a plate in a 5 ml sterile saline solution (0.85% NaCl) to an OD_{600} of 0.08 and making a 1/200 dilution in CAMHB. With a multi-channel pipette, 1 μL of inoculum was carefully added to the appropriate wells on a 96-well plate. Plates were placed in a 37°C incubator for 16-20 hrs. After incubation, plates were scanned to determine the MIC visually (Epson Scanner, Epson Perfection V800 Photo).

2.2.16 Minimal inhibitory concentration (MIC) testing

All strains were grown in CAMBH (Becton Dickinson) at 37°C with aeration for 18 hr. Susceptibility testing was performed using the microdilution broth method, with the inoculum prepared using the colony suspension method, according to CLSI guidelines.[50,51]

To prepare the inoculum, 5-7 colonies from a fresh overnight place were suspended in sterile saline solution (0.85% NaCl). The inoculum was standardized accordingly with saline or colonies to reach an OD_{625} of 0.08. For each sterile 96-well U-bottom MIC plate (Sarstedt), one column served as a sterility control (no inoculum or antibiotic) and another for a growth control (inoculum without antibiotic). A 1/200 dilution of cells was made in CAMHB. With a multi-channel pipette, 1µl of compound and 99 µl of inoculum was added to the appropriate wells on a 96-well plate. Each condition was tested in triplicate. Plates were incubated at 37°C for 16-20 hrs. Plates were shaken to resuspend the bacteria in wells. Plates were read using a Spectramax Plus 384 instrument and analyzed with SoftMax Pro Software (v 5.4.1).

2.2.17 Arabinose Transport Inhibition Assay

This assay was designed to identify potential inhibitors of arabinose transport via a GFP reporter (**Figure 2-11a**). The pA15-*gfp* plasmid was constructed using Gibson assembly. The TPEP[41] expression plasmid was used as the backbone, containing an ampicillin cassette and an arabinose promoter, and the *gfp* gene was derived from pUA66[52]. An empty vector of TPEP without the *xis/int* genes was used as a control to measure baseline fluorescence.

PCR was performed using a reaction mix of 1X HF-Phusion buffer (Fisher Scientific), 0.4 mM dNTP (Fisher Scientific), 1.5 mM MgCl2, 0.5 mM of each primer, 0.5 µl template and 0.5 units of Phusion DNA polymerase (Thermo Fisher) in a final volume of 25 µl. The Backbone TEMP PCR reaction was in a BioRad PCR machine at 98°C for 2 min followed by 30 cycles of 98°C at 10 s, 72°C for 2 min, and 72°C at 30 s, cycles were

finalized at 72°C for 2 min. The Backbone of TPEP FP 5' CAAATAACTCGAGATCTGCAGCTGGTACC and Backbone of TPEP RP 5' GTTCTTCTCCTTTACTCATGGTTAATTCCTCCTGTTAG 3' (**Appendix 2**). The luciferase PCR reaction was in a BioRad PCR machine at 98°C for 2 min followed by 30 cycles of 98°C at 10 s, 69°C for 1 min, and 72°C at 30 s, cycles were finalized at 72°C for 2 min. The luciferase FP 5' CCATGAGTAAAGGAGAAGAACTTTTCAC 3' and luciferase RP 5' 5' GCTGCAGATCTCGAGTTATTTGTACAATTCATC 3' (**Appendix 2**). Primers were ordered from Mobix Labs at McMaster University. PCR constructs were gel purified. The two purified fragments were ligated in a 3:1 ratio of backbone to insert using Gibson assembly. The reaction was comprised of 2X GA buffer (**Appendix 3**), the two fragments, and water to a final volume of 20 μL. The Gibson assembly reaction was carried out for 35 min at 50°C in a Thermocycler (SimpliAmp Thermo Cycler, Thermo Fisher). In a 1.5 ml Eppendorf tube, 4 μL of the Gibson reaction was added to 50 μL of chemically competent TOP10 cells. Cells were incubated for 30 min on ice and heat shocked for 30 s at 42°C. To initiate the recovery process, 700 μL of LB media was added to the cells and the reaction was incubated at 37°C for 1 hr. The transformation was plated on LB agar plates supplemented with 100 μg/ml of Ampicillin and incubated overnight at 37°C. The pA15-*gfp* plasmid and empty vector pA15 constructs were transformed into electrocompetent *E. coli* TOP10 cells, plated on LB (LBL405; BioShop) agar supplemented with 100 μg/mL ampicillin (Sigma), and incubated at 37°C overnight.

The pA15-*gfp* plasmid and empty vector pA15 constructs were streaked from a frozen glycerol stock (10%) on a fresh plate containing ampicillin (100 μg/ml ampicillin)

and incubated overnight at 37°C. A single colony was added to a fresh 5 ml LB containing ampicillin (100 mg/ml). The overnight culture was used to inoculate a fresh 20 ml LB in a 100 ml Erlenmeyer flask. Once the culture reached an OD_{600} between 0.4-0.6, 49 μL of inoculum was added to a black clear bottom 384 well plate (Thermo Fisher) with 1 μL of DMSO in triplicate. The fluorescence signal was read at 5 min intervals for 2 hrs using the Synergy (BioTek) at an emission wavelength of 509 nm and an excitation wavelength of 395 nm.

2.2.18 *In vivo* PCR excision monitoring

This *in vivo* PCR excision monitoring protocol was adapted from Lambersten et al.[41] Assay and control strains were streaked out onto plates from frozen stocks with appropriate antibiotics and 0.4% glucose. Cultures were grown overnight at 37ºC in a stationary incubator. Several colonies were used to inoculate 20 ml of LB with appropriate antibiotics and 0.4% glucose. Cultures were grown overnight at 37ºC with shaking at 250 rpm. With this overnight culture, a 100 ml culture was inoculated to an OD_{600} of 0.05 in LB with 0.4% glucose and appropriate antibiotics. Cultures were grown to the mid-exponential growth phase. Cultures were centrifuged for 15 min at 3000 rpm at room temperature using a TX-400 rotor (Thermo Scientific Sorvall ST16R), the supernatant was removed, and the cell pellet was resuspended in LB for a final OD_{600} of 0.263. A 3:2 ratio of LB induction media (containing IPTG and arabinose for a final concentration of 0.1mM and 0.4% in assay plates) to inoculum was used for each assay (e.g. 15 ml of Induction media and 10 ml of inoculum). Ciprofloxacin was added at a concentration below the IC_{50} value of assay and control strains (0.08 μg/ml). At specific time points, 1 ml culture

samples were taken for PCR analysis. The OD_{600} was measured and cultures were spun down at 4ºC at 5000*g* for 5 min. The supernatant was removed, and pellets were stored at -20ºC. Samples were taken before induction (t=0) and every hour for four hours following induction. Finally, 0.5 µl of supernatant was used as a template in the PCR reaction.

The excised mini-Tn*1549* CI was detected by PCR with primers matching the transposon ends. In addition, the presence or absence of the mini-Tn*1549* in the transposon donor plasmid was tested with PCR primers annealing to the transposon flanking DNA (**Figure 2-11c**). Samples were prepared for PCR by standardizing each sample's optical density with the amount water to resuspend the cell pellet (e.g., OD_{600} = 0.5, the pellet was suspended in 50 µl water). The suspensions were then boiled using the cook setting in a rice cooker (Black+Decker, Model E503 (RC-3) for 10 min, cooled on ice and cell parts were pelleted by centrifugation at 5000*g* for 5 min at 4°C *(*Thermo Scientific Sorvall ST16R). For each PCR reaction: 5 µl of 5X HF-Phusion Buffer (1.5 mM $MgCl_2$), 0.5 µl (0.4 µM) dNTPs, 1.25 µl of 10 mM (0.5 mM) Forward Primer, 1.25 µl of 10 mM (0.5 mM) Reverse Primer, 0.5 µl Template (supernatant), 0.25 µl (0.5 units) Phusion DNA polymerase, and 16.25 µl of Nuclease free water for a final volume of 25 µl. The primers for CI detection are CI Forward (P2) 5' GCGGGATCCTGTTCTCCCAT 3' and CI Reverse (P3) 5' ACGCAAGCTTCGATTCCGCAAG 3' (**Appendix 2**). The primers for DP detection are DP Forward (P1) 5' GAGAGCAGCTGAAGTTACCC 3' and DP Reverse (P4) 5' GTAACTTTAAACGGACCACTAGGAG 3' (**Appendix 2**). The PCR reaction of CI was in a BioRad Thermo Cycler and ran at 98°C for 2 min followed by 25 cycles of 98°C at 10 s, 58°C at 10s (P2 and P3), and 72°C at 30 s, cycles were finalized at 72°C for

2 min. The PCR reaction of DP was in a BioRad Thermo Cycler and ran at 98°C for 2 min followed by 25 cycles of 98°C at 10 s, 55ºC (Primers P1 and P4) or 60ºC (with primers P46 and P47) at 10s, and 72°C at 60 s, cycles were finalized at 72°C for 2 min. Gels were run for 1 hr in 1xTAE buffer (Tris-Acetate-EDTA) at 110 V (BioRad POWER PAC 300 power supply with Thermo Scientific Owl™ EasyCast™ B3 Gel System) in a 1% agarose gel (AGA001; BioShop). ExcelBand™ 1kb (0.25-10kb) DNA Ladder was used as a marker. Gels are stained with GelRed™ after they were run to avoid interacting with the DNA during migration. The gel was visualized with the Typhoon Trio+ (GE) scanner.

2.2.19 Inhibition of Firefly Luciferase Assay

The luciferase inhibition secondary assay was designed to see if compounds inhibited the luciferase reporter of excision activity instead of the integrase. The reporter plasmid was derived from TEMP. The luciferase gene was amplified using Luciferase Fwd primer 5’ GTTACCATATGGAAGACGCC 3' and Luciferase Rev primer 5’ GCATCCTCGAGTTACAATTTG 3' (**Appendix 2**). The luciferase fragment, pGDP-1, and pGDP-2 were digested with *Nde*I and *Xho*I for 1 hr at 37°C. The plasmids and luciferase amplicon were ligated with T4 DNA ligase in a 3:1 ratio overnight at 4°C. The pGDP-1:*luc* construct was transformed into chemically competent TOP10 using the protocol described above.

For the assay, TOP10 containing the construct and TOP10 containing an empty vector was streaked from a frozen stock onto LB agar plates supplemented with 50 µg/ml of kanamycin and grown overnight at 37°C. Several colonies were grown up overnight in 5 ml of LB with 5 µl of kanamycin (50 mg/ml) with shaking (250 rpm) at 37°C. A new 5

ml LB sterile test tube was inoculated to 0.05 OD_{600} for each overnight colony and grown with shaking (250 rpm) at 37°C to an OD_{600} of 0.5. The culture was then diluted to a final OD_{600} of 0.3. 49 µl of the inoculum was added to 1 µl of compound in a black 384 well plate (Thermo Fisher). A control of the assay strain without compound as well as a strain with empty vector is present. Compound plate was incubated for 30 min. The plate was read using a Synergy (Biotek) for 2 hr. Luminescence data was plotted over OD_{600} versus time using Prism.

2.2.21 *In vivo* assay monitoring levels of supercoiling in the cells.

The purpose of this experiment was to determine if ciprofloxacin inhibited *in vivo* excision activity of Tn*1549* Int/Xis by visualizing changes in DNA substrate over time. To conduct the experiment, the Tn*1549* excision assay was scaled up to a final volume of 35 ml (e.g. 14 ml of 0.789 OD_{600} assay or control inoculum and 21 ml of induction media) for each condition. The three conditions were the control strain, the assay strain, and the ciprofloxacin-treated Tn*1549* assay strain with a final concentration of 0.08 µg/ml. At various time points, 5 ml of each condition was centrifuged at 4°C at 3000 rpm for 15 min in 15 ml Falcon Tubes (Thermo Scientific Sorvall ST16R). After centrifugation, the supernatant was removed, and the cell pellets were stored at -20°C until the DNA was ready for extraction. Time points were 0 hrs (before induction), 30 min, 1 hr, 2 hr, 3 hr, and 4 hr. Extract DNA using a column miniprep method and recover DNA in 20 µL of nuclease-free water. 10 µl of each sample was loaded with 2 µl of 6X DNA loading dye (**Appendix 1**). DNA samples were separated for 1 hr in 1xTAE buffer (Tris-Acetate-EDTA) at 110 V in a

1% agarose gel. ExcelBand™ 1kb (0.25-10kb) DNA Ladder was used as a marker. Gels were stained with GelRed™ and visualized with the Typhoon Trio+ (GE) scanner.

2.2.22 *In vivo* conjugation assay

The protocol was adapted from Clewell et al.[53] *E. faecalis* 268-10 carrying Tn*1549* (gift from Orsolya Barabas) was used as the donor and *E. faecalis* JH2-2 was used as the recipient. MICs of donor and recipient strains were done to find an antibiotic that the recipient strain was more resistant to than the donor to select for transconjugants. The MICs of Streptomycin (100 mg/ml stock in DMSO, Sigma), Rifampin (40 mg/ml stock in DMSO, Sigma), Ciprofloxacin (10 mg/ml stock in water, Trimethoprim (50 mg/ml stock in DMSO, Sigma), Fusidic acid (50 mg/ml stock in DMSO, Sigma), Vancomycin (25.6 mg/ml stock in DMSO, Sigma), Blasticidin (12.8 mg/ml stock in DMSO, BLA477; Bioshop), Moenomycin (25.6 mg/ml, Cedarlane), Gentamicin (50 mg/ml stock in water, GTA202; Bioshop), Ampicillin (100 mg/ml stock in water, AMP201; Bioshop), and Chloramphenicol (33.3 mg/ml stock in 70% ethanol, EM Science) were found for donor and recipient strains.

Donor and recipients were grown overnight in 5 ml of BBL™ Brain Heart Infusion (BHI, Becton Dickinson) broth and selected with appropriate antibiotics (e.g. 5µl of 4 µg/ml of vancomycin for the donor and 64 µg/ml of Streptomycin for the recipient). The OD_{600} of each overnight was measured and donor and recipients were serially diluted (10-fold). Serial dilutions were plated on BHI agar plates to count the colony forming units (cfu) of donor and recipient. Each conjugation reaction had 4.5 ml of BHI, 0.5 ml of the Recipient strain, and 0.05 ml of the Donor strain, representing a 1:10 donor to recipient

ratio in 14 ml Polypropylene Round-Bottom Tubes (Falcon). Ciprofloxacin was also added to each conjugation reaction, ranging from above to below the MIC (0, 0.03125, 0.125, 0.5, 1, 2, and 4 μg/ml). Conjugation proceeded over 4 hr in a 37°C incubator with slight rotation of the samples using the TubeRoller from Benchmark Scientific. After 4 hr, reactions were vortexed for 15 s on setting 5 (Fisher Scientific). Conjugation reactions were serially diluted and plated on BHI agar supplemented with 128 μg/ml of Fusidic acid and 8 μg/ml of Vancomycin. Conjugation frequency was counted by dividing the average number of transconjugants over the average number of recipient cells from three replicates.

2.3 Results

2.3.1 Conjugative Transposition Assay

With the aim of finding small molecules that target Tn*1549* gene movement, we targeted the excision step in conjugative transposition. Our high throughput assay uses a firefly luciferase reporter to quantify the rate of excision of the mini-Tn*1549* via integrase (Int) and excisionase (Xis) activity (**Figure 2-3**). Before induction, the P_{tac} promoter on TEMP is repressed by the LacI repressor and glucose represses the expression of Int/Xis through the arabinose promoter on TPEP. IPTG induction allows for downstream luciferase expression by derepressing the P_{tac} promoter and arabinose induction results in Int/Xis expression and mini-Tn*1549* excision. Mini-Tn*1549* consists of a chloramphenicol acetyltransferase (*cat*) flanked by inverted repeats that are recognized by Int and Xis for excision. As a result, the mini-transposon's size is significantly reduced from 33 kb to 1.5

kb (**Figure 2-3**). The compounds we are searching for will ideally lower the luminescence reading, while the optical density will remain unchanged.

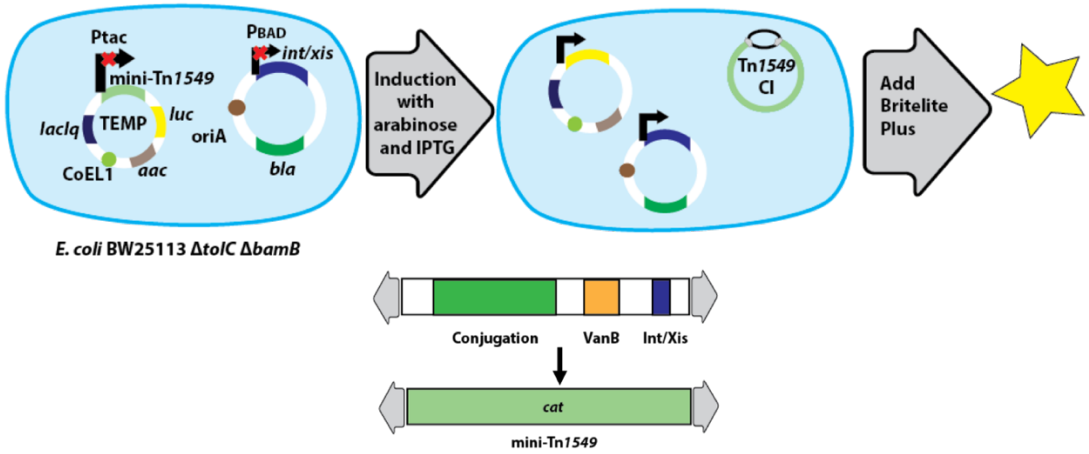

Figure 2-3: Tn*1549* Excision Assay.
The assay models the excision step in conjugative transposition using a firefly luciferase reporter. The luminescence and optical density (OD) are measured after 4 hours to quantify excision of the mini-Tn*1549* via the integrase (Int) and excisionase (Xis). Mini-Tn*1549* consists of a chloramphenicol acetyltransferase flanked by inverted repeats. This significantly reduces the size of the original CTn from 33 kb to 1.5 kb. Before induction, *E. coli* BW25113 Δ*bamB*Δ*tolC* is grown to mid-log phase with glucose present. The glucose repressed the expression of INT/XIS through the arabinose promoter on TPEP. The P_{tac} promoter on TEMP is repressed by the LacI repressor. Induction with arabinose results in Int/Xis expression and min-Tn*1549* excision. IPTG induction allows for downstream luciferase expression after excision. Finally, the luminescence is measured after the addition of Britelite Plus.

2.3.2 Assay Development and Pilot Screen of Tn*1549* Excision Assay

The assay went through an initial development phase, where each step was optimized to make the assay robust (**Figure 2-1**). The screening conditions were determined by comparing the differences in Lum/OD between the control and assay strains with DMSO. The assay strain was *E. coli* BW25113 Δ*bamB*Δ*tolC* containing TEMP and TPEP and the control strain *E. coli* BW25113 Δ*bamB*Δ*tolC* containing TEMP. The Z prime (Z') was 0.64, reflecting a robust assay with acceptable screening conditions (**Figure 2-4**).

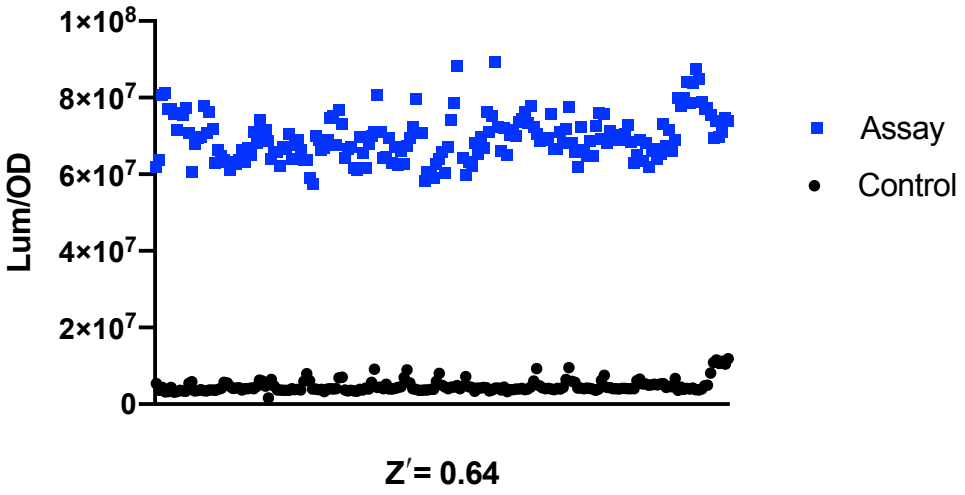

Figure 2-4: Determination of the Z prime for the Tn*1549* excision screen.
The Z prime (Z') test was conducted in a white 384-well clear-bottomed plate, with half of the plate containing the assay strain (*E. coli* BW25113 Δ*bamB*Δ*tolC* cells containing TEMP and TPEP) and the other half containing the control bacteria (*E. coli* BW25113 Δ*bamB*Δ*tolC* cells containing TEMP). The Z' was determined to be 0.64. The y axis is the luminescence signal divided by the optical density at 600 nm. The x axis represents different wells on a 384 well plate.

After establishing the assay, we initiated a pilot screen with the Bioactives library, which has previously validated numerous high throughput screening assays in the CMCB. The purpose of the pilot screen was to make sure that we could generate useful data with an established set of known compounds, and that the assay was robust while scaling up to multiple plates at the same time. The Bioactives library contains 4000 compounds, with known chemical structures, that are either off-patent, have known biological activity or are natural products. **Figure 2-5** shows the replica plot of the assay in duplicate. The x and y axes represent the normalized luminescence/OD data of each replicate, and each data point is a coordinate of the two replicates. The primary screen was performed at an average compound concentration of 10 μM. During screening, it is common practice to define compounds that are 3 standard deviations (SD) from the mean of the dataset as hits.

However, given the high variation in the dataset, we altered the hit cutoff to include compounds below 2SD of the mean normalized luminescence over optical density of both replicates for all compounds screened to identify inhibitors of conjugative transposition. The major factor attributing to the high variation seen in the dataset is explained by our Z' testing method. The Z' test was conducted by only measuring luminescence and optical density in the presence of DMSO. However, the Bioactives library consists of compounds with diverse biological activities, which can have different effects on the Tn*1549* excision assay compared to DMSO. To resolve this issue, optimizing the assay in the presence of a true positive (small molecule that targets excision) and negative control (small molecule with no impact on the assay) would give a more realistic screening window. Other factors contributing to the high variation in the dataset are freeze-thaw cycles of compounds, technical errors in equipment, and the inherent complexity of luminescence and cell-based assays. After screening the Bioactives library, we cherry-picked 90 hits that showed the most reduced signal for dose-response analysis.

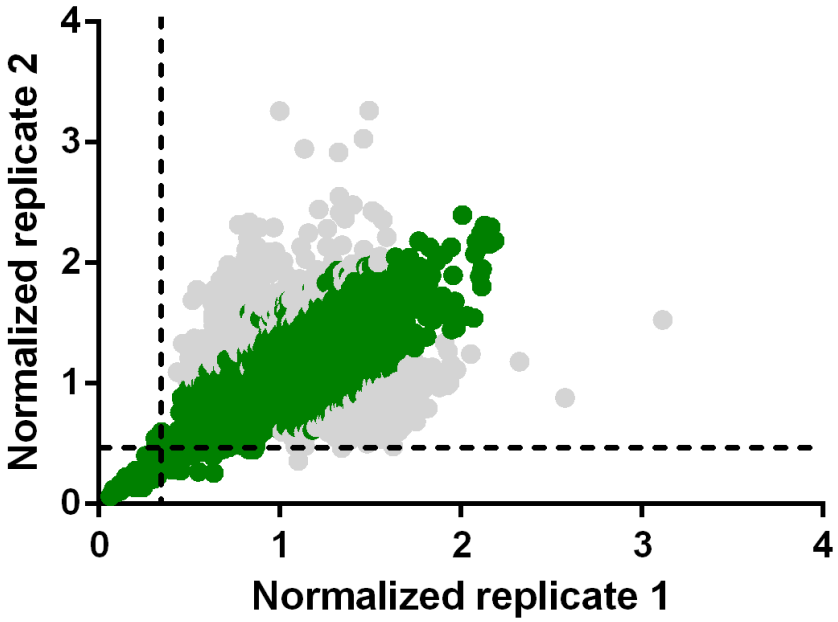

Figure 2-5: Replica plot of the Bioactives Library screen.
Compounds were screened in duplicate and have two luminescence data points normalized to the x and y axes. For this data set, hits were defined below 2SD of the mean normalized luminescence over optical density of both replicates. Compounds in green are along the y=x line and compounds with lower reproducibility are in gray.

2.3.3 Secondary Screening of Hits

Dose response curves of 90 prioritized compounds were screened in duplicate over a range of half-log concentrations (0.5 nM to 50 μM). Half maximal inhibitory concentration (IC_{50}) values were calculated to identify compounds that have a dose-dependent inhibitory effect on the integrase reporter or non-specific compounds (**Table 2-1**). We used this value to determine the concentration of each compound that reduced excision activity by 50% to assign potency to compounds. **Table 2-1** summarizes the dose response curves, IC_{50} values, chemical structure, and other relevant information (i.e. biological target) on the 24 most promising hits (0.6% hit rate) of the pilot screen. Dose

response curves cannot infer the exact mechanism of action of the compounds, without secondary and biochemical assays discussed later. However, given the known structure of compounds it is possible to infer potential mechanisms of action. The most abundant hits were among the fluoroquinolone class, accounting for 14 hits. Every fluoroquinolone in the Bioactives library except for nadifloxacin was identified as a hit. On the replica plot in **Figure 2-5**, nadifloxacin identified as a nonhit (1.3 for replicate 1 and 0.79 for replicate 2). However, given that other fluoroquinolones with similar physiochemical properties to nadifloxacin were identified as hits, it was likely a false negative in this screen. Compounds were screened at 10 µM concentrations, and after several freeze-thaw cycles they can become diluted and decrease their potency. Nadifloxacin will need to be tested again to confirm our hypothesis. Fluoroquinolones are effective bactericidal antibiotics used to treat Gram positive and negative bacterial infections. These antibiotics will be further characterized with respect to Tn*1549* in the following sections.

Table 2-1: Summary of Secondary Screen Hits with Dose-Dependent Activity.
Dose response curves have relative luminescence units (RLU) on the left y-axis, optical density (OD) at 600nm on the right y-axis. RLU and O.D. were measured at various compound concentrations, increasing from left to right. OD measurements are represented by pink squares. RLU measurements have been standardized by OD and are represented as blue circles.

Dose Response Curves	Structure	Background
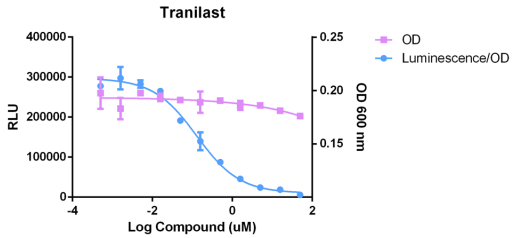 **IC_{50} Luminescence/OD (79-94 min) (µM)** = 0.1286 **IC_{50} OD (µM)** = ~530025	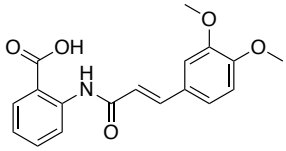	Tranilast is an analog of a metabolite of tryptophan.[54] It inhibits UGT1A1, which can interfere with metabolism of drugs acted on by this enzyme. It also is considered an

		anti-allergy medication by inhibiting the release of histamine from mast cells and has also been found to inhibit proliferation of fibroblasts, but the biological target is currently unknown.[54]
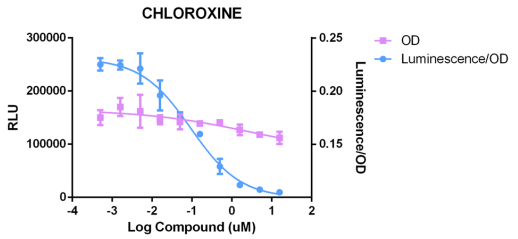 **IC_{50} Luminescence/OD (79-94 min) (µM)** = 0.09361 **IC_{50} OD (µM)** =3.405	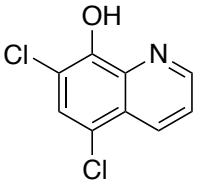	Chloroxine is a synthetic quinolone derivative with bacteriostatic, fungistatic, and antiprotozoal properties. Its mechanism of action is not fully understood. Chloroxine may slow down mitotic activity in the epidermis, leading to anti-dandruff uses.[55] Chloroxine may be genotoxic as it induces SOS-DNA repair in *E. coli*. [56]
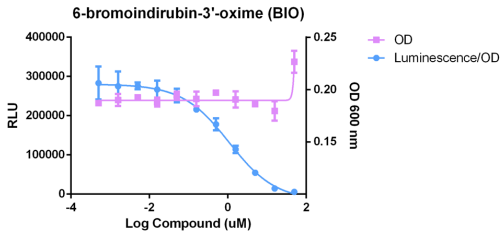 **IC_{50} Luminescence/OD (79-94 min) (µM)** = 1.086 **IC_{50} OD (µM)** = ~87.77	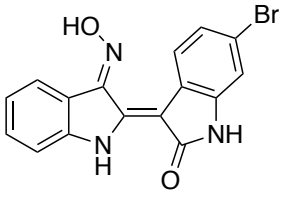	BIO is a general inhibitor of JAK kinases, and more specifically glycogen synthase kinase-3 beta (GSK-3β). GSK-3β is involved in diverse cellular processes, including glycogen

		synthesis, proliferation, development and apoptosis.[57]
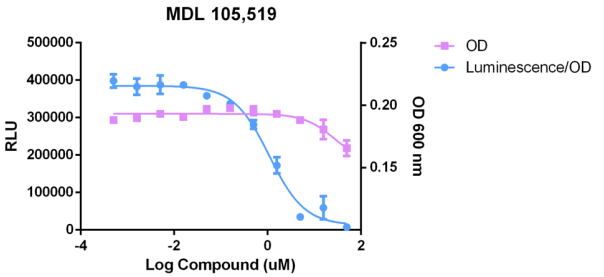 **IC_{50} Luminescence/OD (79-94 min) (µM)** = 1.087 **IC_{50} OD (µM)** = 27.3	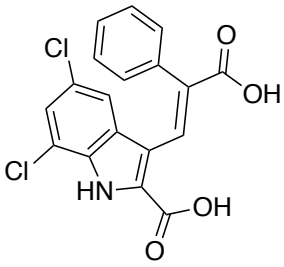	N/A
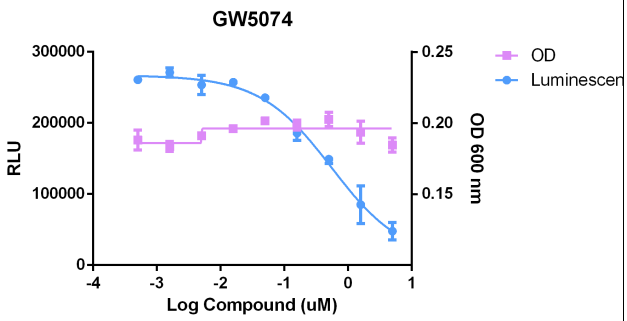 **IC_{50} Luminescence/OD (79-94 min) (µM)** = 0.5546 **IC_{50} OD (µM)** = ~0.005028	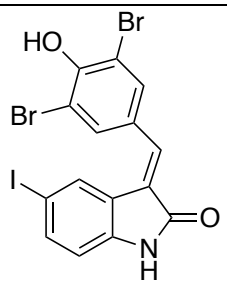	N/A
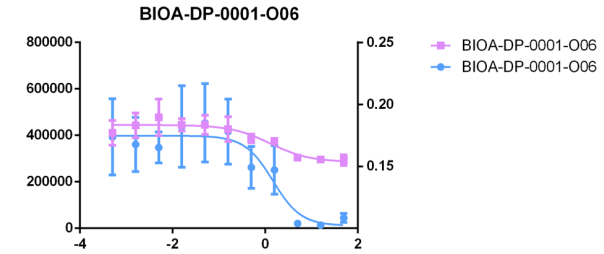 **IC_{50} Luminescence/OD (79-94 min) (µM)** = 1.086 **IC_{50} OD (µM)** = ~87.77	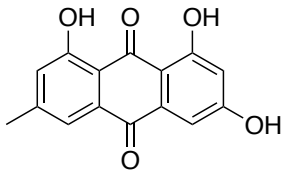	N/A
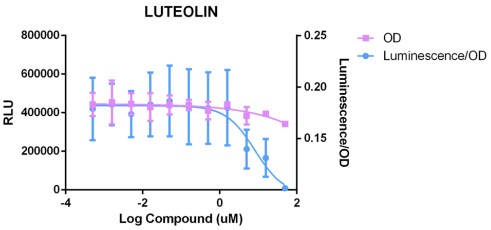 **IC_{50} Luminescence/OD (79-94 min) (µM)** = 8.246	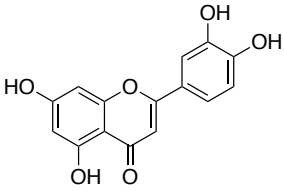	Luteolin is a naturally-occurring flavonoid, with anti-oxidant and anti-inflammatory properties. While the biological target

IC_{50} OD (µM) = 1.50E+12		is unknown, spectroscopic studies have shown that luteolin intercalates with ssDNA more than dsDNA.[58]
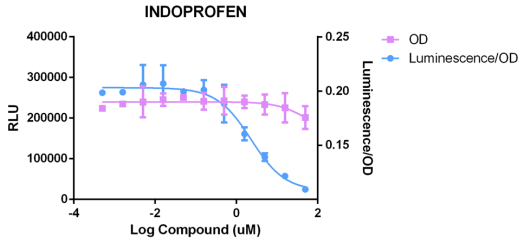 **IC_{50} Luminescence/OD (79-94 min) (µM)** = 2.296 **IC_{50} OD (µM)** = 53.43	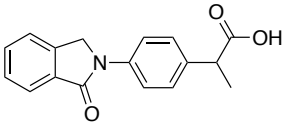	Indoprofen is a nonsteroidal anti-inflamatory drug (NSAID) with analgesic, antipyretic and anti-inflammatory properties. It has been shown to inhibit cyclooxygenase (COX), which blocks the synthesis of prostaglandins.[59]
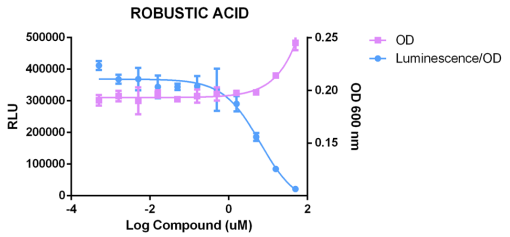 **IC_{50} Luminescence/OD (79-94 min) (µM)** = 6.326 **IC_{50} OD (µM)** = ~2502	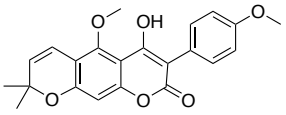	Robustic acid is a potent insecticide and piscicide that targets mitochondrial electron transport at site I (NADH dehydrogenase).[60]
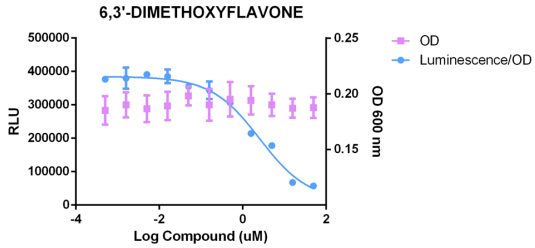 **IC_{50} Luminescence/OD (79-94 min) (µM)** = 2.561 **IC_{50} OD (µM)** = N/A	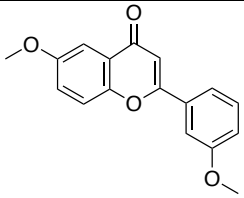	Biological activity is unknown.

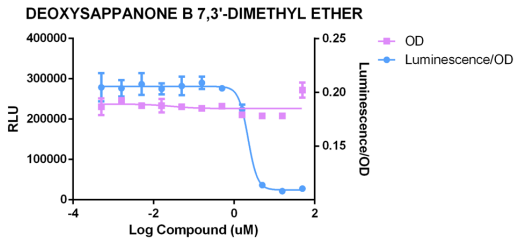 **IC_{50} Luminescence/OD (79-94 min) (µM)** = 2.223 **IC_{50} OD (µM)** = 0.02919	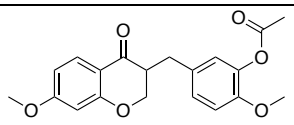	Biological activity is unknown.
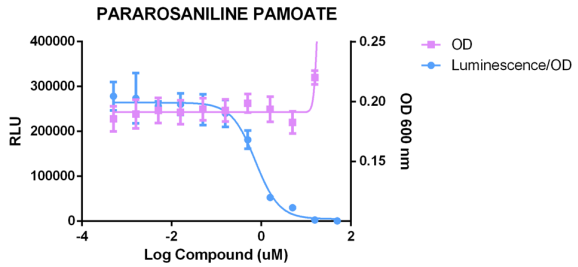 **IC_{50} Luminescence/OD (79-94 min) (µM)** = 0.7391 **IC_{50} OD (µM)** = ~17.59	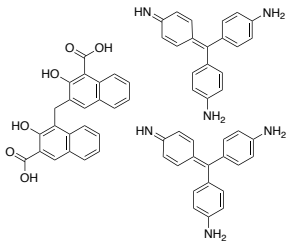	Pararosaniline is a cationic triarylmethane dye and one of the components of basic fuchsin.[61] The pamoate salt of Pararosaniline is better tolerated and produces much less gastrointestinal disturbance than the chloride salt. Research has gone into treating *Schistosoma japonicum* infections. [62]
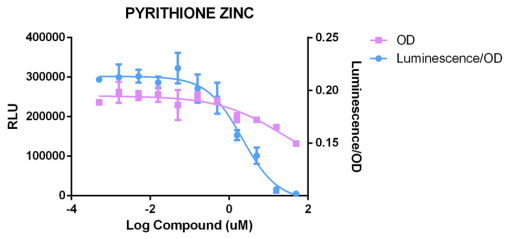 **IC_{50} Luminescence/OD (79-94 min) (µM)** = 2.156 **IC_{50} OD (µM)** = 21.31	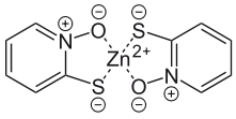	Pyrithione zinc has antifungal activity, which disrupts membrane transport by blocking the proton pump that energizes the transport. It also has bacteriostatic properties. [63]

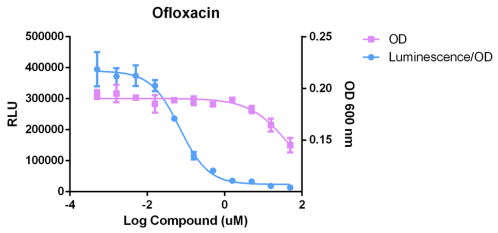 **IC_{50} Luminescence/OD (79-94 min) (µM)** = 0.06863 **IC_{50} OD (µM)** = 43.05	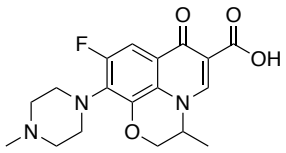	Fluoroquinolone antibiotic that inhibits DNA gyrase and topoisomerase IV.[64]
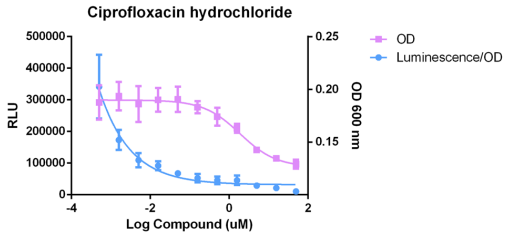 **IC_{50} Luminescence/OD (79-94 min) (µM)** = ~ 3.385e-010 **IC_{50} OD (µM)** = 1.881	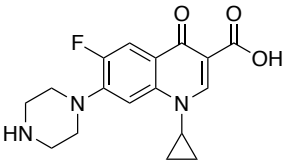	Fluoroquinolone antibiotic that inhibits DNA gyrase and topoisomerase IV. [64]
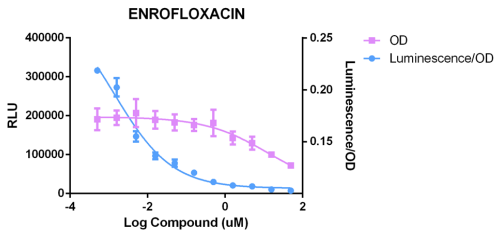 **IC_{50} Luminescence/OD (79-94 min) (µM)** = 72.81 **IC_{50} OD (µM)** = ~132728	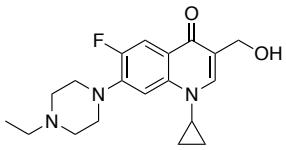	Fluoroquinolone antibiotic that inhibits DNA gyrase and topoisomerase IV. [64]
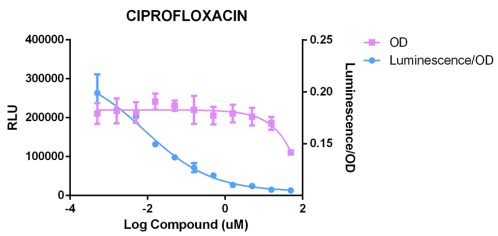 **IC_{50} Luminescence/OD (79-94 min) (µM)** = 0.008578 **IC_{50} OD (µM)** = ~29388	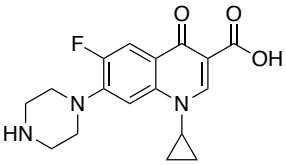	Fluoroquinolone antibiotic that inhibits DNA gyrase and topoisomerase IV. [64]
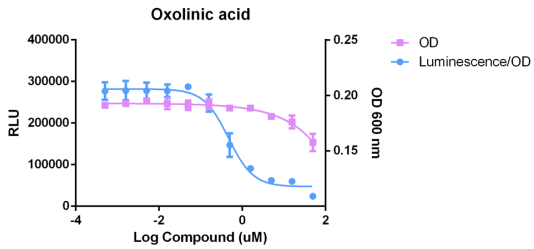 **IC_{50} Luminescence/OD (79-94 min) (µM) = 0.4672** **IC_{50} OD (µM)** = ~ 9.521e+006	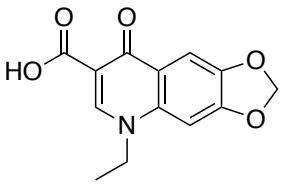	Quinolone antibiotic that inhibits DNA gyrase and topoisomerase IV. [64]

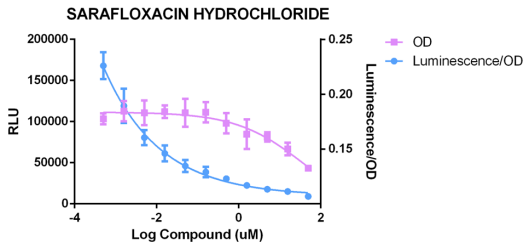 **IC_{50} Luminescence/OD (79-94 min) (µM)** = ~ 1.066e-01 **IC_{50} OD (µM)** = 37.92	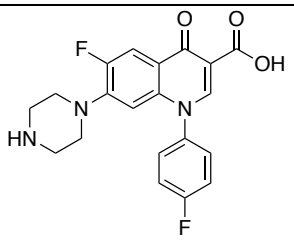	Fluoroquinolone antibiotic that inhibits DNA gyrase and topoisomerase IV. [64]
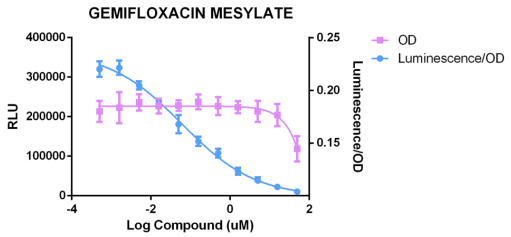 **IC_{50} Luminescence/OD (79-94 min) (µM)** = 0.06165 **IC_{50} OD (µM)** = ~2264	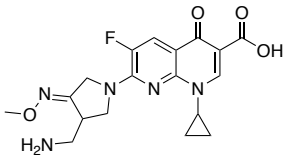	Fluoroquinolone antibiotic that inhibits DNA gyrase and topoisomerase IV. [64]
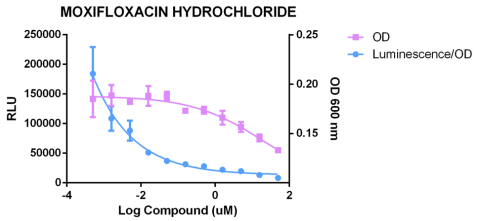 **IC_{50} Luminescence/OD (79-94 min) (µM)** = ~1.451e-011 **IC_{50} OD (µM)** = 18.26	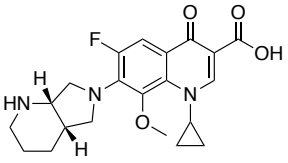	Fluoroquinolone antibiotic that inhibits DNA gyrase and topoisomerase IV. [64]
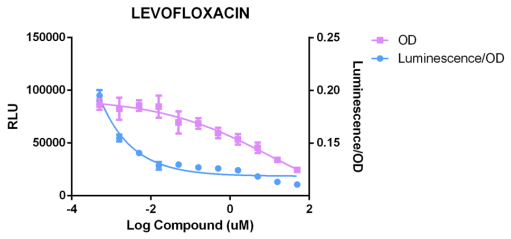 **IC_{50} Luminescence/OD (79-94 min) (µM)** = ~ 7.845e-011 **IC_{50} OD (µM)** = 11.03	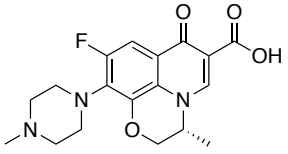	Fluoroquinolone antibiotic that inhibits DNA gyrase and topoisomerase IV. [64]

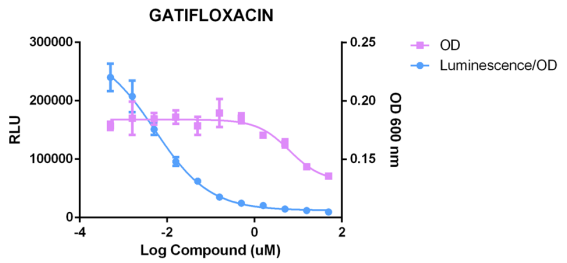 **IC_{50} Luminescence/OD (79-94 min) (µM)** = ~ 0.005289 **IC_{50} OD (µM)** = 6.347	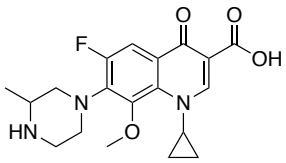	Fluoroquinolone antibiotic that inhibits DNA gyrase and topoisomerase IV. [64]
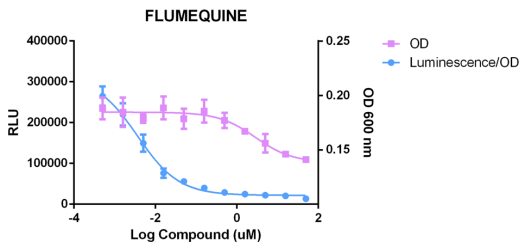 **IC_{50} Luminescence/OD (79-94 min) (µM)** = 0.003697 **IC_{50} OD (µM)** = 2.873	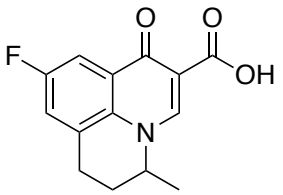	Fluoroquinolone antibiotic that inhibits DNA gyrase and topoisomerase IV. [64]
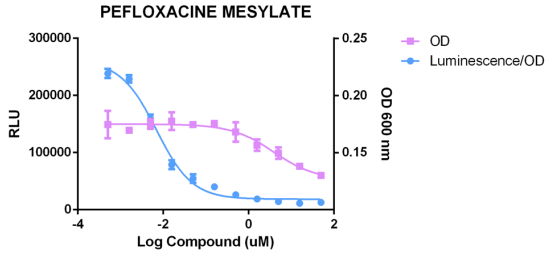 **IC_{50} Luminescence/OD (79-94 min) (µM)** = 0.006972 **IC_{50} OD (µM)** = 3.908	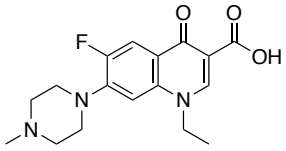	Fluoroquinolone antibiotic that inhibits DNA gyrase and topoisomerase IV. [64]
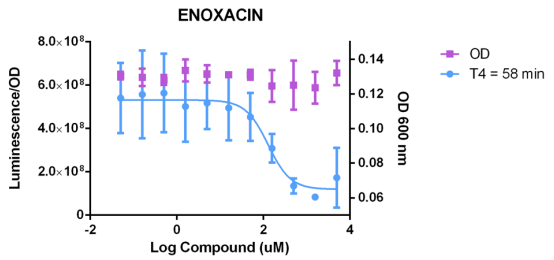 **IC_{50} Luminescence/OD (79-94 min) (µM)** = 2.112 **IC_{50} OD (µM)** = N/A	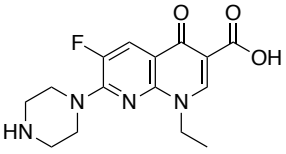	Fluoroquinolone antibiotic that inhibits DNA gyrase and topoisomerase IV. [64]

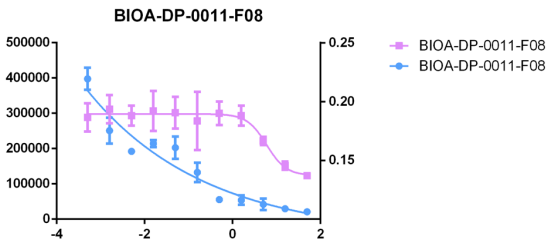 **Norfloxacin** **IC_{50} Luminescence/OD (79-94 min) (µM)** = ~0.0 **IC_{50} OD (µM)** = 5.971	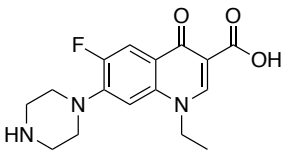	Fluoroquinolone antibiotic that inhibits DNA gyrase and topoisomerase IV. [64]
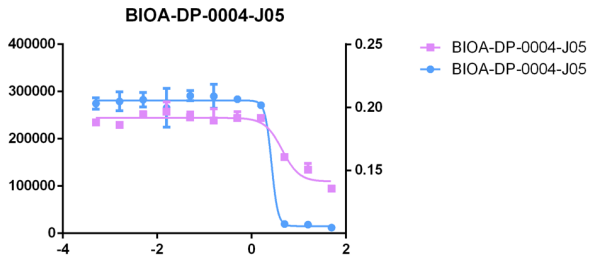 **Lomefloxacin hydrochloride** **IC_{50} Luminescence/OD (79-94 min) (µM)** = ~0.0 **IC_{50} OD (µM)** = 5.971	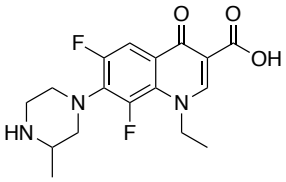	Fluoroquinolone antibiotic that inhibits DNA gyrase and topoisomerase IV. [64]

2.3.4 Fluoroquinolones may indirectly inhibit excision

Fluoroquinolones were the main chemical class hit in the Bioactives library. Dose-response curves demonstrate that fluoroquinolone antibiotics dose-dependently inhibit Tn*1549* excision. Since we know these antibiotics target both DNA gyrase (*gyrA* subunit) and topoisomerase IV (*parC* subunit), it is imperative to establish whether this was a direct effect on the integrase activity or an indirect effect of targeting topoisomerase activity. Topoisomerase activity involves inducing or removing supercoiling. For example, DNA gyrase introduces positive supercoils that accumulate ahead of a translocating DNA polymerase, allowing DNA replication to continue unhindered by topological strain. In the presence of fluoroquinolones, DNA gyrase and topoisomerase IV are inhibited, leading to single and double stranded breaks along the DNA and eventually cell death.

Since DNA gyrase is the major target of fluoroquinolones in bacteria, we generated a 4-fold ciprofloxacin-resistant mutant to evaluate its effects on excision. We screened for mutations in the quinolone resistance determining region of *gyrA* and *parC*. From the colonies screened, we only found a D87Y mutation in *gyrA*. A *gyrA* mutant assay strain was made and tested alongside the wild type assay strain to compare the effect of fluoroquinolones on excision. The DNA gyrase mutant strain displayed dose-dependent inhibition of excision in the presence of ciprofloxacin (**Figure 2-6a**) but the IC_{50} curve shifted towards higher concentrations of inhibitor. The ratio of IC_{50} concentrations reflects the fold-change in MIC values between the wildtype and mutant assay strains (**Table 2-1**). This pattern was also observed for ofloxacin and levofloxacin in the *gyrA* mutant strain (**Figure 2-6a, Table 2-1**). Since more antibiotic is required to inhibit excision in the *gyrA* mutant strain, this result may indicate that the transposition inhibition phenotype is the effect of fluoroquinolones inhibiting DNA gyrase. Alternatively, if fluoroquinolones are directly targeting the integrase, then a decrease in GyrA affinity would make ciprofloxacin more potent because there would be more compound available to bind to the integrase. However, our experiments do not suggest this effect.

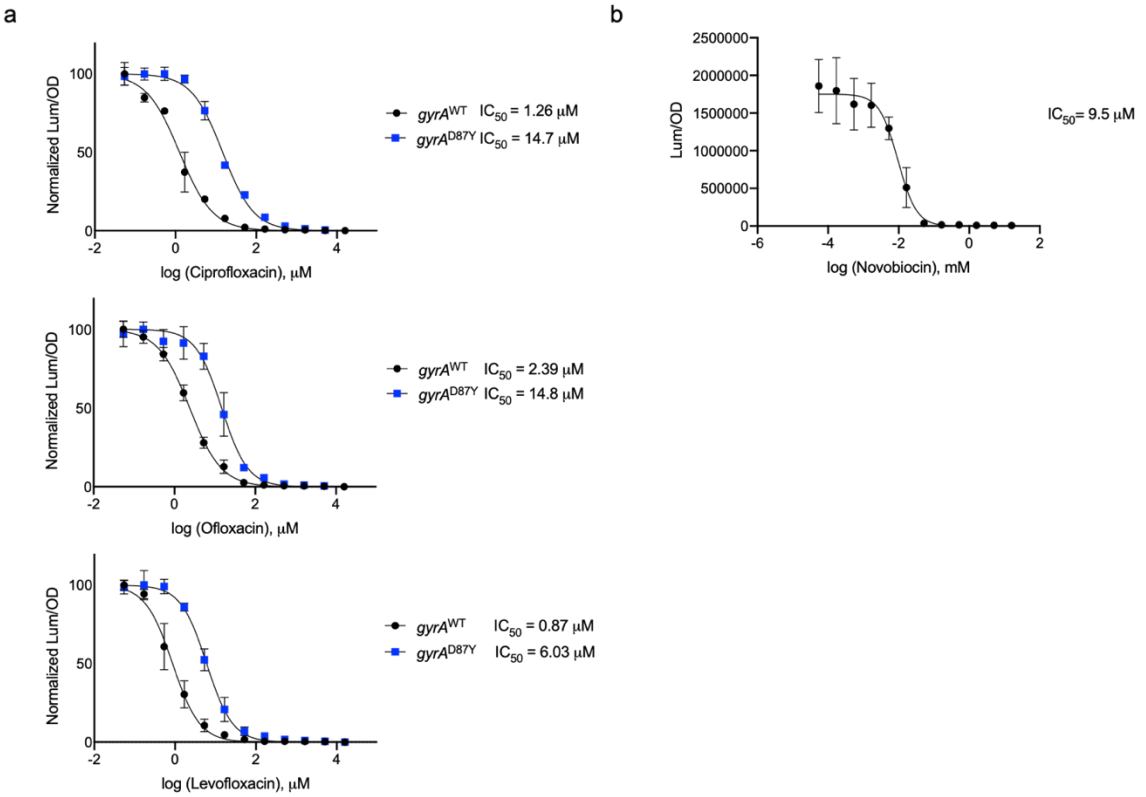

Figure 2-6: DNA gyrase inhibitors can indirectly inhibit Tn*1549* excision.
a) Fluoroquinolones target the *gyrA* subunit of DNA gyrase. Several fluoroquinolones have dose-dependent relationships with both the original assay and a *gyrA* mutant. The *gyrA* mutants have a higher dose-response value, which is proportional to the change in MIC values. b) Novobiocin has a dose-dependent relationship with the wild type assay showing decreasing Lum/OD activity over increasing concentrations. Novobiocin targets ATPase activity in the *gyrB* subunit of DNA gyrase. IC_{50} values are defined as the concentration of compound that reduces the signal (Lum/OD) by 50%.

Table 2-2: MIC values of the original assay versus the *gyrA* mutant assay of several fluoroquinolones.
The minimum inhibitory concentration (MIC) is the lowest concentration of a compounds that prevents visible growth of a bacteria.

Antibiotic	*E. coli* BW25113 Δ*bamB*Δ*tolC* Assay (µg/ml)	*E. coli* BW25113 Δ*bamB*Δ*tolC gyrA* Assay (µg/ml)
Ciprofloxacin	0.004	0.016
Levofloxacin	0.004	0.06
Ofloxacin	0.008-0.016	0.03

With a point mutation in *gyrA* (D87Y), we showed that excision of mini-Tn*1549* was dose-dependent in the presence of ciprofloxacin and that the difference between the wild-type and mutant *gyrA* assays was proportional to the MIC. We wanted to test if a similar effect was seen with other fluoroquinolone-resistance elements. We tested QnrA1, a pentapeptide repeat protein that blocks fluoroquinolones from binding to DNA gyrase. There was a dose-dependence relationship between ciprofloxacin and excision in the presence of QnrA1 (**Figure 2-7)**. The 10-fold increase in IC_{50} value was similar with the change in MIC as well (**Table 2-2**). Overall, these results provide further support that the transposition inhibition phenotype of fluoroquinolones is dependent on inhibiting DNA gyrase and that excision inhibition is independent of Int.

To provide further evidence to point to indirect excision inhibition as the mechanism, we tested novobiocin, an antibiotic that inhibits ATPase activity in the *gyrB* subunit of DNA gyrase. Novobiocin caused dose-dependent inhibition of Tn*1549* excision **(Figure 2-6b)**. Thus, the effects are not specific to *gyrA*, but to DNA gyrase itself. Therefore, DNA gyrase is likely the target of excision inhibition.

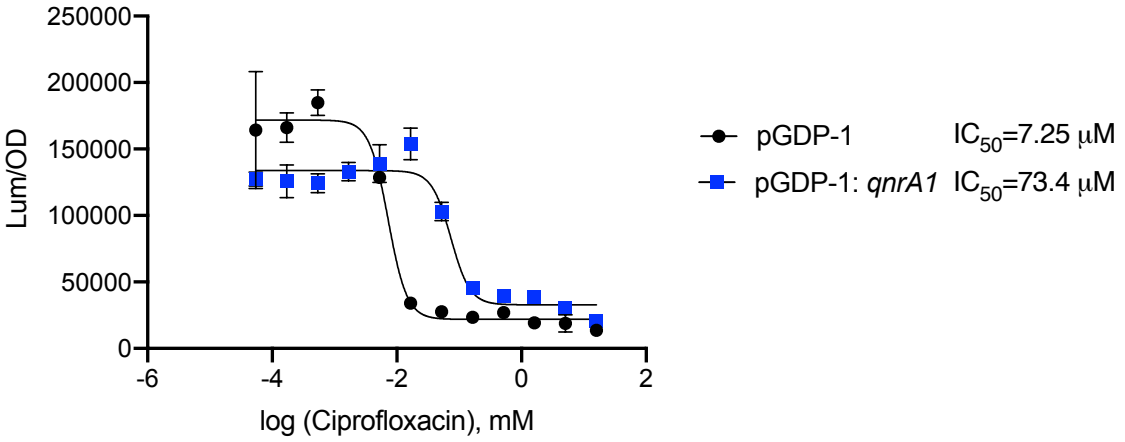

Figure 2-7: Tn*1549* Excision Assay with QnrA1.
E. coli TOP10 containing pGDP-1:*qnrA1*, TEMP, and TPEP was compared to *E. coli* TOP10 containing pGDP-1, TEMP, and TPEP. Luminescence readings were standardized to the OD_{600} values and were measured over various concentrations of ciprofloxacin in triplicate.

Table 2-3: MICs of Fluoroquinolone Resistance Elements.

Strain	Ciprofloxacin (μg/ml)
E. coli BW25113 Δ*bamB*Δ*tolC* Assay	0.004
E. coli TOP10	0.008-0.016
E. coli TOP10 Assay with pGDP-1: *qnrA1*	0.12
E. coli TOP10 Assay with pGDP-1	0.008

2.3.5 Excision is not dependent on induction of the SOS response

Fluoroquinolones alter supercoiling levels and activate the SOS response through dsDNA breaks, whereas novobiocin ~~only~~ alters supercoiling through inhibition of GyrB in DNA gyrase. Since we have determined previously in **Figure 2-6** that both fluoroquinolones and novobiocin can dose-dependently inhibit excision, sharing in common the ability to change supercoiling levels, we wanted to test whether the fluoroquinolone's indirect mechanism of transposition inhibition was also dependent on

the SOS response. RecA is the recombinase that initiates the SOS response, so we used a RecA+ strain (*E. coli* BW25113 Δ*bamB*Δ*tolC*) and a RecA- strain (*E. coli* TOP10) to test our hypothesis. As shown in **Figure 2-8**, both RecA+ and RecA- strains had a dose dependent inhibition signal with ciprofloxacin and novobiocin. The main difference between the two strains is about a 10-fold difference in maximum signal and higher intrinsic resistance against fluoroquinolones in *E. coli* TOP10 (**Table 2-4**). Since both RecA+ and RecA- strains exhibit dose-dependent inhibition of excision, RecA is not likely involved in the mechanism of inhibition.

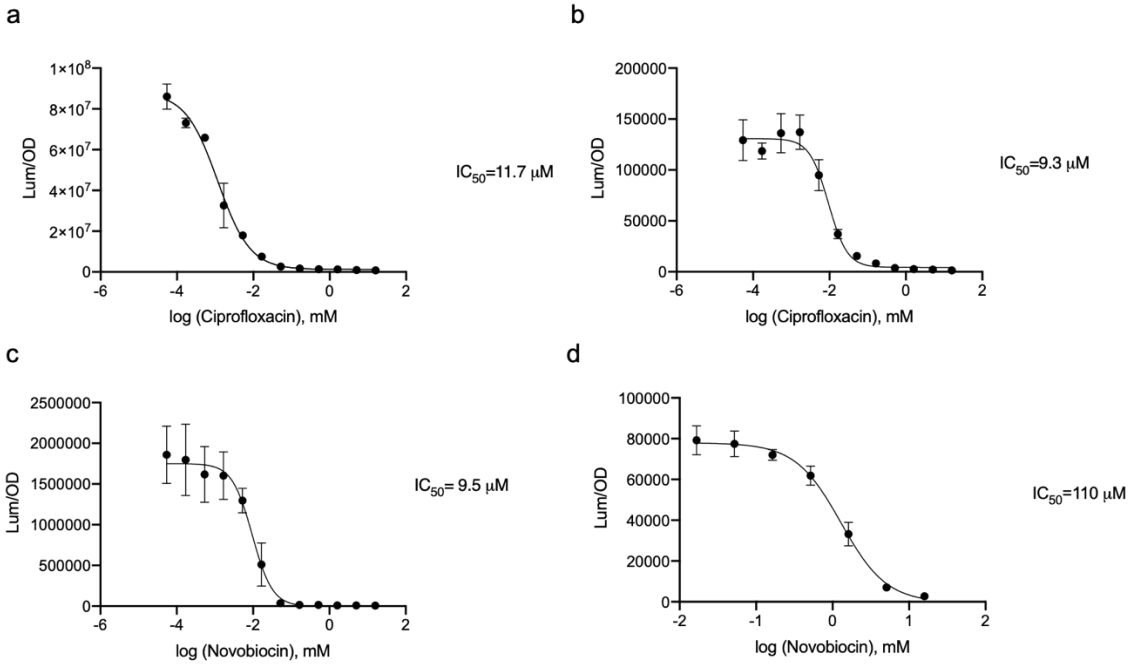

Figure 2-8: Luminescence/OD signal is not dependent on the presence of RecA.
The y-axis is the luminescence over optical density at 600nm and the y-axis is a range of concentrations of ciprofloxacin. a) *E. coli* BW25113 Δ*bamB*Δ*tolC* is a *recA*+ strain with an IC_{50} value of 11.7 μM for ciprofloxacin. b) *E. coli* TOP10 is a *recA*- strain with an IC_{50} value of 9.3 μM for ciprofloxacin. c) *E. coli* BW25113 Δ*bamB*Δ*tolC* is a *recA*+ strain with an IC_{50} value of 9.5 μM for novobiocin. d) *E. coli* TOP10 is a *recA*- strain with an IC_{50} value of 110 μM for novobiocin. Error bars represent the standard deviation of 3 replicates.

Table 2-4: MICs of *E. coli* TOP10 and *E. coli* BW25113 Δ*bamB*Δ*tolC*.

Antibiotic	*E. coli* BW25113 Δ*bamB*Δ*tolC* (μg/ml)	*E. coli* TOP10 (μg/ml)
Ciprofloxacin	0.004	0.008-0.016
Levofloxacin	0.004	0.016
Ofloxacin	0.008-0.016	0.06

2.3.6 Ciprofloxacin decreases luciferase reporter activity

Another alternative explanation to transposition inhibition by fluoroquinolones is that changes in supercoiling prevent transcription of luciferase. As determined in the initial assay development, the control strain has background luminescence signal caused from transcription read-through from $P_{tac.}$ To test this hypothesis, the control strain (TEMP) was tested in the presence of ciprofloxacin, with and without IPTG induction of P_{tac} for luciferase transcription. **Figure 2-9** shows that both the induced and uninduced control strain has background luminescence that decreases dose-dependently with increasing ciprofloxacin concentration. Considering fluoroquinolones alter supercoiling, it is likely that transcription is affected dose-dependently from the presence of ciprofloxacin. However, these data do not exclude the possibility that fluoroquinolones indirectly inhibit excision.

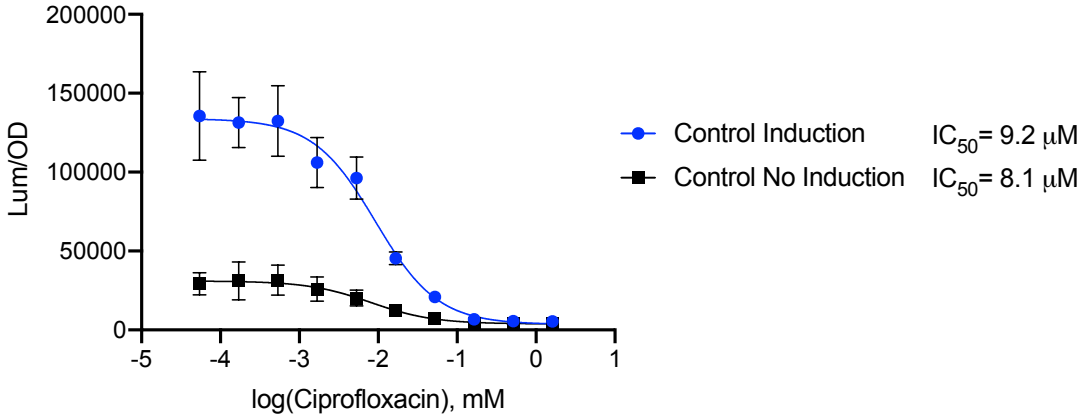

Figure 2-9: Ciprofloxacin changes the expression of the luciferase reporter.
The control strain, *E. coli* BW25113 Δ*bamB*Δ*tolC* containing TEMP, is without Int and Xis that remove mini-Tn*1549* present on TEMP. TEMP contains the luciferase reporter under the control of a tac promoter with mini-Tn*1549* between the two. The control strain was induced (blue with circles) or uninduced (black with squares) with IPTG for 4 hours in the presence of ciprofloxacin. The IC_{50} value of the control induction was 9.2 μM (0.006268 to 0.01307μM with a 95% CI) and the IC_{50} value of the control without induction is 8.1 μM (0.003671 to 0.01797 μM with a 95% CI). Error bars represent the standard deviation of 3 replicates.

2.3.7 Ciprofloxacin both enhanced conjugation at sub-MIC levels and decreased conjugation frequency

Conjugation tests were done to test our hypothesis that fluoroquinolones inhibit excision and subsequent conjugation of Tn*1549*. *E. faecalis* 268-10 carrying Tn*1549* was used as the donor and *E. faecalis* JH2-2 acted as the recipient. MIC tests were conducted to identify an antibiotic that could be used to select for transconjugants (**Table 2-5**). Fusidic acid was used as the marker since the recipient strain was 4 times more resistant than the donor. Conjugation of Tn*1549* in the presence of various concentrations of ciprofloxacin showed a decreased in conjugation frequency (**Figure 2-10**), validating our hypothesis. In addition, there was an apparent increase in conjugation frequency at sub-MIC concentrations (0.03125 and 0.125 μg/ml) (**Figure 2-10**). While we know that the SOS response does not change excision (**Figure 2-8**), whether it enhances conjugation frequency

through activating the SOS response or the induction of several conjugation related genes is unknown.[65]

Table 2-5: MICs of *E. faecalis* 268-10 and *E. faecalis* JH2-2 against various antibiotics

Antibiotic	*E. faecalis* 268-10 (μg/ml)	*E. faecalis* JH2-2 (μg/ml)
Streptomycin	256-512	>512
Rifampin	>400	>400
Ciprofloxacin	2	2
Trimethoprim	>500	<0.25
Fusidic acid	64	256
Vancomycin	128	4
Blasticidin	64-128	64
Moenomycin	0.25	0.125
Gentamicin	256	32
Ampicillin	8	4
Chloramphenicol	8	4

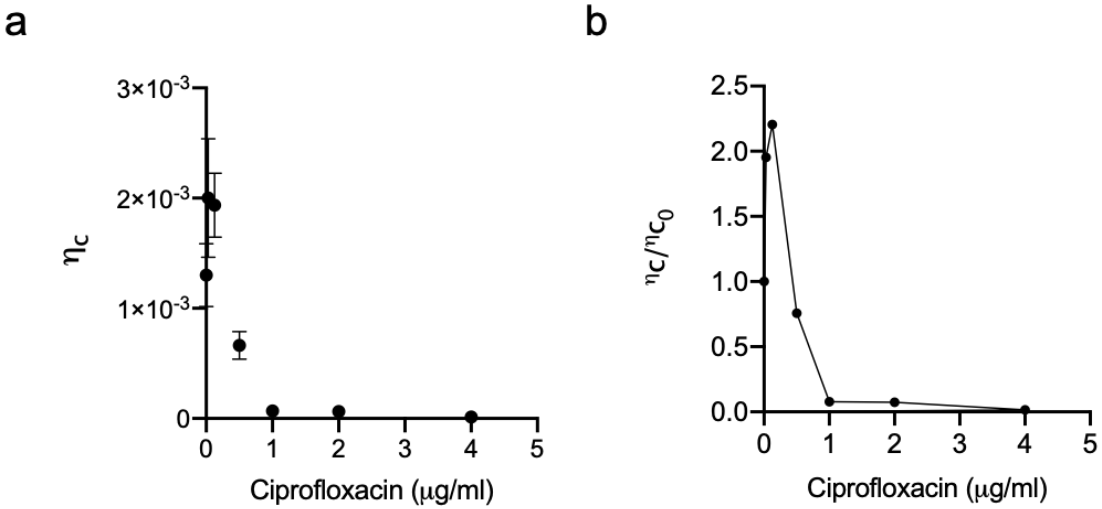

Figure 2-10. Sub-inhibitory concentrations of ciprofloxacin increased conjugation frequency and decreased conjugation frequency at higher concentrations.
E. faecalis 268-10 containing Tn*1549* was used as the donor and *E. faecalis* JH2-2 was used as the recipient. a) Conjugation frequency (η_c) was plotted over various ciprofloxacin concentrations above, at, and below the MIC of donor and recipients (2 μg/ml). Error bars represent the standard deviation of 3 replicates. b) Conjugation frequency of each ciprofloxacin concentration (η_c) was divided by the conjugation frequency without ciprofloxacin present ($^{\eta}c_0$) over various ciprofloxacin concentrations above, at, and below the MIC of donor and recipients (2 μg/ml). For both graphs, the conjugation frequency is increased at sub-inhibitory

concentrations of ciprofloxacin and the conjugation frequency starts to decrease after 0.125 µg/ml of ciprofloxacin. Conjugation frequency was calculated by taking the average of CFU count of transconjugants and dividing by the average CFU count of recipients.

2.3.6 Secondary Screens to identify Off-Target Hits

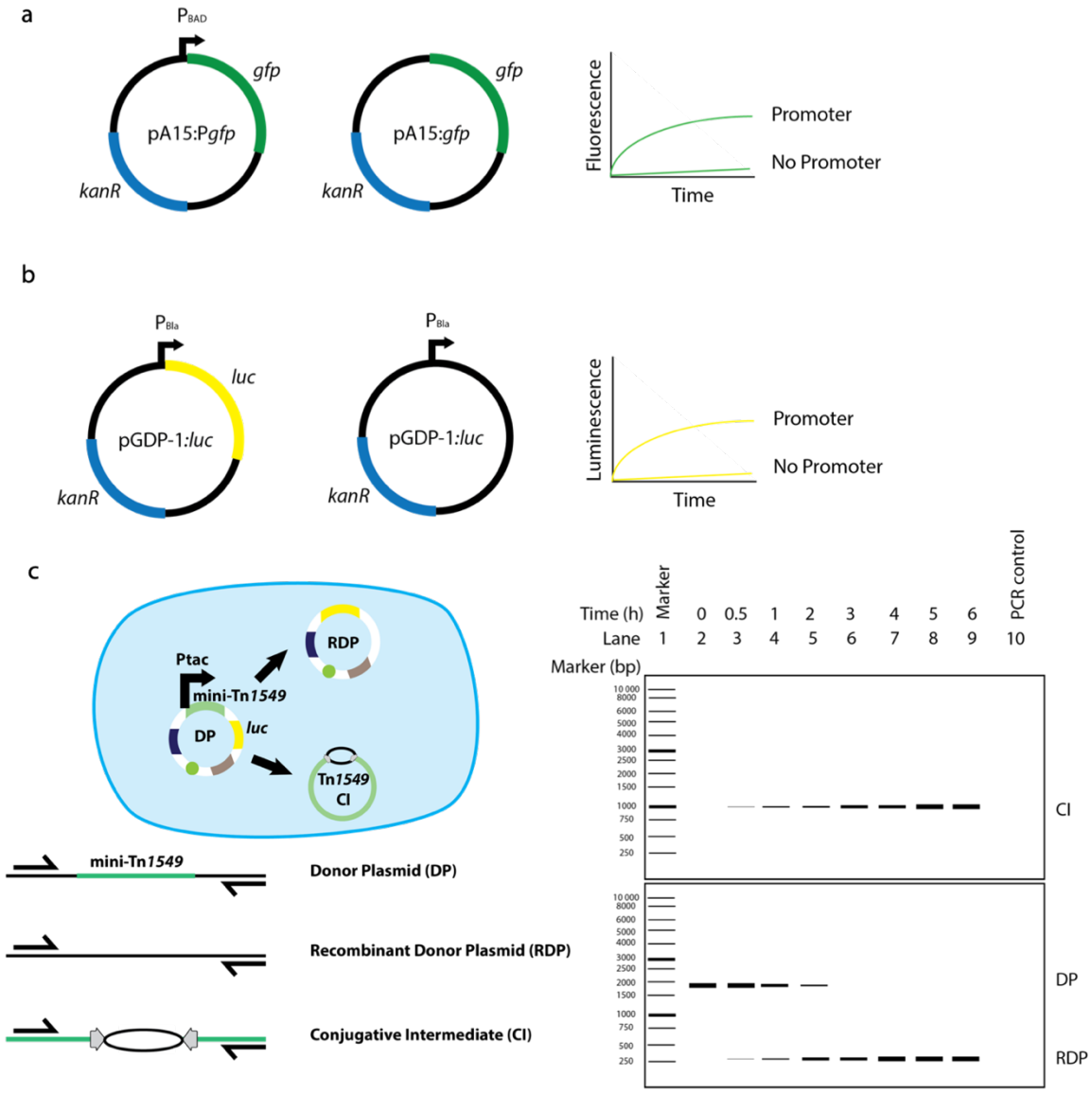

Figure 2-11: Secondary assays to validate primary screening hits.
a)Arabinose transporter inhibition assay This assay is based on the idea that arabinose can be blocked going into a cell and lead to less excision. A construct with a GFP reporter with (pA15:P*gfp*) and without an arabinose promoter (pA15:*gfp)* will be used to monitor compounds inhibiting arabinose transport. b) Luciferase inhibition assay will be used to check if a compound inhibits luciferase activity by comparing an

empty vector without luciferase (pGDP-1) to a vector carrying luciferase (pGDP-1: *luc*). c) The PCR products of the donor plasmid (DP), recombinant donor plasmid (RDP), and conjugative intermediate (CI) were monitored over time and visualized on an agarose gel to determine if there are differences in intermediates compared to the untreated assay.

Secondary assays were designed to filter out non-specific compounds, such as pan-assay interference compounds (PAINs) or compounds that intercalate with DNA. The first secondary assay is designed to identify compounds that inhibit luciferase activity (**Figure 2-11b**). The chemical reaction catalyzed by firefly luciferase requires oxygen, luciferin, and ATP to produce light. Britelite plus contains detergent to lyse the assay cells, as well as excess ATP and luciferin substrate required for luciferase activity. Thus, the assay will detect compounds that directly inhibit luciferase since all components are in order. As shown in **Figure 2-12**, the luciferase inhibition assay is still in development as there is currently no difference in signal between *E. coli* TOP10 containing pGDP-1:*luc* and an empty pGDP-1 vector.

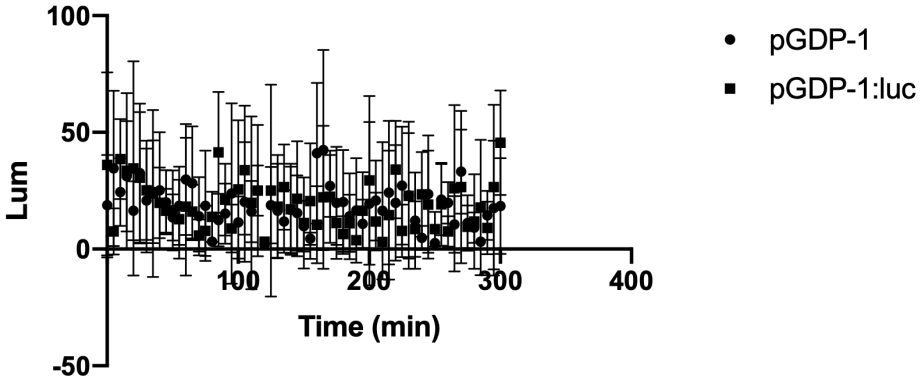

Figure 2-12: Luciferase inhibition assay.
E. coli TOP10 containing empty vector pGDP-1 (circle) was compared to *E. coli* TOP10 containing pGDP-1:*luc* (square).

There is also the potential that a compound blocks arabinose transport into the assay cells leading to less expression of Int/Xis and excision of the mini-Tn*1549*. To model this, we engineered a construct with an arabinose promoter to control GFP expression (**Figure 2-11a**). Thus, if a compound inhibits arabinose transport into the cell, GFP expression will be reduced.

The third secondary assay will be used to confirm if the products of excision are present or absent with a given compound (**Figure 2-11c**). In theory, PCR amplification of the donor plasmid (DP), recombinant donor plasmid (RDP), and conjugative intermediate (CI) can be used to monitor these products before and after the assay with compounds (**Figure 2-11c**). Primers were designed to flank the mini-Tn*1549* in the DP, the lack of the mini-Tn*1549* in RDP, and the transposon flanking DNA for the CI. As an example, we monitored the PCR products of the control strain, assay strain, and the assay strain treated with ciprofloxacin over time. In **Figure 2-13a**, there are faint bands at 1500 bp of DP for the assay strain and ciprofloxacin-treated assay strain beyond time 0 as expected. However, a strong DP band is visible at around 3000 bp, which may indicate that the CI is able to integrate into TEMP with the mini-Tn*1549* present, doubling the size of the PCR product. The RDP is faintly seen for the assay samples (~250 bp) (**Figure 2-13a**). In **Figure 2-13b**, the CI is seen after time 0 for both the assay strain and ciprofloxacin-treated assay strain. Whereas the control assay does not have the CI present (~450 bp). The ciprofloxacin-treated assay strain had a noticeably dimmer band than the assay strain counterpart. However, treating the assay with various concentrations of ciprofloxacin will determine if this result is meaningful.

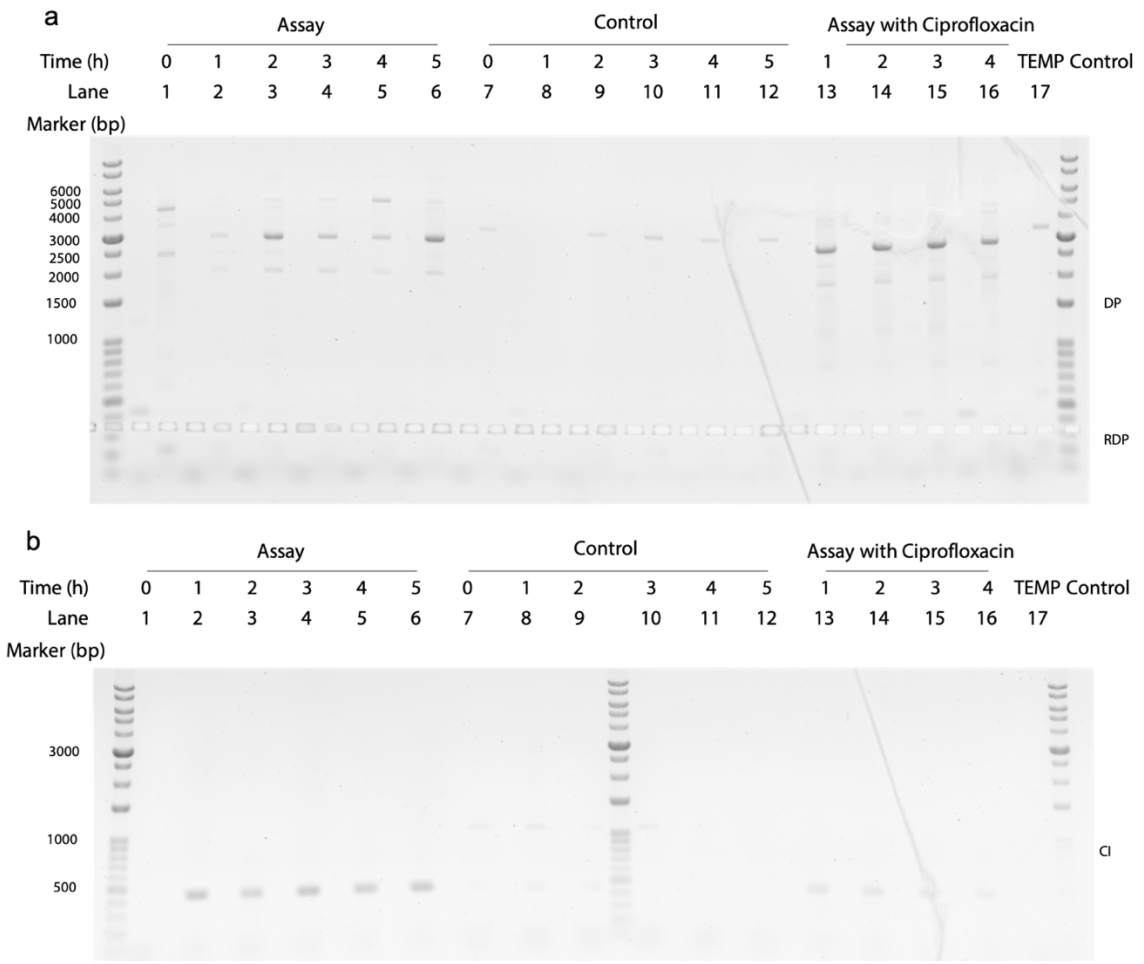

Figure 2-13: PCR excision assay of various time points in the assay.
The PCR products of donor plasmid (DP), recombinant donor plasmid (RDP), and conjugative intermediate (CI) were monitored. The assay and control samples were monitored for 5 hours, and the ciprofloxacin treated assay was monitored for 4 hours. A concentration of ciprofloxacin was added (0.08 μg/ml) such that it was above the IC_{50} value, but before a decrease in cell death in the assay conditions. a) DP and RDP bands are located around 1500 bp and 250 bp, respectively. B) The CI band is located around 500 bp.

2.3.7 Secondary assay to identify specific hits

In vivo Tn*1549* assay to measure excision

As with the PCR excision assay, we wanted to measure the *in vivo* activity of the assay. Instead of using PCR, we scaled up the assay and isolated plasmid intermediates. We tested the control, assay, and ciprofloxacin-treated assay strains overtime to visualize

the changes in DNA intermediates (**Figure 2-15**). There were no clear differences between the assay and assay treated with ciprofloxacin, except for a potential decrease in concentration of DNA in the treated condition. In the future, time points between 0 and 60 minutes will be explored to identify changes early on in the excision process. The expected banding patterns in **Figure 2-14** were found in **Figure 2-15** with several additional bands around 2000 and 3000 that likely represent a CI with an additional CI integrated into it. This hypothesis can be checked by isolating and sequencing the DNA intermediate.

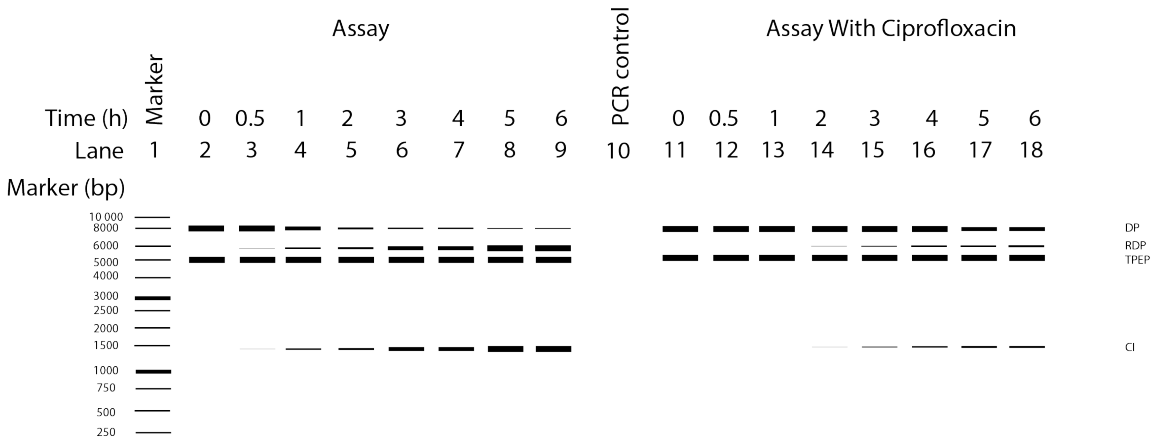

Figure 2-14: *In vivo* mini-Tn*1549* excision assay expected results.
Based off of the excision assay, the reactants (donor plasmid, DP) and products (recombinant donor plasmid, RDP and conjugative intermediate, CI) are extracted and visualized on an agarose gel. The expected results are that the assay with ciprofloxacin has delayed excision of Tn*1549*.

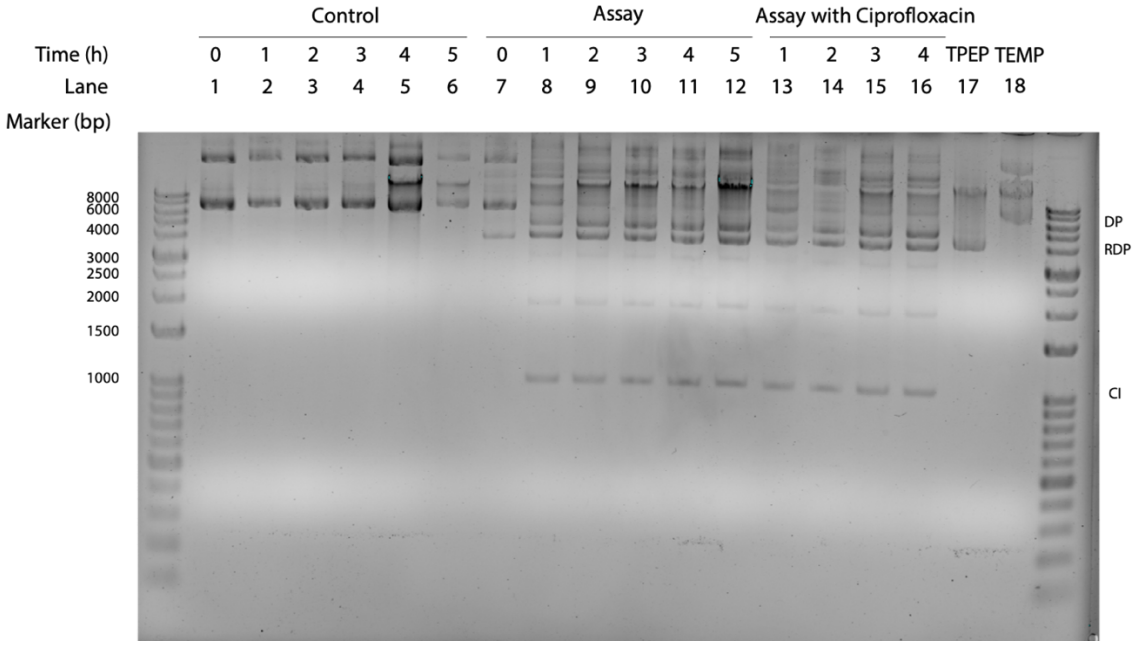

Figure 2-15: DNA isolated from assay, control, and ciprofloxacin-treated assay conditions at various time points.
The PCR products of donor plasmid (DP), recombinant donor plasmid (RDP), and conjugative intermediate (CI) were monitored over time. The assay and control samples were monitored for 5 hours (hr), and the ciprofloxacin treated assay was monitored for 4 hours. A concentration of ciprofloxacin was added (0.08 μg/ml) such that it was above the IC_{50} value, but before a decrease in cell death in the assay conditions. DP and RDP bands are located around 1500 bp and 250 bp, respectively. The CI band is located around 500 bp.

In vitro testing of Integrase activity with fluoroquinolones

The gold standard for testing the specificity of an enzyme is using *in vitro* assays. Since we know that the luciferase reporter is sensitive to changes in supercoiling, it was necessary to test whether Int is too. This experiment was a proof of principle test to determine whether integrase activity is dependent on the supercoiled state of the substrate. The first step to do this experiment is to separate the supercoiled substrate into various topoisomers using chloroquine gels. Chloroquine will insert into the DNA and unwind the double helix. This process converts highly negatively supercoiled topoisomers into less supercoiled ones, allowing their resolution in a gel. Topoisomers with various levels of

supercoiling can be extracted and used as a substrate to measure if Int activity is dependent on the supercoiling level of the substrate. The initial optimization steps in substrate preparation are found in **Figure 2-16**. The next steps would be to purify Int and Xis to test the *in vitro* activity against different topoisomers and visualize the reaction on an agarose gel. *In vitro* experiments with fluoroquinolones or other hits present can be used to determine if they specifically inhibit Int or Xis with a regular supercoiled substrate.

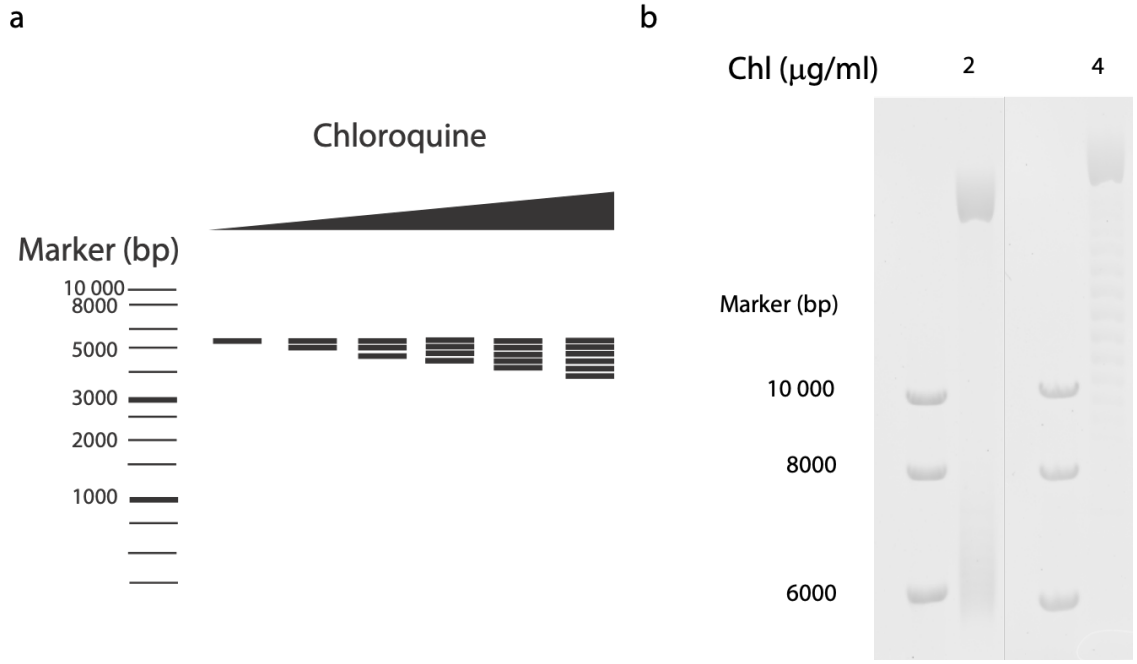

Figure 2-16: TEMP substrate preparation.
a)DNA substrates of varying degrees of supercoiling will be prepared in various concentrations of chloroquine gels. From left to right, each lane represents the expected banding pattern of the same supercoiled DNA sample run in different gels with increasing concentrations of chloroquine. b) Chloroquine gels were used to separate TEMP into various topoisomers. Chloroquine (Chl) was added to 1% agarose gels, 2 μg/ml on the left and 4 μg/ml on the right gel. Gels were run at 4V/cm for 30 hours at 4°C.

2.3.8 Screening Tn*1549* excision assay against a library of prefractionated natural products

After successfully screening the Bioactives library, the Tn*1549* excision assay was screened against the prefractionated library (PFL) (**Figure 2-17**). The PFL is a growing collection of 382 microbial extracts separated into 8 methanolic fractions each, along with the crude extract and conditioned media control (**Figure 2-2)**. The two main benefits of this library are increasing hits compared to screening crude extracts only and compound solubility is known based on the fraction. Like the Bioactives screen hit cut off, we defined a hit as below 2SD of the mean normalized luminescence over optical density of both replicates for all compounds in the library. Moving forward, hits will need reconfirmation and further characterization to identify inhibitors of conjugative transposition.

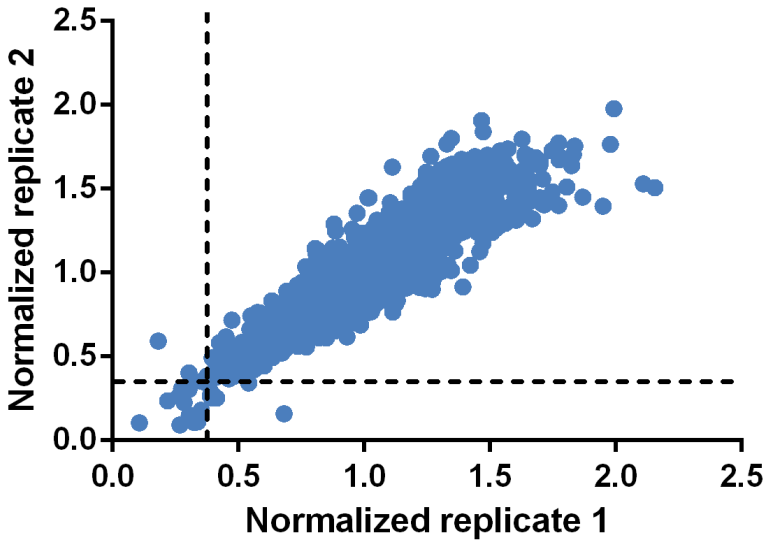

Figure 2-17: PFL Screen replica plot.
Compounds were screened in duplicate and have two luminescence data points normalized to the x and y axes. For this data set, hits were defined below 2SD of the mean normalized luminescence over optical density of both replicates.

2.4 Discussion

2.4.1 Tn*1549* Excision Assay Screening

This research focused on identifying specific inhibitors that can prevent AMR gene transfer. We directed our efforts to target Tn*1549*, a conjugative transposon that is linked to the emergence of VRE in clinical isolates. We designed an assay to model the excision step in CTn movement by targeting the two key molecular targets (Xis/Int) involved in this process. This assay was successfully validated and screened against the Bioactives and PFL. The PFL initial follow up and hit re-confirmation is currently in progress. As for the Bioactives screen, 24 promising hits were obtained with dose-dependent activity. 14 of the 24 hits belong to the fluoroquinolone class of antibiotics and will be discussed in the next section. The other 10, in addition to the fluoroquinolone hits will need to be validated against the three secondary assays outlined in **Figure 2-11.**

While we have not been successful in identifying specific hits against Int or Xis, this assay has been fully validated and can be used to screen more compound libraries to find specific hits. However, given that the Tn*1549* excision assay is the first of its kind built to identify compounds that target conjugative transposons, the chemical space is largely unexplored. Like with antibiotics, in the search for compounds that inhibit MGEs, it may be useful to look in natural product sources. Our hypothesis is that microbial secondary metabolites have been selected by evolution to modulate bacterial gene transfer. MGEs are ancient so it is possible that bacteria have developed secondary metabolites that either increase or inhibit gene transfer.[66,67] Similarly, many natural product compounds have been

found that have targeted the conjugation step in the movement of conjugative plasmids.[37,38] Rubio-Cosials et al. designed an antagonistic peptide to the active site of Int to block *in vitro* activity as a proof of principle.[68] Despite the lack of early success in finding new compounds that inhibit conjugative transposition, we found that fluoroquinolones indirectly inhibited excision in this assay.

2.4.2 Fluoroquinolones in Gene Transfer

Fluoroquinolones acted as dose-dependent hits in secondary screening, so to test if they were specific to the excision process or targeting DNA gyrase and inhibiting excision through an indirect mechanism, we developed a *gyrA*^{D87Y} mutant assay strain and compared dose-response curves (**Figure 2-6a**). Dose-response curves displayed a shift to higher concentrations of inhibitor in the *gyrA*^{D87Y} assay. The differences in MIC and IC_{50} values of *gyrA*^{D87Y} and *gyrA*^{WT} change by a similar factor (**Table 2-2** and **Figure 2-6**). This trend was consistent for ciprofloxacin, levofloxacin, and ofloxacin. Given that there is a relationship between the changes in MIC and IC_{50} values in the *gyrA*^{D87Y} and *gyrA*^{WT} assays, we hypothesize that ciprofloxacin is targeting GyrA instead of Int. In the *gyrA*^{D87Y} assay, more ciprofloxacin would have been available to bind Int from fewer interactions in GyrA than the *gyrA*^{WT} assay. If Int was the true target, we would expect a decrease in the IC_{50} value relative to the changes in MICs we observed with a GyrA mutation.

A single point mutation in *gyrA* can lead to a significant increase in excision in the presence of equivalent ciprofloxacin concentrations. While a *gyrA* point mutation is one mechanism of fluoroquinolone resistance, we wanted to investigate if these observations held for another mechanism. We tested the protein QnrA1, which protects DNA gyrase

from interacting with fluoroquinolones. A collection of Qnr proteins have been identified worldwide, mostly in Gram-negative bacteria. Qnrs are pentapeptide repeat proteins, likely originating in aquatic organisms. These proteins act as DNA mimics, by decreasing the binding of DNA gyrase and topoisomerase IV to DNA. By binding DNA gyrase and topoisomerase IV Qnrs inhibit quinolones from entering cleavage complexes formed by the enzymes.[69] Testing the QnrA1 assay strain against an equivalent wild-type assay strain we see the same relationship between MIC and IC_{50} values as the *gyrA* experiment **Figure 2-7**). Another fluoroquinolone resistance mechanism uses AAC(6')-Ib-cr, which is an enzyme that can acetylate aminoglycosides, in addition to a free piperazinyl amine found in ciprofloxacin and norfloxacin.[70] This enzyme is present on a plasmid and has rapidly spread among *Enterobacteriaceae*.[71] These resistance elements have the potential to mitigate the inhibition of MGE transfer by protecting the cells, which can help give the MGE a chance to propagate.

The significance of fluoroquinolones involved in indirectly inhibiting excision is related to the presence of fluoroquinolone resistance transfer through MGEs. If fluoroquinolones prevent gene transfer, the fitness of a mobile genetic element would increase by carrying these resistance elements. In addition, when fluoroquinolones are used clinically to treat bacterial infections, they have a secondary benefit of indirectly inhibiting resistance gene transfer. Some bacteria possess transmissible resistance elements that confer resistance to fluoroquinolones and carry other resistance mechanisms.[72,73]

As discussed above, GyrA is dependent on the excision inhibition phenotype seen in the presence of fluoroquinolones, which lead to dsDNA breaks and altered supercoiling.

To isolate the mechanism that fluoroquinolones use to inhibit excision, we tested novobiocin because it inhibits ATPase activity in the *gyrB* subunit of DNA gyrase only leading to changes in supercoiling. In **Figure 2-6b**, we see that novobiocin has dose-dependent inhibition of Tn*1549* excision. This result validated that the effects are not specific to *gyrA*, but to DNA gyrase itself. In addition, this result also validated our hypothesis that altered supercoiling levels led to changes in excision, which were determined to be independent of the SOS response (**Figure 2-8).** This provides evidence that changes in supercoiling may indirectly inhibit excision.

In the presence of fluoroquinolones, DNA gyrase is inhibited and cannot introduce negative supercoils into DNA and dsDNA breaks occur, leading to cell death.[74] While fluoroquinolones certainly target DNA gyrase, the downstream targets have two possible effects. The first possibility is that the integrase is dependent on DNA supercoiling in its function, which is not known at the moment. The second hypothesis is that the supercoiling changes induced by fluoroquinolones prevent Xis from properly interacting with DNA and lead to a significantly reduced excision.[41,75] We suggest that changes in supercoiling likely affect both integrase and excisionase function. To understand if the integrase is dependent on DNA supercoiling, DNA from the Tn*1549* excision assay can be isolated in the presence and absence of fluoroquinolones and visualized on various chloroquine gels. If the integrase function is supercoiling dependent, then more or less supercoiled mini-Tn*1549* will not be excised, leading to differences in the abundance of conjugative intermediates (**Figure 2-15**). *In vitro* assays can test various TEMP topoisomers (i.e. **Figure 2-16**) using Int with and without Xis to test the changes in efficiency of excision.

In addition to modulating ICE transfer, fluoroquinolones and aminocoumarin antibiotics are effective plasmid curing agents.[76,77] Theoretically, plasmid curing agents are dependent on the concentration of compound and not on *gyrA* mutation. Therefore, one would expect no difference between the two conditions. During our assay, plasmids were maintained through antibiotic selectable markers, making the possibility of plasmid loss unlikely.

Another alternative explanation to transposition inhibition by fluoroquinolones is that changes in supercoiling prevent transcription of luciferase in a dose dependent manner. To test this hypothesis, the control strain (TEMP) was tested with fluoroquinolones and with and without IPTG induction of P_{tac} for luciferase transcription. The control strain exhibited a dose-dependent response in Lum/OD as observed for the assay strain (**Figure 2-6** and **Figure 2-9**). This assay can be used to determine compounds with off target effects. For example, if a compound inhibits luciferase or if the compound changes transcription of either the luciferase reporter or Int/Xis. While we have shown that luciferase transcription is affected by ciprofloxacin in a dose-dependent manner, it does not exclude the possibility that ciprofloxacin can also indirectly or directly inhibit excision. An experiment using *E. coli* BW25113 Δ*bamB*Δ*tolC* with the TEMP plasmid without the mini-Tn*1549* can be used to determine the magnitude ciprofloxacin has on excision versus changing the transcription of the reporter or Int/Xis. However, biochemical experiments directly testing Int/Xis with fluoroquinolones present will be useful to separate these effects.

Although we have not yet identified specific inhibitors of MGE, these results are promising for additional screens. The Tn*1549* excision assay can be customized to find

inhibitors against other integrases involved in resistance dissemination. To date, there are no other screens that have reported inhibitors of integrases involved in conjugative transposition.

We provided evidence that fluoroquinolones may indirectly inhibit excision, and potentially gene transfer. However, fluoroquinolones, in addition to tetracyclines, have been shown to enhance gene transfer as well.[78–81] Subinhibitory concentrations of ciprofloxacin can indirectly promote excision and conjugation of SXT ICE from *Vibrio cholerae* through SOS induction.[78,79] In contrast, the rate of conjugative transposition in *Bacteroides* spp. and *Enterococcus faecalis* increased through an SOS-independent mechanism in the presence of low concentrations of tetracycline.[80,81] When fluoroquinolones are used to treat infections, they have the mixed benefit of potentially promoting gene transfer and the formation of MDR pathogens while preventing gene transfer.

Since we isolated the excision step in our Tn*1549* assay, it was important to test ciprofloxacin against the full Tn*1549* element to see if ciprofloxacin inhibited conjugation. We showed that the conjugation frequency of Tn*1549* decreased in the presence of various concentrations of ciprofloxacin (**Figure 2-10**). These findings validated our hypothesis that ciprofloxacin decreases the conjugation frequency beyond excision. In addition, at sub-MIC concentrations (0.03125 and 0.125 μg/ml) there was an apparent increase in conjugation frequency (**Figure 2-10**). While we know that the SOS response does not change excision (**Figure 2-8**), it is unknown whether it enhances conjugation frequency through activating the SOS response or the induction of several conjugation related genes.[65]

Other antibiotics will be tested in the future to determine if this effect is specific to fluoroquinolones.

Biochemical experiments will need to be performed to define the relationship between fluoroquinolones and integrases. However, looking at their mechanism of action and comparing them to a related enzyme, DNA gyrase, provides molecular insights into the potential interaction between the integrase and fluoroquinolones. The main similarities between these two enzymes are that they both use DNA as substrates and use a catalytic tyrosine residue for nucleophilic attack on the DNA backbone. DNA gyrases however require ATP in their reaction and create dsDNA breaks to introduce negative supercoils (**Figure 2-18**), whereas tyrosine recombinases only need to introduce ssDNA breaks for recombination (**Figure 2-19**). It is known that fluoroquinolones stabilize dsDNA breaks induced by DNA gyrase and change global supercoiling levels in the cell. Based on our findings and the literature, ciprofloxacin may be either indirectly inhibiting excision by changing the supercoiled state of the substrate that the Integrase binds or directly inhibiting Int by stabilizing the HJ intermediate and preventing the resolution of excision.

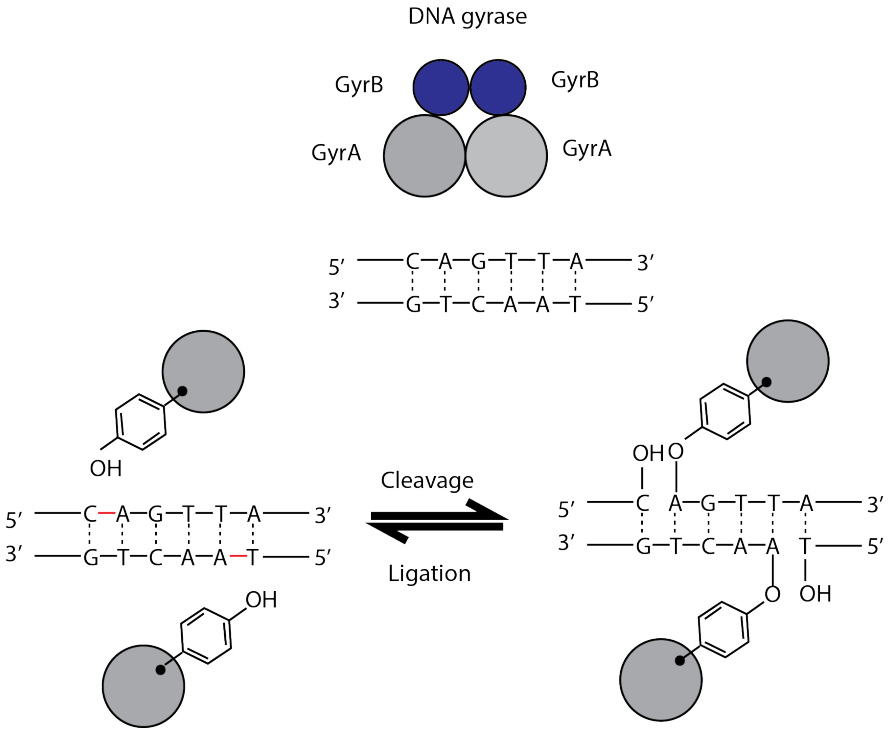

Figure 2-18: Mechanism of DNA gyrase.
DNA gyrase is a tetrameric enzyme that consists of 2 GyrA (gray oval) and 2 GyrB (purple oval) subunits. The GyrA subunit contains a catalytic tyrosine nucleophile responsible for creating staggered dsDNA breaks, which are necessary to introduce negative supercoils into dsDNA. GyrB contains an ATPase subunit that hydrolyzes ATP to power this process.

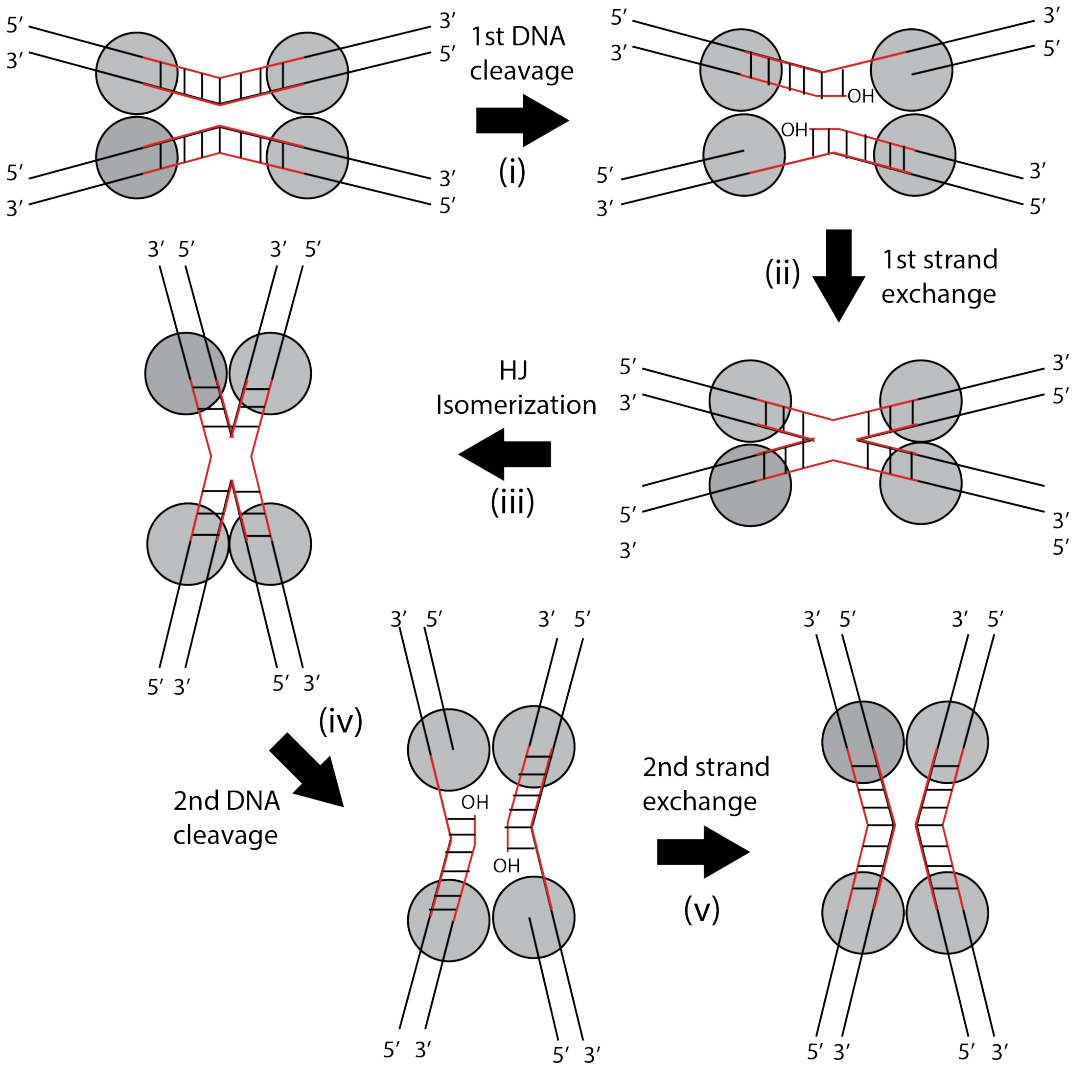

Figure 2-19: Mechanism of Tyrosine Recombinases
Tyrosine recombinases (gray ovals) recombine DNA in a stepwise fashion. (i) First, two tyrosine recombinase dimers bind dsDNA and cleave one strand of each dsDNA using a tyrosine nucleophile. This creates a covalent a 3'-phosphotyrosyl bond (black bots) and a free 5'-hydroxyl (5'OH) group; (ii) each free 5'OH group attacks the opposite 3'-phosphotyrosol bond, making a four-way Holliday junction (HJ) intermediate; (iii) The HJ intermediate isomerizes triggering the second protein pair to cleavage (iv) and exchange (v) the other DNA strands, generating the final recombined products. ATP-independent strand exchange is dependent on homology in the dsDNA substrates (red). Figure was adapted from Rubio-Cosials et al.[68]

2.4.3 Future Work and Conclusions

This work serves as the foundation for future work and screening to find novel inhibitors of ICEs, such as CTns. First, secondary assays for on-target and off-target effects will be used to identify hits. The next step would be to test hits against the full Tn*1549* element in enterococci to evaluate the efficacy of inhibitors. In addition, existing structural information for Int bound to DNA intermediates will be used to logically design probes with higher specificity.[68]

Ciprofloxacin and other fluoroquinolones are unlikely to be used to prevent the transfer of MGEs because it puts a selective pressure on bacteria to become resistant and potentially transfer AMR genes. These antibiotics are routinely used in the armamentarium available to medical practitioners. However, their use is declining in certain cases because of the threat of spontaneous resistance.

In addition, it will be important to test the effects of common antibiotics against these MGEs to see if they promote, reduce or have no effect on transfer. Furthermore, it would be useful to test if MGE inhibitors or enhancers have a significantly change the transmission of AMR genes in an animal model.[82] The efficacy of a potential inhibitor will need to be validated in animal models to have a real-world application.

By targeting key MGEs, we will gain a greater understanding of which compounds influence their movement in the environment. This is critical to monitoring and preventing the formation of MDR pathogens in livestock and hospitals. For example, *C. difficile* is a pathogen that is a leading cause of antibiotic-associated diarrhea with few classes of effective antibiotics remaining.[83] Treatment of MDR *C. difficile* relies on the antibiotic

vancomycin as an effective first line treatment and clinical isolates are commonly susceptible.[84] However, the ability to evade vancomycin may soon arise in *C. difficile* considering Tn*1549* carries a vancomycin resistance cassette and can transfer to *C. difficile*.[85] This scenario could be prevented through small molecule inhibition.

In conclusion, our research demonstrated that we can target excision responsible for the movement of the AMR genes. These molecules can potentially be used to prevent the transmission of antibiotic resistance genes and the emergence of MDR pathogens. However, much work is needed to turn these goals into reality.

Chapter 3.

Developing a High Throughput Conjugation Assay to Screen for Novel Conjugation Inhibitors

3.1 Introduction

Conjugation, the process by which a donor cell transfers DNA to a recipient cell through direct cell-to-cell contact to form a transconjugant, was first reported by Tatum and Lederberg in 1946 and has since been extensively studied. As the most common mechanism of antimicrobial resistance (AMR) gene transfer, understanding the underlying molecular biology and regulation of transfer is important in preventing the dissemination of AMR genes and the formation of multi-drug resistant (MDR) pathogens. Furthermore, as the body of sequencing data grows, both the role of MGEs in bacterial evolution as well as their diversity become increasingly clear. It is especially concerning to consider the potential MGEs to transfer AMR genes.

Several MDR pathogens with MGEs carrying AMR genes are currently problematic and the emergence of new 'superbugs' is likely to continue in the future. To prevent further spread of AMR genes, our goal is to find small molecule inhibitors of conjugation without antimicrobial properties by using a high throughput conjugation assay to screen libraries of small molecules and microbial extracts.

Previous high throughput conjugation assays are presented in **Figure 3-1**. Both assays use R388, an F plasmid derivative, but differ in their reporter. The first uses a *lux* reporter on a mobilizable plasmid that is repressed in the donor strain through LacI repression, and derepressed in the transconjugant from the absence of LacI (**Figure 3-1a**).

The second uses a GFP reporter on a mobilizable plasmid under the control of a T7 promoter, which can only be expressed after transfer to the transconjugant with induction of T7 Polymerase (**Figure 3-1b**). These were the first assays used to screen for conjugation inhibitors (COINs), however, in our assay design we made several improvements. Our system uses the F plasmid, which is well researched, and the regulation is understood. The F plasmid is related to many other elements and carries several resistance elements.[86]The assay works by transferring a mobilizable plasmid containing a portion of the *lux* operon through conjugation into a recipient strain containing the complementary part. By splitting up the *lux* operon this nullifies the requirement for the leaky repressor system (LacI), which increases sensitivity by reducing background luminescence from donor cells and only getting signal in the transconjugants. Our design has the benefit of not using an inducer (i.e. IPTG) and luminescence is more sensitive than GFP fluorescence. Since *lux* is highly sensitive, we can potentially find enhancers of conjugation in addition to conjugation inhibitors (COINs). This chapter outlines the progress of building and testing a high throughput conjugation assay and considerations to fully develop this assay.

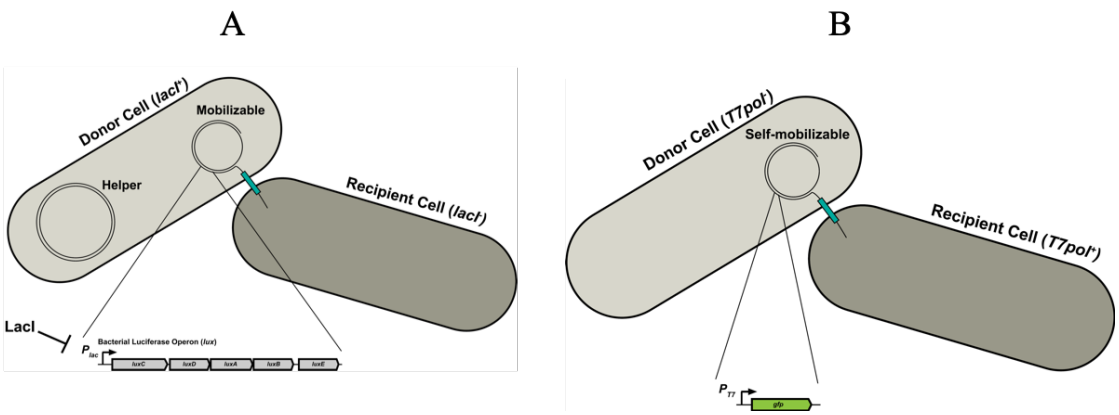

Figure 3-1: Previously reported High Throughput Conjugation Assays.
a) This assay models R388, a conjugative plasmid. A non-transferable, R388 helper plasmid mobilizes a co-resident plasmid containing the *lux* operon. The expression of the *lux* operon is repressed in the donor cell by the *lac* repressor (LacI) acting on the *lac* promoter. After conjugation, the *lux* operon is expressed to only visualize transconjugants.[37] b) This assay uses a self-mobilizable plasmid (R388) containing a GFP reporter under a T7 promoter. This reporter is only expressed in recipient cells that have the T7 RNA polymerase (induced by IPTG) for exclusive fluorescence in transconjugants. Figure illustrations made by Matthew Surette.

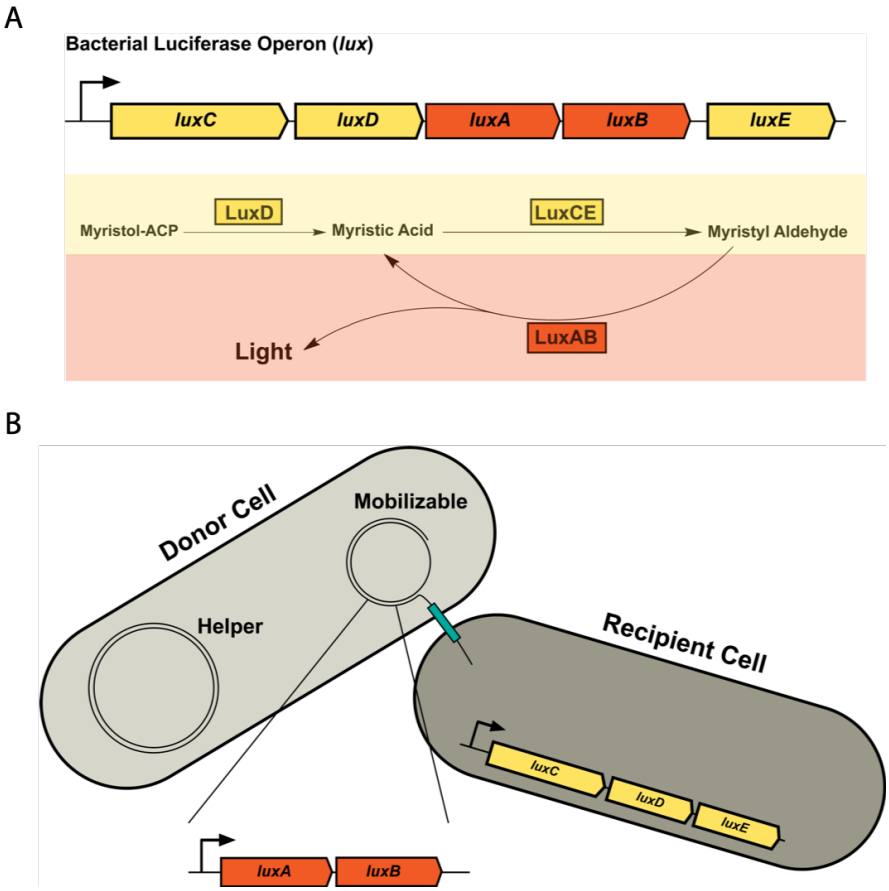

Figure 3-2: High Throughput Conjugation Assay Design
a) The *lux* operon (*luxCDABE*) light production pathway. The substrate is myristyl aldehyde and the product is myristic acid. The reaction forms an excited hydroxyflavin intermediate, and emits blue-green light once the intermediate is dehydrated into flavin mononucleotide (FMN).[87]
b) The donor cell contains a helper plasmid (F' with a chloramphenicol resistance marker inserted into the *oriT*) which facilitates conjugal transfer of a mobilizable plasmid (pCSCDE) to a recipient cell (F-). Once the mobilizable plasmid is transferred to the recipient cell, the full *lux* operon is expressed, and luminescence is visualized only in transconjugants. Figure illustrations made by Matthew Surette.

3.2 Materials and Methods

All primer sequences used in the following protocols can be found in Appendix 2.

3.2.1 Donor Strain Construction

The mobilizable reporter plasmids, pCSAB and pCSCDE, were constructed through Gibson assembly according to NEB guidelines. pCSAB is made up of PCR

amplicons of pBla from pINT-1, *oriT* from the F plasmid in *E. coli* JM105, *luxAB* from pCS26-Pac, and a fragment containing a terminator for *luxAB* transcription extending through the kanamycin cassette from pCS26-Pac (**Figure 3-3**). pCSCDE is made up of PCR amplicons of pBla from pINT-1, *oriT* from the F plasmid in *E. coli* JM105, *luxCD* from pCS26-Pac, and a fragment starting from *luxE* extending through the kanamycin cassette from pCS26-Pac (**Figure 3-3**). Fragments were purified using a Thermo Scientific PCR purification kit according to the protocol, where *oriT* PCR reaction purification using an isopropanol step was used to obtain a higher yield. For each Gibson assembly reaction, the fragments were ligated using a backbone to insert molar ratio of 3:1. The reaction also contained 2X GA buffer (**Appendix 1**) and nuclease free water. The Gibson assembly reaction was carried out for 1 hr at 50°C in a Thermocycler (SimpliAmp Thermo Cycler, Thermo Fisher). 1 µl of a 3-fold dilution of the Gibson reaction was added to 50 µl of electrocompetent *E. coli* TOP10 cells and electroporated. The reaction was transferred to a 1.5 ml Eppendorf tube with 950 µl of SOC media and placed in a shaking incubator (250 rpm) at 37°C for 1 hr. Transformations were plated on 50 µg/ml kanamycin and incubated at 37°C overnight. pCSCDE was verified through digestion (**Figure 3-3b**) and the MOBIX sequencing facility at McMaster University was used to verify that no mutations were present between fragments.

In the donor strain *E. coli* XL Blue, a chloramphenicol resistance marker (chloramphenicol acetyltransferase, *cat*) knocked out a portion of the *oriT* found in the F' plasmid. This modification turned the F' into a helper plasmid used to mobilize the reporter plasmid. Insertion was accomplished using the Wanner integration method.[88] First, primers

were designed to have regions of homology on the *oriT* that would knockout the *nic* site found in the F' plasmid. *cat* was amplified off of pLysS flanked with regions of homology from the *oriT* and purified using a PCR gel purification kit. Primers were made using PAGE ultramer^{TM} DNA oligo (IDT, McMaster University). pKD46 was electroporated into *E. coli* XL Blue. *E. coli* XL Blue containing pKD46 was grown in the presence of arabinose to induce production of λ Red recombinase and made electrocompetent. 400 ng of the amplicon was electroporated into these cells. Transformations were grown overnight at 37°C to remove the pKD46 plasmid on LB agar plates supplemented with 33 mg/ml of chloramphenicol. Colony PCR of overnight colonies was used to determine successful integration of the chloramphenicol cassette in the *oriT* of the F' plasmid.

3.2.2 Recipient Strain Construction

The first step to integrate *lux* genes into *E. coli* was clone pINT-1 plasmids containing those genes.[88,89] pINT-1: *luxAB* was made by amplifying *luxAB* from pCS26-Pac. pINT-1 and *luxAB* were digested using *Nde*I and *Xho*I, and gel purified. pINT-1 and *luxAB* were then ligated overnight at room temperature using T4 DNA ligase (Thermo Scientific). pINT-1: *luxCDE* was made by amplifying *luxCD* and *luxE* from pCS26-Pac. These amplicons were ligated using Gibson Assembly and transformed into *E. coli* TOP10. pINT-1: *luxAB* and pINT-1: *luxCDE* were verified through digestion (**Figure 3-5**) and the MOBIX sequencing facility at McMaster University verified that no mutations were present. PCR was used to amplify a product containing the *lux* genes and a removable kanamycin cassette, flanked by *polB* and *araC*. *E. coli* BW25113 Δ*tolCΔbamB* was transformed with pKD46. *E. coli* BW25113 Δ*tolCΔbamB* containing pKD46 was grown in

the presence of arabinose to induce production of λ Red recombinase and made into electrocompetent cells. The amplicon (200 ng) was then electroporated into *E. coli* BW25113 Δ*tolC*Δ*bamB* cells expressing the recombinase and grown at 37°C in the presence of 25 mg/ml of kanamycin overnight. Successful integrations were determined using colony PCR.[88]

Table 3-1: Strain list for high throughput conjugation assay

Strain	Construct	Resistance Marker	Notes
E. coli XL Blue	F′, Mutated *oriT*, pCSCDE	Chloramphenicol, Kanamycin	Donor for proposed assay
E. coli XL Blue	F′, pCSCDE	Kanamycin	Donor
E. coli BW25113 Δ*bamB*Δ*tolC*	Integrated *luxAB* into arabinose operon	Kanamycin	Recipient for proposed assay
E. coli TOP10		Rifampin	Frequency mating recipient
E. coli TOP10	pCS26*lux*:C6	Kanamycin	Low
E. coli TOP10	pCS26*lux*:C10	Kanamycin	Medium
E. coli TOP10	pCS26*lux*:C35	Kanamycin	Hight

3.2.3 Testing Luminescence Production of Conjugation Assay Strains

A donor and a recipient strain were streaked on separate halves of the same LB agar plate with overlap in the middle to facilitate conjugation. The donor strain was *E. coli* XL Blue containing F′ with an *oriT* knockout and pCSCDE. The recipient strain was *E. coli* BW25113 Δ*bamB* Δ*tolC* with *luxAB* integrated into the arabinose operon. The plate was grown overnight in a stationary incubator at 37°C. The plate was then visualized with an Ivis instrument. Several controls were used to show varying levels luminescence from the bacterial luciferase reporter in *E. coli* TOP10 (pCS26*lux*:C6, low, pCS26*lux*:C10, medium,

pCS26*lux*:C35, high) based on promoter strength. Controls were grown on LB agar plates supplemented with 50 μg/ml of kanamycin. Controls were provided by Dr. Michael Surette (McMaster University).

3.2.4 Testing Conjugation Efficiency

To test the conjugation efficiency, overnights of the donor strains (*E. coli* XL Blue containing wildtype F′ and pCSCDE or F′ with an *oriT* knockout and pCSCDE) and the recipient (*E. coli* TOP10 rifampin resistant strain) with appropriate antibiotics were incubated at 37°C with shaking (250 rpm). The OD_{600} was measured in the three overnights. 1 ml of each overnight was centrifuged (6000*g* for 3 min), spent media discarded, and the cell pellet resuspended in LB media with no antibiotic to standardize the OD_{600} among samples. The donor and recipients (100 μl of each) were mixed in a 1:1 ratio and plated on a LB agar plate with no antibiotic in 15 μl droplets. The plates were incubated overnight without shaking at 37°C for 20 hrs. 1ml of LB was then added to plates to suspend the colonies. Eight 1:10 serial dilutions of the inoculum were made with LB and 10 μl of each dilution was plated in triplicate on 40 μg/ml of rifampin (Recipients) and 50 μg/ml kanamycin and 40 μg/ml rifampin (Transconjugant) plates. Plates were incubated overnight without shaking at 37°C for 16 hrs. Pictures of plates were taken with the Epson Scanner. Conjugation frequency is calculated with the following formulas.

$$\frac{Cfu}{ml} = \frac{\#\ of\ colonies}{volume} \times dilution\ factor$$

$$Conjugation\ efficiency = \frac{cfu\ of\ transconjugants}{cfu\ of\ recipients + cfu\ of\ transconjugants} \times 100$$

3.3 Results

3.3.1 Assay Overview and Assembly

When designing an assay for high throughput conjugation, it is important to quantitatively visualize conjugation in real-time and to distinguish transconjugants from donor and recipient cells. We decided to use the *lux* operon from *Photorhabdus luminescens*. This well-studied system is quantitative, sensitive, and can be measured in real-time.[87] The genes producing bioluminescence are located on an operon comprised of five genes, *luxCDABE*. LuxA and LuxB form luciferase, whereas LuxC, LuxD and LuxE produce its fatty acid substrate (**Figure 3-2**). In our design, *luxCDE* and *luxAB* are split between the donor and recipient strains, respectively. This feature of the assay distinguishes the donor and recipient populations from transconjugants. The luciferase genes are kept together so they are expressed in the same stoichiometric ratio. Overall, our assay design improves on previous assay designs by reducing background luminescence from the donor strain (**Figure 3-1a**) and by not requiring an inducible system (i.e. IPTG) or using GFP, which is less sensitive than *lux* (**Figure 3-1b**).[90] There is also the added benefit of *lux* making its own substrate, which does not affect central carbon metabolism.

Donor cells contain a non-transmissible F′ helper plasmid and a mobilizable reporter plasmid. The reporter plasmid contains a portion of the *lux* operon as well as an origin of transfer (*oriT*) that is compatible with the helper plasmid conjugation system. Reporter plasmids were constructed through Gibson assembly (**Figure 3-3**) and transformed into a cell lines containing an F′ plasmid to make the donor strain. This F′ plasmid is non-mobilizable due to a knockout in the native *oriT* with a chloramphenicol

acetyltransferase (*cat*) that removes the *nic* site. The F′ helper plasmid acts only in *trans* because the relaxase is unable nick the F′ plasmid DNA and initiate conjugation. However, it can mobilize the donor plasmid because it contains the wild-type F plasmid *oriT*. This will ensure that all transconjugants luminesce.

Recipient cells contain the complementary portion of the *lux* operon integrated into the bacterial chromosome. The process used to construct the recipient strain was similar to the methods used by Wanner et al.[89] The first step was to clone *luxAB* and *luxCDE* into pINT-1 (**Figure 3-5**). pINT-1 was designed to integrate into the arabinose operon through homologous recombination using portions of *polB* and *araC* present on the plasmid. PCR amplification products have *polB* and *araC* on the ends (**Figure 3-6a**). Within these genes, the amplicon contains a kanamycin cassette with flanking FRT sites as well as a beta-lactamase promoter controlling *lux* transcription. *E. coli* strains with pKD46 were grown in the presence of arabinose to induce production of phage λ red recombinase, which was used to integrate the amplicon into the chromosome.[88] Successful integrants (**Figure 3-6b**) will be transformed with pCP20, which contains a flippase for removal of the kanamycin cassette. *Lux* genes are now present in the arabinose operon. Both pKD46 and pCP20 have a temperature sensitive origin of replication and are cured between steps (**Appendix 2**).

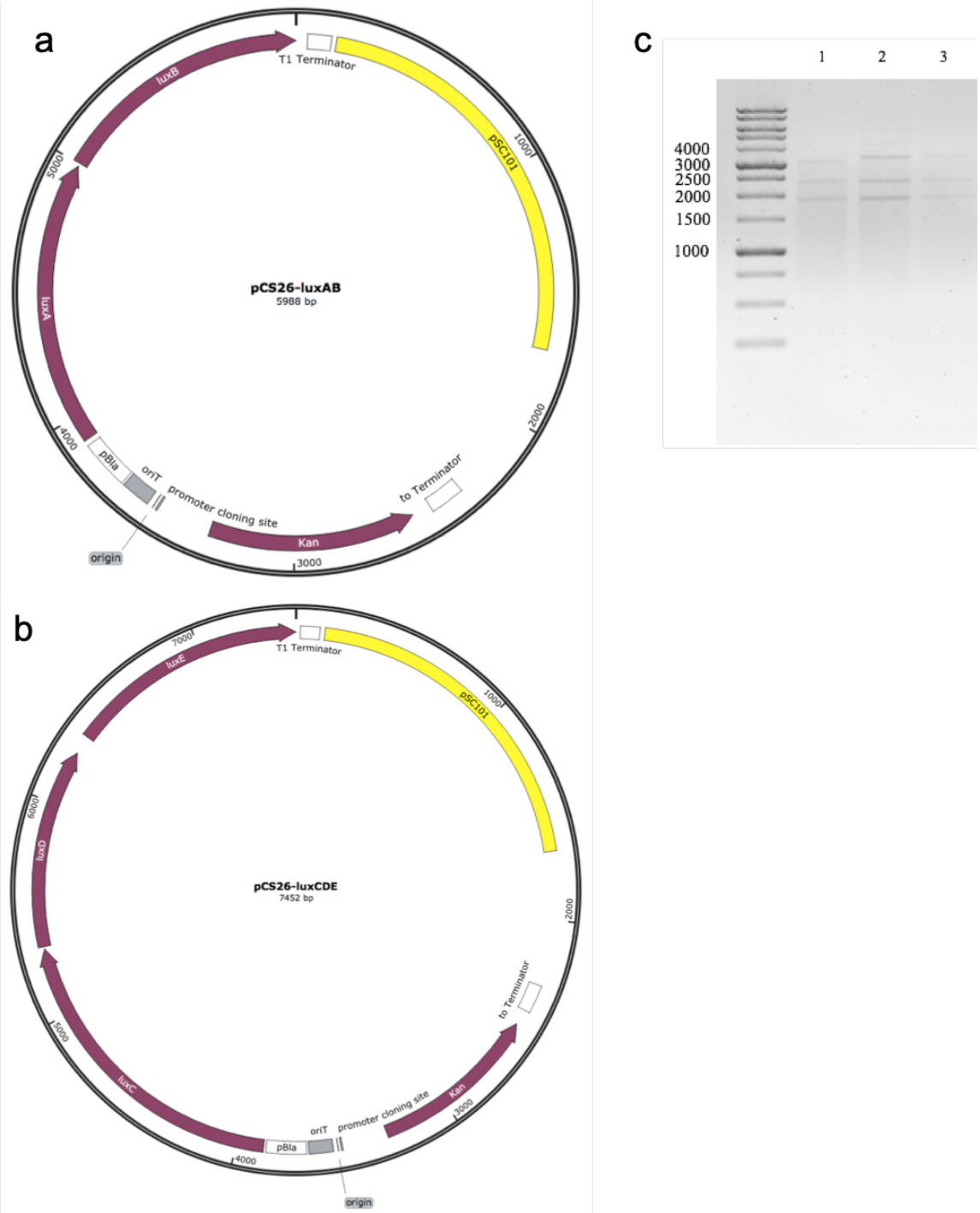

Figure 3-3: Donor plasmids constructed through Gibson assembly.
a) pCSAB (left) and pCSCDE (right) contain pSC101 low copy origin of replication, kanamycin resistance marker, *oriT* from the F plasmid, and the corresponding *lux* genes under the control of a beta-lactamase promoter. b) Restriction mapping of pCSCDE**.** pCSCDE was digested with *Nde*I/*Pst*I. The expected digestion pattern of 1862, 2373, and 3407 bp using *Nde*I/*Pst*I was seen in lane 2.

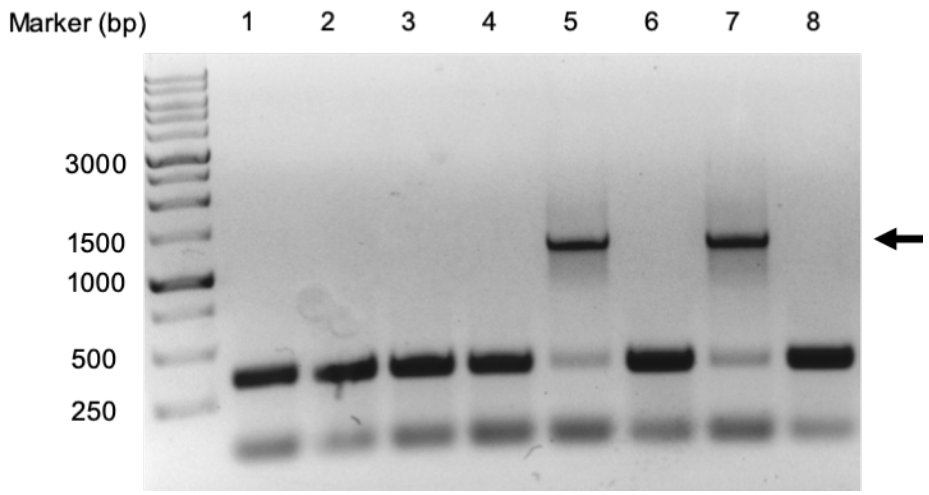

Figure 3-4: Chloramphenicol resistance marker inserted into the F plasmid *oriT* within *E. coli* XL Blue.
Colony PCR of chloramphenicol resistant *E. coli* XL Blue colonies with *oriT* knockout visualized at the arrow with the expected band size of 1399 bp.

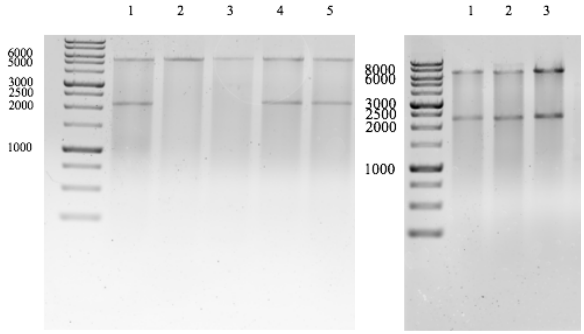

Figure 3-5: Restriction mapping of pINT-1: *luxAB* and pINT-1: *luxCDE*.
pINT-1: *luxAB* (left) has an expected digestion pattern of 2100 and 5450 using *Nde*I/*Xho*I. *luxAB* insert is contained in lanes 1, 4, and 5. pINT-1: *luxCDE* (right) has an expected digestion pattern of 2265 and 6882 using *Nde*I/*Sca*I. Restriction mapping suggests insert is present in each lane.

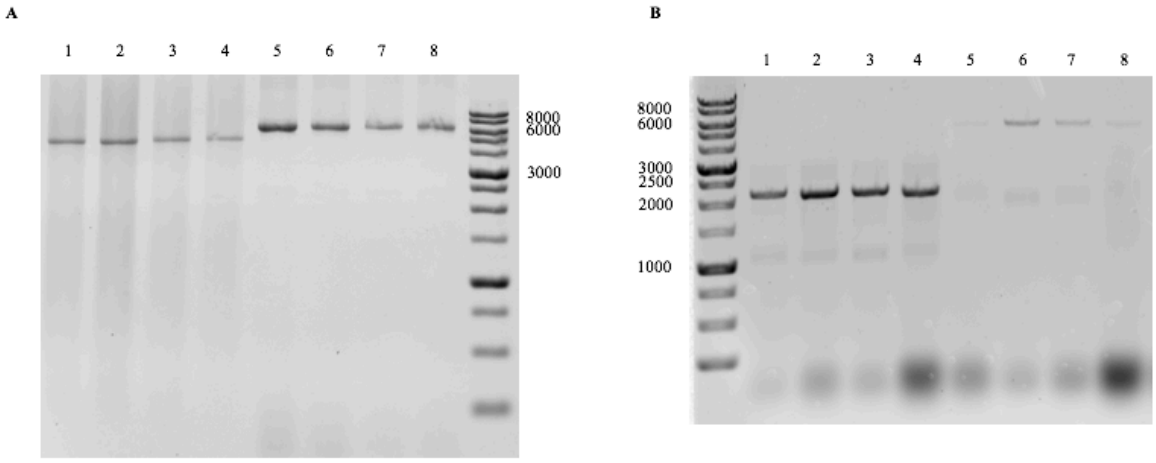

Figure 3-6: Colony PCR amplification of *luxAB* integrated into the arabinose operon of *E. coli* BW25113 Δ*tolC*Δ*bamB*.
a) *luxAB* amplicon used to integrate *luxAB* into the arabinose operon. Bands 5-8 were gel purified and electroporated into *E. coli* BW25113 Δ*tolC*Δ*bamB* cells containing pKD46 expressing the lambda recombinase. b) Lane 1 shows *E. coli* BW25113 Δ *tolC* Δ*bamB* cells. Lanes 2-8 are colonies plated from a kanamycin plate. *luxAB* has been integrated into the genome in colonies from lanes 6 and 7 with an expected band of 8000 bp.

3.3.2 Light production viability and conjugation frequency

The following section describes the current progress towards making a functional high throughput conjugation assay. The first experiment focused on detecting luminescence from transconjugants between donor (*E. coli* XL Blue containing F′ with an *oriT* knockout and pCSCDE) and recipient (*E. coli* BW25113 Δ*tolC*Δ*bamB* with integrated *luxAB*) assay strains. **Figure 3-7a** shows three luminescing strains with constructs containing synthetic promoters directing transcription of the *lux* operon. **Figure 3-7b** shows an absence of luminescence, indicating the lack of movement of the reporter plasmid between assay strains.

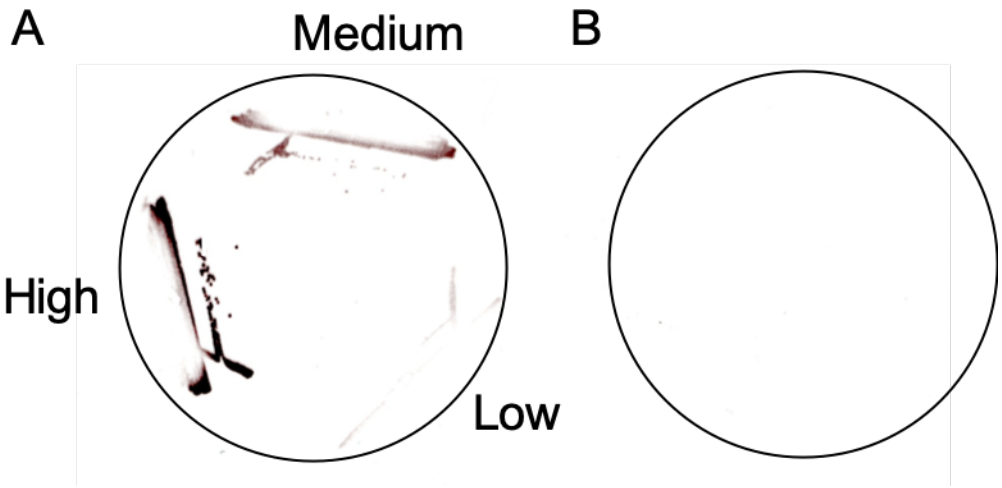

Figure 3-7: Detecting luminescence from conjugation.
a) This figure shows a high, medium, and low strength promoters of *lux* expression in *E. coli* TOP10. b) The luminescence signature of a donor (*E. coli* XL Blue with F' (mutated *oriT*) and pCSCDE) and recipient (*E. coli* TOP10 with *luxAB* integrated into the arabinose operon). Images were taken with Ivis.

Since luminescence was undetected during conjugation experiments, we needed to determine whether the previous issue stems from a lack of reporter plasmid mobilization to recipients or if there is an issue with luciferase expression. To test if the conjugation frequency was insufficient, we mated two donor strains, *E. coli* XL Blue with a wild type F′ and pCSCDE or F′ with an *oriT* knockout and pCSCDE, with a rifampin resistant *E. coli* TOP10 recipient (**Table 3-1**). The conjugation frequency in the wildtype pairing is estimated at 6.15×10^{-6}, whereas the conjugation frequency of the *oriT* knockout strain is zero (**Table 3-2**).

Table 3-2: Conjugation frequency of pCSCDE mobilization using different donor strains

Donor and Recipient Strains	Conjugation Frequency
E. coli XL Blue with F' and pCSCDE and *E. coli* TOP10	6.15×10^{-6}
E. coli XL Blue with F' (mutated *oriT*) and pCSCDE and *E. coli* TOP10	0

3.4 Discussion

3.4.1 Assay Construction

The assembly of the proposed system in **Figure 3-2** is complete. The donor strain has a mobilizable plasmid (pCSCDE), along with the option for a functional *oriT* present in the host F′ plasmid. The recipient strain has the complementary portion of the *lux* operon, *luxAB*. Although complete, the reversal of *lux* components expressing both combinations in donor and recipient strains may need to be done for assay optimization. pCSAB needs to be made and *luxCDE* integrated into *E. coli* TOP10. As for *luxCDE* integration, the precursor integration plasmid pINT-1: *luxCDE* has been constructed.

The donor strain has a knockout *oriT* with a chloramphenicol cassette (**not sequenced yet**). If the cassette needs to be removed or swapped, the integration process can be redone with FRT sites in the primers so that the cassette can be excised from the F plasmid using pCP20. The current recipient strain still has the kanamycin cassette as part of the integration process from the pINT-1: *luxAB*. This cassette needs to be removed because the mobilizable plasmid also has a kanamycin cassette and therefore it is not possible to select both.

3.4.2 Assay Function

Assay construction is positive news, but assay functionality needs improvement. First, the conjugation frequency values are low (**Figure 3-7**) compared to expected values of 4.8×10^{-1} for F plasmid conjugation frequency in *E. coli.*[91] The calculated conjugation frequency of the wild-type condition was 6.15×10^{-6}. Comparing the wild-type F′ plasmid to the *oriT* knockout experiments, there are only colonies in the wild-type experiments in

the lowest dilution. Given a high initial cell count of 2.66×10^9 cfu/ml**,** it is possible to have rifampin resistant mutants originating from donor cells. The experimental spontaneous mutation rate of *E. coli* to confer rifampin resistance is 2.6×10^9 cfu/ml.[92] To test our hypothesis, transconjugants would need to be sent for sequencing to check for rifampin resistance (in the *rpoB* gene). This experiment will be verified to see if the observed colonies are artifacts or represent a low conjugation frequency. Moving forward the conjugation frequency needs to be improved. First, the *oriT* in the reporter plasmids needs to be sequenced for a second time to confirm there is no mutation preventing mobilization. This will rule out the possibility that the reporter plasmid is not recognized as a substrate for conjugation.

The rationale to use an *oriT* knockout was to ensure that the mobilizable plasmid is the only DNA transferred to recipient cells and that all transconjugants have the mobilizable plasmid. Before knocking out oriT, optimizing the conjugation frequency between donor and recipient strains first will save time.

The wide selection of F plasmid derivatives (e.g. Hfr, F+, and F′ strains) offers flexibility in optimizing the donor strain. While optimizing the recipient strain, it is important to make sure they are without the F plasmid (F-) or they will be unable to accept the reporter plasmid.

When testing the functionality of the assay, luminescence was not detected in the conjugation condition compared to controls (**Figure 3-7**). The low conjugation frequency seen in **Figure 3-7** is likely evidence for a complete lack of conjugation occurring between the assay strains. However, to measure if the luciferase expression is active, pCSCDE can

be transferred into *E. coli* TOP10 with *luxAB* integrated, and luminescence measured. If luciferase expression cannot be separated from background signal, then new promoters need to be cloned into pCSCDE and possibly the integrated strain. The constitutive beta lactamase promoter could be swapped for a high or medium synthetic promoter that we have used as controls**.** Since it has been observed that light production can adversely affect cell growth,[37] we decided to initially experiment with a combination of a strong promoter (pBla) and a low copy number (pSC101) origin of replication for the donor plasmid (pCS26-Pac see **Appendix 2**). pSC101 has a stringent copy number that will presumably avoid toxicity issues. The backbone vector, pCS, has been successfully used in a wide range of applications.[52,93] Additionally, this vector contains *Pac*I sites adjacent to pSC101 that will facilitate the cloning of other origin of replication fragments if required.[52] The consequences of light production on cell growth will be mitigated in part by the other portion of the *lux* operon being inserted as a single copy in the recipient strain.[37]

The next step will be to optimize the light production for intensity and stability. pCSAB will need to be cloned, and *luxAB* and *luxCDE* will need to be integrated into several strains. A beta-lactamase promoter has been cloned into pCS26-Pac to compare signal intensity of the assay as a high control (**Figure 3-12**). However, the construct **Figure 3-12c** has low levels of luminescence compared to the low control using in earlier experiments. Cloning will be redone since pBla is a strong promoter and should be giving a high signal.

Another aspect of assay development is ensuring reproducible and steady light production. Plasmid transmission kinetics can be approximated by measuring light

production over time. Signal variability is expected between different combinations of *lux* genes and donor-recipient *E. coli* strains. As a result, we will test each scenario and choose the best combination for screening. Other variables include optimizing the amount and ratio of donor-recipient cells, the growth phase (stationary versus exponential) of cells, media types, and the duration of conjugation.

3.4.3 Future Directions in Assay Development

This high throughput conjugation assay is in the early development stage. With the assay fully assembled, the next step is to optimize the assay to make it robust before high throughput screening occurs (Discussed in sections **3.4.1** and **3.4.2**). The Z prime test is the gold standard in screening practice to measure the robustness of an assay. With a robust assay having a Z prime score of over 0.5, and ideally closer to 1 to generate strong hits. The Z prime is calculated using equation 1. Equation 1 is defined in terms of four parameters: the means (μ) and standard deviations (σ) of both the high (H) and low (L) controls (μ_H, μ_s, σ_c and σ_s). The assay set up will resemble **Figure 3.3.2b** for high signal. The low control will be a modified version of the proposed assay in which the donor plasmid (e.g. pCSCDE) is missing the *oriT* site and will not be mobilized. This control is expected to have no luminescence.

$$Z\ prime = 1 - \frac{3(\sigma_H + \sigma_L)}{|\mu_H - \mu_L|} \quad (1)$$

After the strains are developed, the assay must be optimized and prepared for high throughput screening. Another group has already published several papers with a high throughput conjugation assay protocol that will be used as a starting point.[37] The previous

conjugation screen by Fernando de la Cruz et al. was performed using the R388 conjugation system, which requires LB-agar instead of liquid media for growth due to the fragility of the conjugative pilus.[37,44] Therefore, library compounds must added to molten LB agar and stored over night to allow diffusion before screening. Furthermore, using LB agar restricted the throughput of the assay to 96-well plates. Using the F plasmid system, conjugation is possible in liquid media, which expands the assay throughput to 384-well plates.[94,95] This improvement can be attributed to a more stable conjugative pilus in the F plasmid compared to R388.[44] Both solid and liquid media will be tested to see if we can leverage this feature of the full F plasmid in the assay.

HTS requires a high level of attention to detail in order to find molecules that specifically inhibit the desired target. Below are several considerations that need to be addressed before screening. Proper aeration of the assay is necessary since luminescence is an oxygen-dependent process.[87] In addition, the assay needs to be functional with DMSO as this is the solvent of microbial extracts and many compound libraries. Enzymes involved in conjugation such as relaxase require a divalent cation; thus, having sufficient divalent cation concentrations for the reaction is critical to avoid finding non-specific chelating agents.[32,96] Previously identified conjugation inhibitors, linoleic acid and oleic acid, targeting F plasmid conjugation will serve as positive controls for screening.[37]

Once the assay is optimized for high throughput screening, we will perform a pilot screen using the Natural Product Library (NPL) to find COINs. The NPL consists of ~10,000 natural product extracts of environmental microorganisms, in which ~90% are actinomycetes bacteria. During the screening process, the assay will use known inhibitors

(e.g. linoleic and oleic acid) as a reference against hits. An inhibitor hit will be defined as a compound that reduces light production equal to or more than 95%, whereas compounds that enhance conjugation will be defined as those that are 3SD above mean luminescence. Dose response analyses of selected hits will separate compounds that inhibit or enhance conjugation versus bacterial growth. In the future, we plan to screen more libraries and different conjugation systems in order to find novel COINs and conjugation enhancing compounds.

A major challenge following screening will be identifying the target of inhibition. Since the entire conjugation system is targeted in the assay, extensive follow up and target identification will be required upon hit identification, as well as activity-guided purification (e.g. conjugation inhibition) and fractionation of extracts. The complexity of the F plasmid, as it has around 100 genes, will present difficulties in determining the target.[44] To address this obstacle, we have designed secondary assays that will be used to identify if compounds have off-target effects. An *E. coli* strain with a plasmid containing the entire *lux* operon can be incubated with compound/extract in liquid (**Figure 3-10a**) or on solid media (**Figure 3-10b**). Activity of compounds can be found by measuring the OD_{600} and luminescence over time. In liquid media, hypothetical situations are the compound 1) inhibits light production, 2) inhibits conjugation, or 3) inhibits cell growth and light production (**Figure 3-10a**). For the second assay, a lawn of *E. coli* TOP10 with pCS26-pBla can be grown on a plate and spotted with the desired compound. In theory, the potential effects of the compound are 1) cell death, 2) luminescence inhibition and cell death, or 3) inhibits luminescence without cell death (**Figure 3-10b**). The solid media assay has a concentration gradient of compound

unlike the liquid assay, which can be beneficial if the compound has concentration-dependent effects. For example, the compound may inhibit conjugation at lower concentrations, but have antimicrobial activity at higher concentrations.

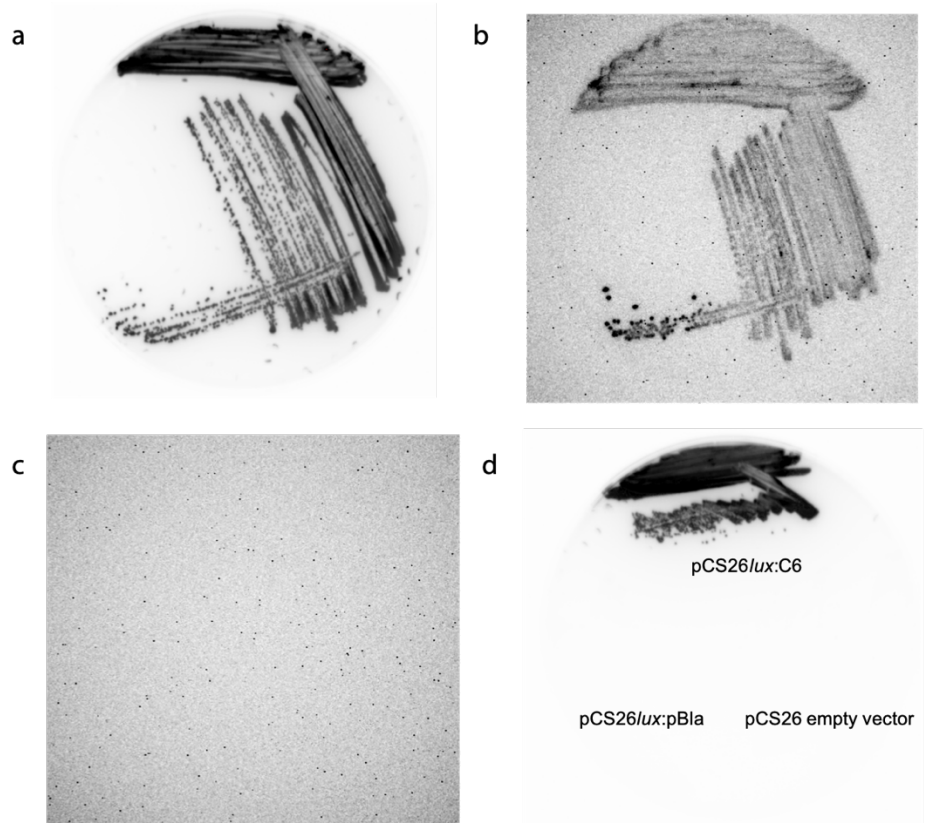

Figure 3-8: Luminescence of *E. coli* strains carrying pCS26 constructs with different promoters.
E. coli TOP10 cells with a) pCS26*lux*:C6, b) pCS26-PBla, c) pCS26 empty vector, and d) all three were streaked out onto LB agar plates supplemented with 50 ug/ml kanamycin. Chemiluminescence was measured using ChemiDoc imager with AutoExpose feature.

The secondary assays described above identify compounds with off-target or undesirable effects and will help identify the target responsible for conjugation inhibition. One approach would be to purify essential conjugation proteins (e.g. relaxases, ATPases) to see if the putative compounds inhibit their function. Alternatively, an unbiased approach would involve inducing mutations (e.g. using UV light). When conjugation strains are

incubated with a compound of interest, a mutation in the target will rescue the conjugation frequency. Luminescing colonies can be sequenced to determine if the acquired mutation(s) are specific to a target. Compounds can also be tested on a range of conjugation systems to see if they are specific to a particular system or general inhibitors of conjugation. A low throughput filter mating method is outlined in **Figure 3-11** that can be used to measure the conjugation efficiency. Additional steps in characterizing potential conjugation inhibitors include NMR, mass spectrometry, and bioassays to determine their spectrum of activity against Gram-positive and Gram-negative microorganisms.

AMR gene transfer through conjugation can be targeted using small molecules. The high throughput conjugation assay described in this chapter will serve as a platform to find compounds that target many other conjugation systems. The ultimate goal will be to prevent the spread of AMR genes and the formation of MDR pathogens.

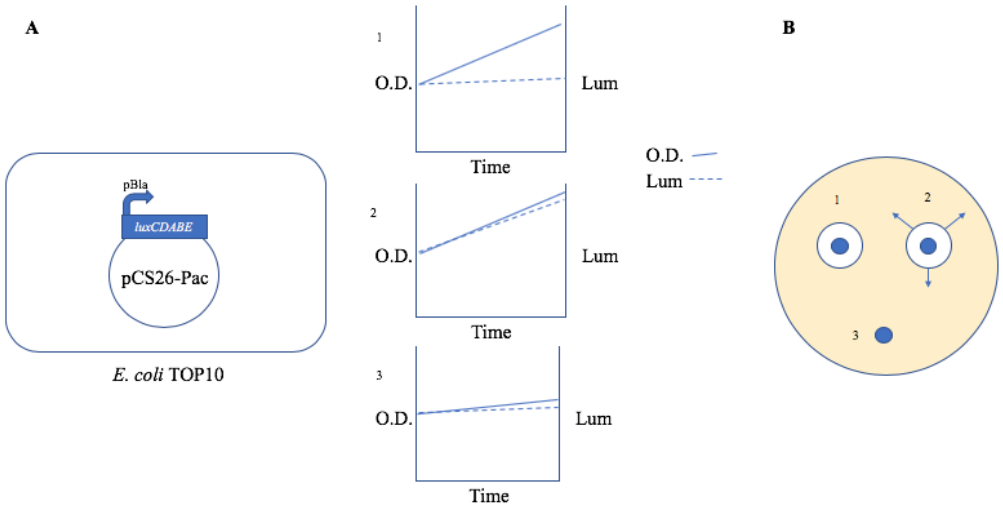

Figure 3-9: Luciferase reporter assay.
E. coli TOP10 containing a plasmid expressing the *lux* operon under the control of a beta lactamase promoter. This strain will be used to measure if a compound inhibits luminescence and can be tested in liquid or solid media. a) In LB media, the results of the assay can be 1) inhibits light production, 2) inhibits conjugation, or 3) inhibits cell growth and light production b) In solid media, the possibilities are 1) cell death, 2) luminescence inhibition and cell death, or 3) inhibits luminescence without cell death.

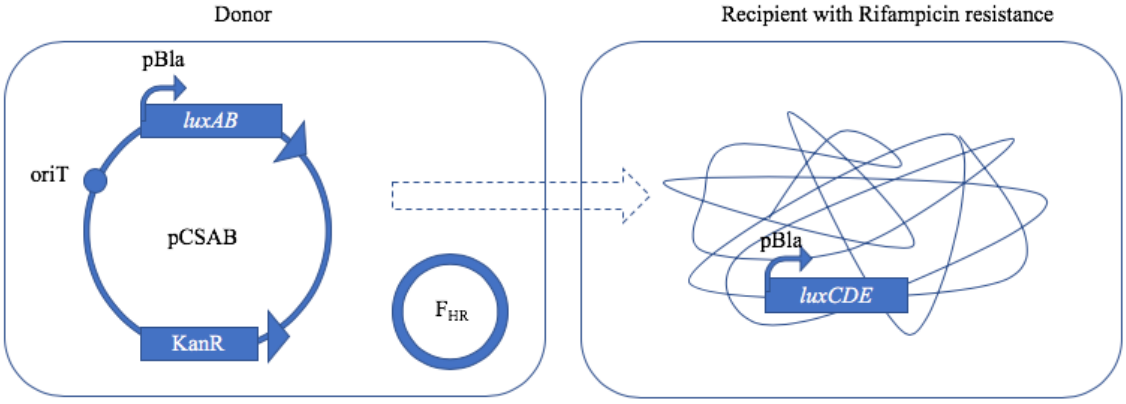

Figure 3-10: Secondary assay to determine the conjugation frequency.
Donor cells carry a mobilizable plasmid with a kanamycin resistance cassette and a F helper plasmid that is transferred to recipients containing a complementary portion of the *lux* operon and are resistant to rifampin. Therefore, only transconjugants will luminesce and these can be selected with kanamycin and rifampin through filter mating experiments.

Chapter 4.

Conclusions and Future Directions

4.1 Conclusions and Future Directions

The overarching theme of this work was to find small molecules through high throughput screening that prevent or promote antibiotic resistance gene mobilization. The first project in Chapter 2 focused on targeting the enzymes used to mobilize a conjugative transposon and Chapter 3 was dedicated to the identification of broad-spectrum conjugation inhibitors against a conjugative plasmid. Together, these approaches complement each other by targeting two different MGEs.

Known compounds in the Bioactives Library as well as microbial extracts in the PFL were screened using the Tn*1549* excision assay. Fluoroquinolones were shown to indirectly inhibit excision in a dose-dependent manner, and independently of SOS induction. We also showed that the conjugation frequency of Tn*1549* decreased in the presence of various concentrations of ciprofloxacin while at sub-MIC concentrations there was an apparent increase in conjugation frequency. Further *in vitro* and *in vivo* work is needed to validate the hypothesis that fluoroquinolones change the supercoiled state of the plasmid substrate leading to less excision, instead of directly targeting Int. The Bioactives library and PFL hits will be validated using secondary assays and specific inhibitors will be identified.

The high throughput conjugation assay described in Chapter 2 (**Figure 2-2**) is still in the development stage. The goal of assembling the assay has been reached, but much work is needed to reach a Z' amenable to high throughput screening. This simple assay

design is customizable with other conjugation systems and secondary assays have been put in place to find conjugation inhibitors in the future.

By beginning to target and screen key MGEs we will gain a greater understanding of which compounds influence their movement in the environment. This is critical to monitoring and preventing the formation of MDR pathogens in livestock and hospitals. Targeting MGEs is a promising strategy, but this approach is still in its infancy. First of all, these compounds need validation in animal models, in addition to evidence of efficacy in a practical application. COINs lower the frequency of conjugation, but the barriers to significant limit gene transfer are unknown. The discovery of molecular probes will give a richer understanding of the dynamics and mechanisms of MGEs movement in the environment. By learning which compounds inhibit or enhance transfer we can make better decisions involving antibiotic stewardship by avoiding drugs that select for transfer. In the future, these inhibitors may be used to prevent MGE-mediated AMR transfer in environmental hotspots.

References

1. D'Costa, V. M., McGrann, K. M., Hughes, D. W. & Wright, G. D. Sampling the Antibiotic Resistome. *Science (80-.).* **311**, 374–377 (2006).

2. Perry, J. A. & Wright, G. D. The antibiotic resistance "mobilome": searching for the link between environment and clinic. *Front. Microbiol.* **4**, 138 (2013).

3. Forsberg, K. J. *et al.* The shared antibiotic resistome of soil bacteria and human pathogens. *Science* **337**, 1107–11 (2012).

4. Wright, G. D. The antibiotic resistome: the nexus of chemical and genetic diversity. *Nat. Rev. Microbiol.* **5**, 175–186 (2007).

5. Lerminiaux, N. A. & Cameron, A. D. S. Horizontal transfer of antibiotic resistance genes in clinical environments. *Can. J. Microbiol.* **65**, 34–44 (2019).

6. Gillings, M. R. Lateral gene transfer, bacterial genome evolution, and the Anthropocene. *Ann. N. Y. Acad. Sci.* **1389**, 20–36 (2017).

7. Hens, D. K., Chatterjee, N. C. & Kumar, R. New temperate DNA phage BcP15 acts as a drug resistance vector. *Arch. Virol.* **151**, 1345–1353 (2006).

8. Dzidic, S. & Bedeković, V. Horizontal gene transfer-emerging multidrug resistance in hospital bacteria. *Acta Pharmacol. Sin.* **24**, 519–26 (2003).

9. Zhao, W.-H. & Hu, Z.-Q. Epidemiology and genetics of CTX-M extended-spectrum β-lactamases in Gram-negative bacteria. *Crit. Rev. Microbiol.* **39**, 79–101 (2013).

10. Oliver, A. *et al.* CTX-M-10 Linked to a Phage-Related Element Is Widely Disseminated among Enterobacteriaceae in a Spanish Hospital. *Antimicrob. Agents Chemother.* **49**, 1567–1571 (2005).

11. Johnston, C., Martin, B., Fichant, G., Polard, P. & Claverys, J.-P. Bacterial transformation: distribution, shared mechanisms and divergent control. *Nat. Rev. Microbiol.* **12**, 181–196 (2014).

12. Traglia, G. M., Chua, K., Centrón, D., Tolmasky, M. E. & Ramírez, M. S. Whole-Genome Sequence Analysis of the Naturally Competent Acinetobacter baumannii Clinical Isolate A118. *Genome Biol. Evol.* **6**, 2235–2239 (2014).

13. Halary, S., Leigh, J. W., Cheaib, B., Lopez, P. & Bapteste, E. Network analyses structure genetic diversity in independent genetic worlds. *Proc. Natl. Acad. Sci.* **107**, 127–132 (2010).

14. Amábile-Cuevas, C. F. & Chicurel, M. E. Bacterial plasmids and gene flux. *Cell* **70**, 189–199 (1992).

15. Sørensen, S. J., Bailey, M., Hansen, L. H., Kroer, N. & Wuertz, S. Studying plasmid horizontal transfer in situ: a critical review. *Nat. Rev. Microbiol.* **3**, 700–710 (2005).

16. Getino, M. & de la Cruz, F. Natural and Artificial Strategies To Control the Conjugative Transmission of Plasmids. *Microbiol. Spectr.* **6**, (2018).

17. Low, H. H. *et al.* Structure of a type IV secretion system. *Nature* **508**, 550–553 (2014).

18. Clarke, M., Maddera, L., Harris, R. L. & Silverman, P. M. *F-pili dynamics by live-cell imaging*. (2008).

19. Burrus, V. & Waldor, M. K. Shaping bacterial genomes with integrative and conjugative elements. *Res. Microbiol.* **155**, 376–386 (2004).

20. Delavat, F., Miyazaki, R., Carraro, N., Pradervand, N. & van der Meer, J. R. The hidden life of integrative and conjugative elements. *FEMS Microbiol. Rev.* **41**, 512–537 (2017).

21. Wozniak, R. A. F. & Waldor, M. K. Integrative and conjugative elements: mosaic mobile genetic elements enabling dynamic lateral gene flow. *Nat. Rev. Microbiol.* **8**, 552–563 (2010).

22. Mazel, D. Integrons: agents of bacterial evolution. *Nat. Rev. Microbiol.* **4**, 608–620 (2006).

23. Thomas, C. M. & Nielsen, K. M. Mechanisms of, and Barriers to, Horizontal Gene Transfer between Bacteria. *Nat. Rev. Microbiol.* **3**, 711–721 (2005).

24. Johnson, C. M. & Grossman, A. D. Integrative and Conjugative Elements (ICEs): What They Do and How They Work. *Annu. Rev. Genet.* **49**, 577–601 (2015).

25. Smyshlyaev, G., Barabas, O. & Bateman, A. Sequence analysis allows functional annotation of tyrosine recombinases in prokaryotic genomes. *bioRxiv* 542381 (2019). doi:10.1101/542381

26. Liu, J. *et al.* Staphylococcal chromosomal cassettes mec (SCCmec): A mobile genetic element in methicillin-resistant Staphylococcus aureus. *Microb. Pathog.* **101**, 56–67 (2016).

27. Alekshun, M. N. & Levy, S. B. Molecular mechanisms of antibacterial multidrug resistance. *Cell* **128**, 1037–50 (2007).

28. Uemura, S. *et al.* Acquisition of a transposon encoding extended-spectrum beta-lactamase SHV-12 by Pseudomonas aeruginosa isolates during the clinical course of a burn patient. *Antimicrob. Agents Chemother.* **54**, 3956–9 (2010).

29. Rideout, M. C. *et al.* Potent antimicrobial small molecules screened as inhibitors of

tyrosine recombinases and Holliday junction-resolving enzymes. *Mol. Divers.* **15**, 989–1005 (2011).

30. Rideout, M. C. *et al.* wrwyrggrywrw is a single-chain functional analog of the Holliday junction-binding homodimer, (wrwycr)2. *Peptides* **40**, 112–22 (2013).

31. Boldt, J. L., Pinilla, C. & Segall, A. M. Reversible inhibitors of lambda integrase-mediated recombination efficiently trap Holliday junction intermediates and form the basis of a novel assay for junction resolution. *J. Biol. Chem.* **279**, 3472–83 (2004).

32. Lujan, S. A., Guogas, L. M., Ragonese, H., Matson, S. W. & Redinbo, M. R. Disrupting antibiotic resistance propagation by inhibiting the conjugative DNA relaxase. *Proc. Natl. Acad. Sci. U. S. A.* **104**, 12282–7 (2007).

33. Nash, R. P., McNamara, D. E., Keith Ballentine III, W., Matson, S. W. & Redinbo, M. R. Investigating the impact of bisphosphonates and structurally related compounds on bacteria containing conjugative plasmids. *Biochem. Biophys. Res. Commun.* **424**, 697–703 (2012).

34. Casu, B. *et al.* Structural Analysis and Inhibition of TraE from the pKM101 Type IV Secretion System. *J. Biol. Chem.* **291**, 23817–23829 (2016).

35. Casu, B., Arya, T., Bessette, B. & Baron, C. Fragment-based screening identifies novel targets for inhibitors of conjugative transfer of antimicrobial resistance by plasmid pKM101. doi:10.1038/s41598-017-14953-1

36. Ripoll-Rozada, J. *et al.* Type IV traffic ATPase TrwD as molecular target to inhibit bacterial conjugation. *Mol. Microbiol.* **100**, 912–21 (2016).

37. Fernandez-Lopez, R. *et al.* Unsaturated fatty acids are inhibitors of bacterial conjugation. *Microbiology* **151**, 3517–3526 (2005).

38. Getino, M. *et al.* Tanzawaic Acids, a Chemically Novel Set of Bacterial Conjugation Inhibitors. *PLoS One* **11**, e0148098 (2016).

39. Getino, M. *et al.* Synthetic Fatty Acids Prevent Plasmid-Mediated Horizontal Gene Transfer. *MBio* **6**, e01032-15 (2015).

40. Burrus, V., Pavlovic, G., Decaris, B. & Guédon, G. Conjugative transposons: the tip of the iceberg. *Mol. Microbiol.* **46**, 601–10 (2002).

41. Lambertsen, L., Rubio-Cosials, A., Patil, K. R. & Barabas, O. Conjugative transposition of the vancomycin resistance carrying Tn *1549* : enzymatic requirements and target site preferences. *Mol. Microbiol.* **107**, 639–658 (2018).

42. Roberts, A. P. & Mullany, P. A modular master on the move: the Tn916 family of mobile genetic elements. *Trends Microbiol.* **17**, 251–258 (2009).

43. Tsvetkova, K., Marvaud, J.-C. & Lambert, T. Analysis of the Mobilization Functions of the Vancomycin Resistance Transposon Tn1549, a Member of a New Family of Conjugative Elements. *J. Bacteriol.* **192**, 702–713 (2010).

44. Smillie, C., Garcillán-Barcia, M. P., Francia, M. V., Rocha, E. P. C. & de la Cruz, F. Mobility of plasmids. *Microbiol. Mol. Biol. Rev.* **74**, 434–52 (2010).

45. User Guide: GeneJET Gel Extraction Kit. Available at: https://www.thermofisher.com/document-connect/document-connect.html?url=https%3A%2F%2Fassets.thermofisher.com%2FTFS-Assets%2FLSG%2Fmanuals%2FMAN0012661_GeneJET_Gel_Extraction_UG.pdf&title=VXNlciBHdWlkZTogR2VuZUpFVCBHZWwgRXh0cmFjdGlvbiBLaXQ=. (Accessed: 2nd May 2019)

46. DreamTaq Green PCR Master Mix (2X) - Thermo Fisher Scientific. Available at: https://www.thermofisher.com/order/catalog/product/K1081. (Accessed: 2nd May 2019)

47. GeneJET PCR Purification Kit - Thermo Fisher Scientific. Available at: https://www.thermofisher.com/order/catalog/product/K0702. (Accessed: 2nd May 2019)

48. PureLink Quick Plasmid Miniprep Kit - Thermo Fisher Scientific. Available at: https://www.thermofisher.com/order/catalog/product/K210010. (Accessed: 22nd May 2019)

49. Mangat, C. S., Bharat, A., Gehrke, S. S. & Brown, E. D. Rank ordering plate data facilitates data visualization and normalization in high-throughput screening. *J. Biomol. Screen.* **19**, 1314–20 (2014).

50. Wiegand, I., Hilpert, K. & Hancock, R. E. W. Agar and broth dilution methods to determine the minimal inhibitory concentration (MIC) of antimicrobial substances. *Nat. Protoc.* **3**, 163–175 (2008).

51. (CLSI)., C. Methods for Dilution Antimicrobial Susceptibility Tests for Bacteria that Grow Aerobically. **M7-A8**, (2012).

52. Bjarnason, J., Southward, C. M. & Surette, M. G. Genomic profiling of iron-responsive genes in Salmonella enterica serovar typhimurium by high-throughput screening of a random promoter library. *J. Bacteriol.* **185**, 4973–82 (2003).

53. Clewell, D. B., An, F. Y., White, B. A. & Gawron-Burke, C. Streptococcus faecalis sex pheromone (cAM373) also produced by Staphylococcus aureus and identification of a conjugative transposon (Tn918). *J. Bacteriol.* **162**, 1212–20 (1985).

54. Darakhshan, S. & Pour, A. B. Tranilast: A review of its therapeutic applications. *Pharmacol. Res.* **91**, 15–28 (2015).

55. Knox, C. *et al.* Chloroxine. *Nucleic Acids Res.* **39**, D1035–D1041 (2011).

56. Malaveille, C., Brun, G. & Bartsch, H. Genotoxicity of ochratoxin A and structurally related compounds in Escherichia coli strains: studies on their mode of action. *IARC Sci. Publ.* 261–6 (1991).

57. Chon, E., Flanagan, B., de Sá Rodrigues, L. C., Piskun, C. & Stein, T. J. 6-Bromoindirubin-3'oxime (BIO) decreases proliferation and migration of canine melanoma cell lines. *Vet. J.* **205**, 305–12 (2015).

58. Zou, N., Wang, X. & Li, G. Spectroscopic and electrochemical studies on the interaction between luteolin and DNA. *J. Solid State Electrochem.* **20**, 1775–1782 (2016).

59. indoprofen (CHEBI:76162). Available at: https://www.ebi.ac.uk/chebi/searchId.do?chebiId=CHEBI:76162. (Accessed: 9th October 2018)

60. Lyddiard, J. R. A., Whitfield, P. J. & Bartlett, A. ANTISCHISTOSOMAL BIOACTIVITY OF ISOFLAVONOIDS FROM MILLETTIA THONNINGII (LEGUMINOSAE). *http://dx.doi.org/10.1645/0022-3395(2002)088[0163:ABOIFM]2.0.CO;2* (2001). doi:10.1645/0022-3395(2002)088[0163:ABOIFM]2.0.CO;2

61. Küçükkılınç, T. & Özer, İ. Inhibition of human plasma cholinesterase by malachite green and related triarylmethane dyes: Mechanistic implications. *Arch. Biochem. Biophys.* **440**, 118–122 (2005).

62. Pesigan, T. P., Banzon, T. C., Santos, A. T., Noseñas, J. & Zabala, R. G. Pararosaniline pamoate (CI-403-A) in the treatment of Schistosoma japonicum infection in the Philippines. *Bull. World Health Organ.* **36**, 263–74 (1967).

63. Reeder, N. L. *et al.* The antifungal mechanism of action of zinc pyrithione. *Br. J. Dermatol.* **165**, 9–12 (2011).

64. Andriole, V. T. The Quinolones: Past, Present, and Future. *Clin. Infect. Dis.* **41**, S113–S119 (2005).

65. Shun-Mei, E. *et al.* Sub-inhibitory concentrations of fluoroquinolones increase conjugation frequency. *Microb. Pathog.* **114**, 57–62 (2018).

66. Dobrindt, U., Hochhut, B., Hentschel, U. & Hacker, J. Genomic islands in pathogenic and environmental microorganisms. *Nat. Rev. Microbiol.* **2**, 414–424 (2004).

67. Boyd, E. F., Almagro-Moreno, S. & Parent, M. A. Genomic islands are dynamic, ancient integrative elements in bacterial evolution. *Trends Microbiol.* **17**, 47–53 (2009).

68. Rubio-Cosials, A. *et al.* Transposase-DNA Complex Structures Reveal Mechanisms for Conjugative Transposition of Antibiotic Resistance. *Cell* **173**, 208-220.e20 (2018).

69. Aldred, K. J., Kerns, R. J. & Osheroff, N. Mechanism of quinolone action and resistance. *Biochemistry* **53**, 1565–74 (2014).

70. Fullerton, M. D. *et al.* Single phosphorylation sites in Acc1 and Acc2 regulate lipid homeostasis and the insulin-sensitizing effects of metformin. *Nat. Med.* **19**, 1649–54 (2013).

71. Hawkey, P. M. & Jones, A. M. The changing epidemiology of resistance. *J. Antimicrob. Chemother.* **64**, i3–i10 (2009).

72. Liu, L. *et al.* Antimicrobial Resistance and Cytotoxicity of Citrobacter spp. in Maanshan Anhui Province, China. *Front. Microbiol.* **8**, 1357 (2017).

73. Botelho, J., Mourão, J., Roberts, A. P. & Peixe, L. Integrative and conjugative elements, the neglected drivers of carbapenemase-encoding genes. doi:10.1101/678748

74. Morgan-Linnell, S. K., Hiasa, H., Zechiedrich, L. & Nitiss, J. L. Assessing sensitivity to antibacterial topoisomerase II inhibitors. *Curr. Protoc. Pharmacol.* **Chapter 3**, Unit3.13 (2007).

75. Abbani, M., Iwahara, M. & Clubb, R. T. The Structure of the Excisionase (Xis) Protein from Conjugative Transposon Tn916 Provides Insights into the Regulation of Heterobivalent Tyrosine Recombinases. *J. Mol. Biol.* **347**, 11–25 (2005).

76. Hooper, D. C., Wolfson, J. S., Tung, C., Souza, K. S. & Swartz, M. N. Effects of inhibition of the B subunit of DNA gyrase on conjugation in Escherichia coli. *J. Bacteriol.* **171**, 2235–7 (1989).

77. Weisser, J. & Wiedemann, B. Inhibition of R-plasmid transfer in Escherichia coli by 4-quinolones. *Antimicrob. Agents Chemother.* **31**, 531–4 (1987).

78. Couce, A. & Blázquez, J. Side effects of antibiotics on genetic variability. *FEMS Microbiol. Rev.* **33**, 531–538 (2009).

79. Beaber, J. W., Hochhut, B. & Waldor, M. K. SOS response promotes horizontal dissemination of antibiotic resistance genes. *Nature* **427**, 72–74 (2004).

80. Stevens, A. M., Shoemaker, N. B., Li, L. Y. & Salyers, A. A. Tetracycline regulation of genes on Bacteroides conjugative transposons. *J. Bacteriol.* **175**, 6134–41 (1993).

81. Torres, O., Korman, R., Zahler, S. & Dunny, G. The conjugative transposon Tn925: enhancement of conjugal transfer by tetracycline in Enterococcus faecalis

and mobilization of chromosomal genes in Bacillus subtilis and E. faecalis. *MGG Mol. Gen. Genet.* **225**, 395–400 (1991).

82. Launay, A., Ballard, S. A., Johnson, P. D. R., Grayson, M. L. & Lambert, T. Transfer of Vancomycin Resistance Transposon Tn1549 from Clostridium symbiosum to Enterococcus spp. in the Gut of Gnotobiotic Mice. *Antimicrob. Agents Chemother.* **50**, 1054–1062 (2006).

83. Peng, Z. *et al.* Update on Antimicrobial Resistance in Clostridium difficile: Resistance Mechanisms and Antimicrobial Susceptibility Testing. *J. Clin. Microbiol.* **55**, 1998–2008 (2017).

84. Goudarzi, M. *et al.* Antimicrobial susceptibility of clostridium difficile clinical isolates in iran. *Iran. Red Crescent Med. J.* **15**, 704–11 (2013).

85. Knight, D. R., Androga, G. O., Ballard, S. A., Howden, B. P. & Riley, T. V. A Phenotypically Silent *vanB2* Operon Carried on a Tn *1549* -Like Element in *Clostridium difficile*. *mSphere* **1**, (2016).

86. Koraimann, G. Spread and Persistence of Virulence and Antibiotic Resistance Genes: A Ride on the F Plasmid Conjugation Module. *EcoSal Plus* **8**, (2018).

87. Close, D. *et al.* The evolution of the bacterial luciferase gene cassette (lux) as a real-time bioreporter. *Sensors (Basel).* **12**, 732–52 (2012).

88. Cox, G. *et al.* A Common Platform for Antibiotic Dereplication and Adjuvant Discovery. *Cell Chem. Biol.* **24**, 98–109 (2017).

89. Datsenko, K. A. & Wanner, B. L. One-step inactivation of chromosomal genes in Escherichia coli K-12 using PCR products. *Proc. Natl. Acad. Sci.* **97**, 6640–6645 (2000).

90. Hakkila, K., Maksimow, M., Karp, M. & Virta, M. Reporter Genes lucFF, luxCDABE, gfp, and dsred Have Different Characteristics in Whole-Cell Bacterial Sensors. (2002). doi:10.1006/abio.2001.5517

91. Encinas, D. *et al.* Plasmid conjugation from proteobacteria as evidence for the origin of xenologous genes in cyanobacteria. *J. Bacteriol.* **196**, 1551–9 (2014).

92. Lee, H., Popodi, E., Tang, H., Foster, P. L. & Modrich, P. Rate and molecular spectrum of spontaneous mutations in the bacterium Escherichia coli as determined by whole-genome sequencing. doi:10.1073/pnas.1210309109

93. Cox, R. S., III, Surette, M. G. & Elowitz, M. B. Programming gene expression with combinatorial promoters. *Mol. Syst. Biol.* **3**, (2007).

94. Bergstrom, C. T., Lipsitch, M. & Levin, B. R. Natural selection, infectious transfer and the existence conditions for bacterial plasmids. *Genetics* **155**, 1505–1519

(2000).

95. Achtman, M. Mating aggregates in Escherichia coli conjugation. *J. Bacteriol.* **123**, 505–15 (1975).

96. Lucas, M. *et al.* Relaxase DNA Binding and Cleavage Are Two Distinguishable Steps in Conjugative DNA Processing That Involve Different Sequence Elements of the nic Site * □ S. (2010). doi:10.1074/jbc.M109.057539

Appendices

Appendix 1: Media and Master mixes

PSI broth (100 ml, autoclave)

Reagent	Amount	Supplier
Bacto Yeast Extract	0.5 g	BD Biosciences
Bacto Tryptone	2.0 g	TRP402, BioShop
Magnesium sulphate, monohydrate	0.5 g	Sigma
Sodium hydroxide	Enough to reach a pH of 7	EMD

TfBI (dissolved in water, filter sterilized, and stored at 4°C)

Reagent	Amount	Supplier
Potassium Acetate, dihydrate	30 mM	EM Science
Rubidium Chloride	100 mM	BioShop
Calcium Chloride	10 mM	Fisher Scientific
Manganese Chloride	50 mM	Sigma
Glycerol	15% (v/v)	GLY001, BioShop
Dilute acetic acid	Enough to reach a pH of 5.8	Caledon

TfBII (dissolved in water, filter sterilized and stored at 4°C)

Reagent	Amount	Supplier
MOPS	10 mM	MOP001, BioShop
Rubidium Chloride	10 mM	Bioshop

Calcium Chloride (75 mM)	75 mM	Fisher Scientific
Glycerol	15% (v/v)	GLY001, BioShop
Sodium hydroxide	Enough to reach a pH of 6.5	EMD

2X Gibson Master Mix
320 µl 5X ISO buffer
6.4 µl 1U/µl T5 exonuclease (M0363S; NEB)
20 µl 2U/µl Phusion polymerase (non hot start) (F-530L; ThermoFisher)
40 µl 40U/µl Taq ligase (L6060L; D-Mark Bio)
413.6 µl ddH2O

Dilute T5 exonuclease stock 10-fold in 1X ISO to get 1 U/µl.

5X ISO Buffer
3 ml 1M Tris-HCl pH 7.5
300 µl 1M $MgCl_2$
1.5g PEG-8000
300 µl 1M DTT
0.0199g NAD
60 µl 100 mM dGTP
60 µl 100 mM dATP
60 µl 100 mM dCTP
60 µl 100 mM dTTP
2.16 ml ddH_2O

50X TAE buffer
Tris base 242 g (BioShop)
Acetic acid 57.1 ml (Caledon)
EDTA 37.2 g (Fisher)
To 1 L of dH_20

Gels are made with 1X TAE buffer.

6X DNA loading dye
0.25% Bromophenol Blue (2 mg) (300 bp)
30% glycerol in dH_2O (3ml + 7 ml dH_2O)
0.25% xylene (4kb)
5-Bromo-n-xylene, (Sigma)

Bromophenol blue sodium salt (Sigma)

Induction Media
83.3 µl of 100 mg/ml Ampicillin (Ampicillin sodium salt Sigma)
83.3 µl of 33.3 mg/ml Chloramphenicol (OmniPur®)
16.6 µl of 50 mg/ml Gentamycin sulfate GTA202
83.3 µl of 1 mM IPTG IPT-001 BioShop
1.66 ml of 20% (w/v) Arabinose (L-(+)-Arabinose W325501 Sigma)
48.25 ml LB media (LBL405; BioShop)

Notes: Arabinose is dissolved in LB. Ampicillin is not added to the induction media when working with the control strain.

Appendix 2: Primers

Chapter 2

Primer name	Sequence	Ref
pGDP Rev	5’ CCA ACT CAG CTT CCT TTC 3’	[2]
pBla Fwd	5’ CAT GAG ACA ATA ACC CTG 3’	[2]
pLac Fwd	5’ ATA AGG GAG AGC GTC GAG 3’	[2]
gyrA seq	5’ GGATATACACCTTGCCGC 3’	This study
parC seq	5’ CGAAGTTTGGCACCCAGTC 3’	This study
gyrA PCR	Fwd: 5’ CTTCCACTTCTGCGCGAGCGC 3’ Rev: 5’ CCGAGATGGCCTGAAGCCGG 3’	This study
parC PCR	Fwd: 5’ GTTTGGCAGACGGGCAGGTAGC 3’	This study
	Rev: 5’ CGATATGGCAGAGCGCCTTGCG 3’	This study
Backbone of TPEP	Fwd: 5’ CAAATAACTCGAGATCTGCAGCTGGTACC 3’	This study
	Rev:5’GTTCTTCTCCTTTACTCATGGTTAATTCCTCCTGTTAG 3’	This study
pUA66 gfp	Fwd: 5’ CCATGAGTAAAGGAGAAGAACTTTTCAC 3’	This study
	Rev: 5’ GCTGCAGATCTCGAGTTATTTGTACAATTCATC 3’	

Luciferase	Fwd: 5’ GTTACCATATGGAAGACGCC 3'	This study
	Rev: 5’ GCATCCTCGAGTTACAATTTG 3'	This study
CI	Fwd: 5’ GCGGGATCCTGTTCTCCCAT 3’	[1]
	Rev: 5’ ACGCAAGCTTCGATTCCGCAAG 3’	[1]
DP	Fwd: 5’ GAGAGCAGCTGAAGTTACCC 3’	[1]
	Rev: 5’ GTAACTTTAAACGGACCACTAGGAG 3’	[1]
Forward Seq Primer for pA15: *gfp*	Fwd: 5’ CACACTTTGCTATGCCATAGC 3’	This study
Reverse Seq Primer for pA15: *gfp*	Rev: 5’ GACCGCTTCTGCGTTCTG 3’	This study

Chapter 3

Primer Set	Sequence (5’ to 3’)
pINT-1: *luxCDE* PS1	Fwd: 5’CGAAACACGGAAACCGAAGACC 3’
	Rev: 5’GGAACTTCGAAGCAGCTCCAGC 3’
	(pINT-1: *luxAB* PS1)
pINT-1: *luxCDE* PS2	Fwd: 5’ GCCTGCGCCACGCTGAAAATCC 3’
	Rev: 5’ GGCGAAGTGCCGGGGCAG 3’
	(pINT-1: *luxAB* PS2)
pINT-1: *luxCDE* PS3	Fwd: 5’ CGCTTGGTGGTCGAATGGGC 3’
	Rev: 5’ GGACAAGGGAAAACGCAAGCGC 3’
	(pINT-1: *luxAB* PS3)
pINT-1: *luxCDE* PS4	Fwd: 5’ CGCCCCAGCTGGCAATTCCG 3’
	(pINT-1: *luxAB* PS4 FP)
	Rev: 5’ CGGGAAAGATTTCAACCTGGCCG 3’
	(pINT-1: *luxCDE*)
pINT-1: *luxCDE* PS5	Fwd: 5’ GCAGCGGCCTGGTGCCG 3’
	(pINT-1: *luxAB* PS5 FP)
	Rev: 5’ GGCCTCTAGCTTAGCCATTTCTTC 3’
	(pCSCDE PS1 RP)
pINT-1: *luxCDE* PS6	Fwd: 5’ CTCTATACGGTAGGGCAAAGATGG 3’
	Rev: 5’ GAGCCGCACCTGTCGCTGC 3’
	(pCSCDE PS2)

pINT-1: *luxCDE* PS7	Fwd: 5’ GGGCGGTAGAGCATGCGCC 3’ Rev: 5’ CAACCGCAACATCCTTAGCCG 3’ (pCSCDE PS3)
pINT-1: *luxCDE* PS8	Fwd: 5’ GGTGCGGAAAGGATTGTAGAAGC 3’ Rev: 5’ CCGGCAATTCATTAATGGGTAGACTG 3’ (pCSCDE PS4)
pINT-1: *luxCDE* PS9	Fwd: 5’ CGTTTTTAATCACCGCAGTCGGTG 3’ Rev: 5’ GACCACACTAATGGATCGCTCG 3’ (pCSCDE PS5)
pINT-1: *luxCDE* P10	Fwd: 5’ GCCGCTATCGCGATGGATAATGAT 3’ Rev:5’ GAGCATTAAATCTATCTGGTCCCAAATTG 3’ (pCSCDE PS6)
pINT-1: *luxCDE* P11	Fwd: 5’ CTCTTAGGCTCTGTGAGTTATGGC 3’ Rev: 5’ CGAGCACGCCGGGATACTTACC 3’ (pCSCDE PS7)
pINT-1: *luxCDE* P12	Fwd: 5’ CCTGATGGAACGCCGGGGTTG 3’ (pCSCDE PS8 FP) Rev: 5’ CCAGAAGGCCATCCTGACGG 3’ (pINT-1: *luxAB* PS8)
pINT-1: *luxCDE* P13	Fwd: 5’ CCACCACCACCACCACTGAG 3’ RP- CAGGGTTATTGTCTCATGAGCGG 3’ (pINT-1: *luxAB* PS9)
pINT-1: *luxAB* PS1	Fwd: 5’ CGAAACACGGAAACCGAAGACC 3’ Rev: 5’ GGAACTTCGAAGCAGCTCCAGC 3’
pINT-1: *luxAB* PS2	Fwd: 5’ GCCTGCGCCACGCTGAAAATCC 3’ Rev: 5’ GGCGAAGTGCCGGGGCAG 3’
pINT-1: *lux*AB PS3	Fwd: 5’ CGCTTGGTGGTCGAATGGGC 3’ Rev: 5’ GGACAAGGGAAAACGCAAGCGC 3’
pINT-1: *luxAB* PS4	Fwd: 5’ CGCCCCAGCTGGCAATTCCG 3’ Rev: 5’ GGGGAGGTTGGTATGTAAGCAAAAAG 3’
pINT-1: *luxAB* PS5	Fwd: 5’ GCAGCGGCCTGGTGCCG 3’ Rev: 5’ CCAACTTAATATCATCGGTAGGCC 3’
pINT-1: *luxAB* PS6	Fwd: 5’ CGCGGCGTATAGCAGAGGTG 3’ Rev: 5’ CCTGCATGCGAACTATACTTTGTTC 3’
pINT-1: *luxAB* PS7	Fwd: 5’ GCCATTTCTTAAAGAAAAACAACGTTCGC 3’ Rev: 5’ CCGCAACGGCTTTATATCTTTCAGC 3’
pINT-1: *luxAB* PS8	Fwd: 5’ GGCGGACCTCGGAAATATGTAAC 3’ Rev: 5’ GTGCCACCAGAAGGCCATCC 3’
pINT-1: *luxAB* PS9	Fwd: 5’ CCACCACCACTGAGATCCGG 3’ Rev: 5’ CAGGGTTATTGTCTCATGAGCGG 3’
pCSAB PS1	Fwd: pCSCDE PS1 Rev: pINT1: *luxAB* PS4
pCSAB PS2	Fwd: 5’ CGCGTTAAATTTTTGTTAAATCAGCTC 3’ (pCSAB FP2)

	Rev: pINT-1: *luxAB* PS5
pCSAB PS3	pINT-1: *luxAB* PS6
pCSAB PS4	pINT-1: *luxAB* PS7
pCSAB PS5	Fwd: pINT-1: *luxAB* PS8
	Rev: 5’ CCATGTGGTACTTCTTAATATTATC 3’
	(pCSAB PS5)
pCSAB PS6	FP-GTGTATTGCTGTCCTTTGAACCAATG 3’
	(FP pCSAB PS6)
	RP pCSCDE PS8
pCSAB PS7	PS9 pCSCDE
pCSAB PS8	PS10 pCSCDE
pCSAB PS9	PS11 pCSCDE
pCSAB PS10	PS12 pCSCDE
pCSAB PS11	PS13 pCSCDE
pCSAB PS12	PS14 pCSCDE
pCSCDE PS1	Fwd: 5’ CGGTGTCGGCGCGGCTAC 3’
	Rev: 5’ GGCCTCTAGCTTAGCCATTTCTTC 3’
pCSCDE PS2	Fwd: 5’ CTCTATACGGTAGGGCAAAGATGG 3’
	Rev: 5’ GAGCCGCACCTGTCGCTGC 3’
pCSCDE PS3	Fwd: 5’ GGGCGGTAGAGCATGCGCC 3’
	Rev: 5’ CAACCGCAACATCCTTAGCCG 3’
pCSCDE PS4	Fwd: 5’ GGTGCGGAAAGGATTGTAGAAGC 3’
	Rev: 5’ CCGGCAATTCATTAATGGGTAGACTG 3’
pCSCDE PS5	Fwd: 5’ CGTTTTTAATCACCGCAGTCGGTG 3’
	Rev: 5’ GACCACACTAATGGATCGCTCG 3’
pCSCDE PS6	Fwd: 5’ GCCGCTATCGCGATGGATAATGAT 3’
	Rev: 5’ GAGCATTAAATCTATCTGGTCCCAAATTG 3’
pCSCDE PS7	Fwd: 5’ CTCTTAGGCTCTGTGAGTTATGGC 3’
	Rev: 5’ CGAGCACGCCGGGATACTTACC 3’
pCSCDE PS8	Fwd: 5’ CCTGATGGAACGCCGGGGTTG 3’
	Rev: 5’ GTTCTCGTCATCAGCTCTCTGG 3
pCSCDE PS9	Fwd: 5’ CCTACAAGGAAAGAACGGACGG 3’
	Rev: 5’ GTCCGTTACGTAGGTAGGAATCTG 3’
pCSCDE PS10	Fwd: 5’ CCAAGTTGAACTAGATAGACAAATGG 3’
	Rev: 5’ CCCCACGGGAGGCGTCAC 3’
pCSCDE PS11	Fwd: 5’ CTCAACAGTCACACATAGACAGCC 3’
	Rev: 5’ GCCTGTAGTGCCATTTACCCCC 3’
pCSCDE PS12	Rev: 5’ CCGACCATCAGGCACCTGAG 3’
	Rev: 5’ CATCGACTGTGGCCGGCTG 3’
pCSCDE PS13	Fwd: 5’ GCACGAGGAAGCGGTCAGCC 3’
	Rev” 5’ GGCTATTCGGCTATGACTGGGC 3’
pCSCDE PS14	Fwd: 5’ GAACCGGGCGCCCCTGC 3’
	Rev: 5’ CGCCGCTAGCAGCACCCC 3’

Appendix 3: Plasmid maps

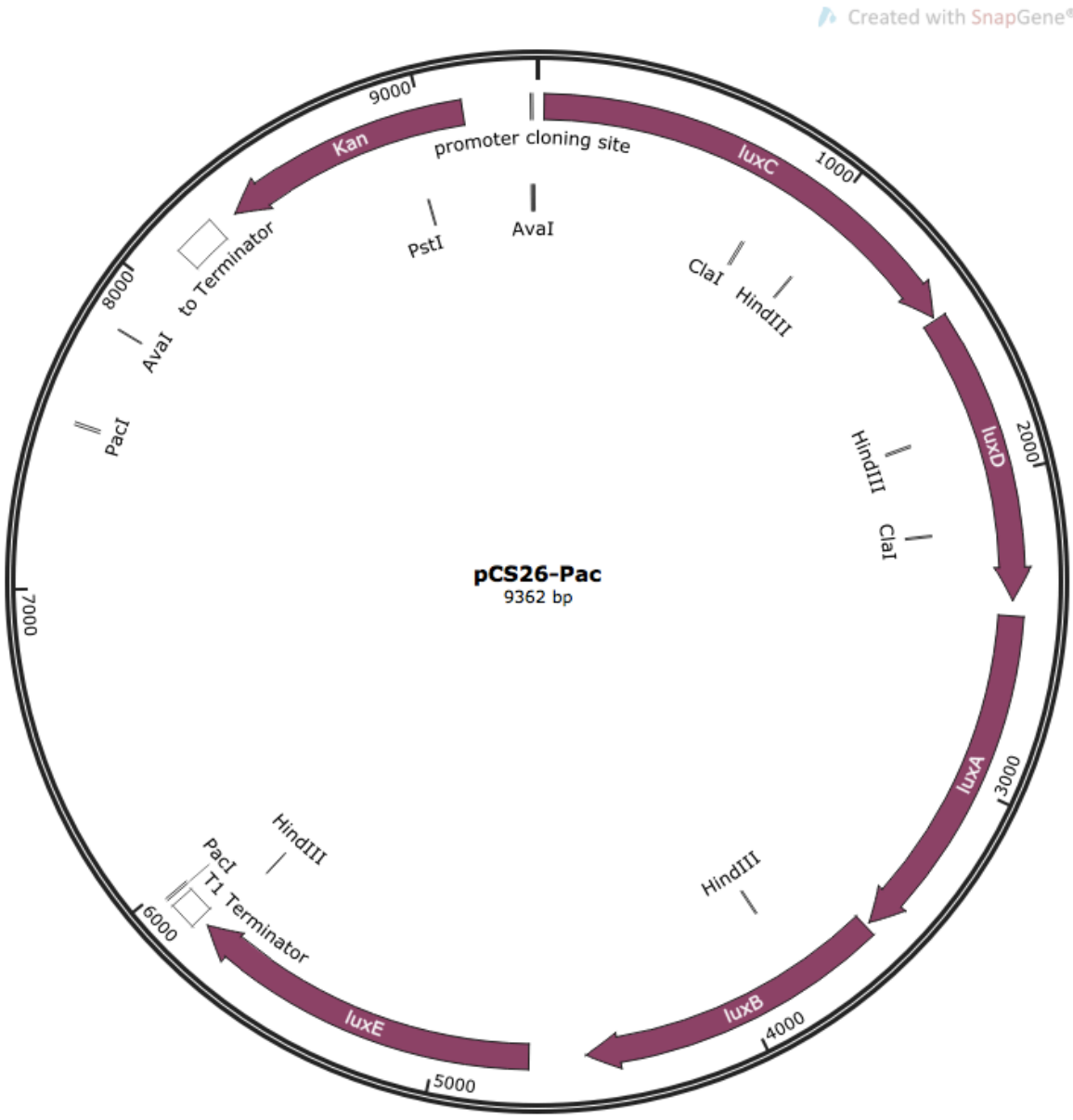

Figure S1: pCS26-Pac from Dr. Surrette's lab and originally described in Bjarnason et al.[52] This plasmid will serve as the backbone to clone in the *oriT*, beta lactamase promoter, and *lux* genes. This plasmid contains a kanamycin resistance cassette and a terminator, as well as a terminator for the *lux* operon. It also possesses a low copy number origin of replication (pSC101) that is flanked by PacI sites to allow movement into other vectors or to replace the current origin of replication.

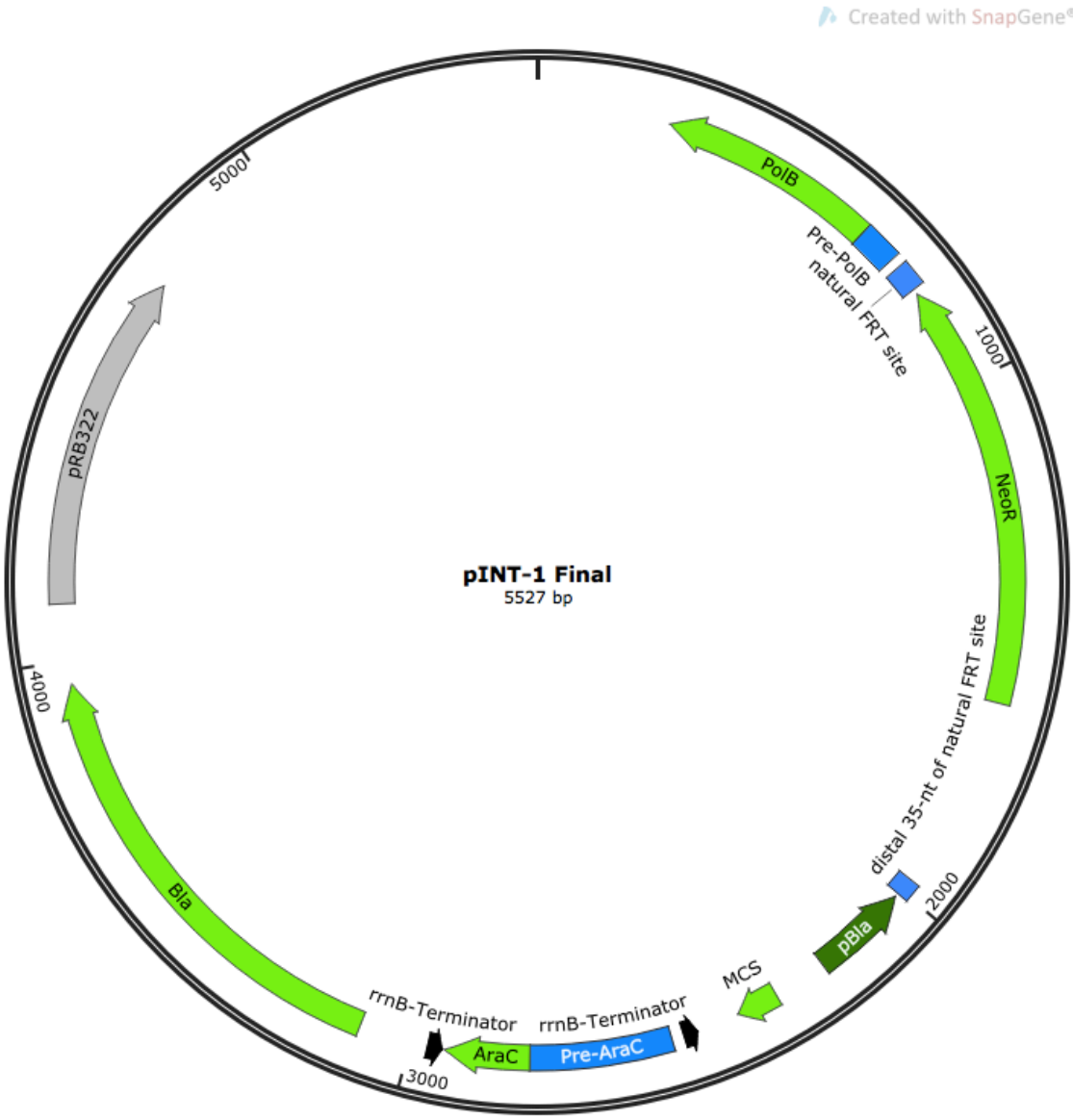

Figure S2: pINT-1 plasmid map. This plasmid contains a kanamycin and ampicillin cassette. Genes can be cloned into the multiple cloning site to later integrate into the arabinose operon in *E. coli* genome, based on *PolB* and *AraC* homology located in the plasmid.

Figure S3: pKD46 plasmid map. pKD46 encodes lambda red genes (*exo*, *bet*, *gam*) synthesized under the control of an inducible arabinose promoter. It additionally encodes *araC*, which represses the arabinose promoter. The native terminator (tL3) is positioned after the *exo* gene for controlled transcription. This is a low copy number plasmid with an easily curable temperature sensitive replication origin (repA101ts). After the amplicon is integrated into the arabinose operon of *E. coli*, the plasmid can be cured by growing up at 37°C.

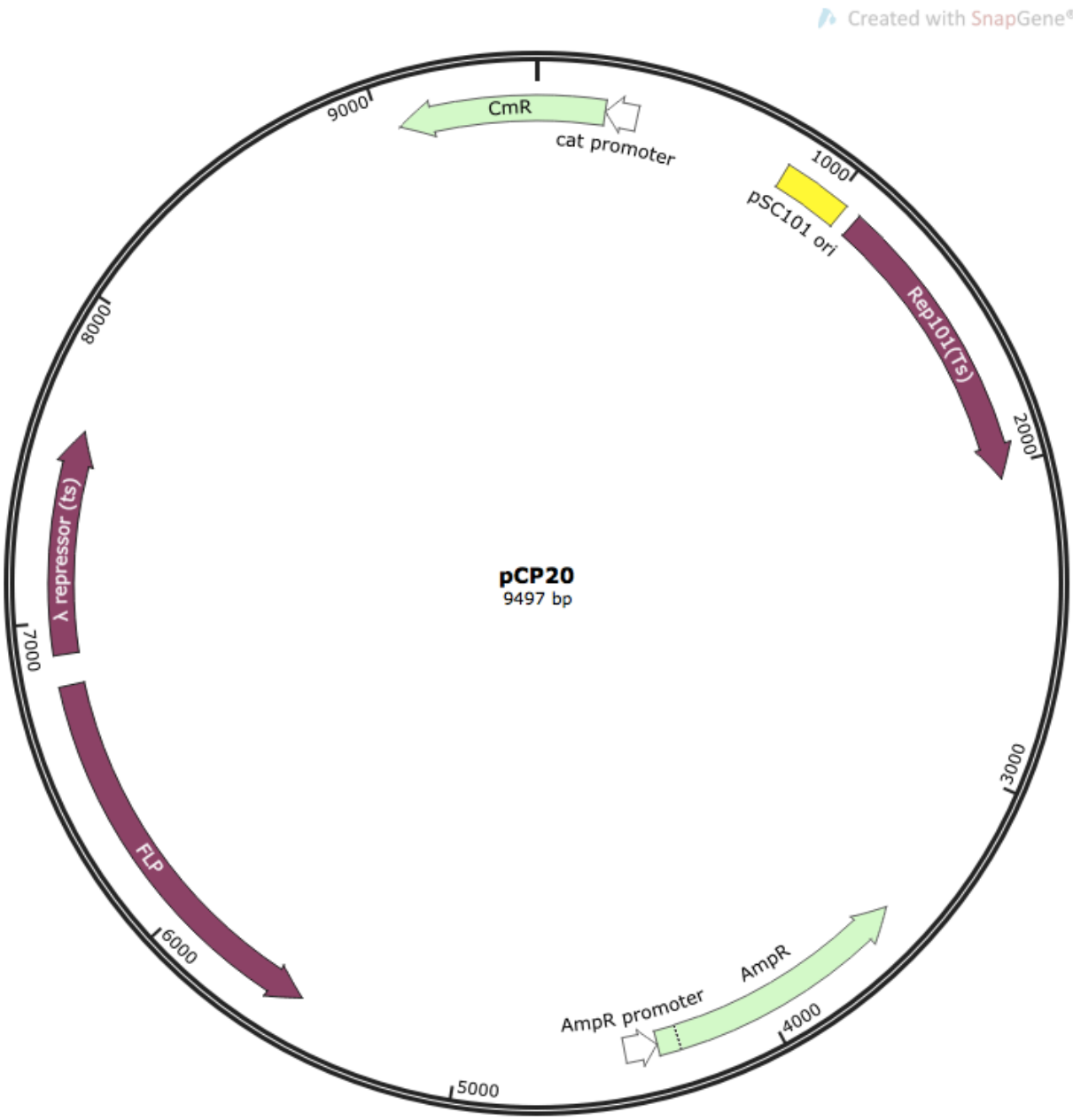

Figure S4: pCP20 plasmid map. This plasmid has a temperature-sensitive origin of replication, confers ampicillin and chloramphenicol resistance, and encodes the FLP recombinase. It is used to remove kanamycin cassette from the chromosomal insert, by recognizing FRT sites flanking the kanamycin cassette. After the flippase takes out the kanamycin cassette from the plasmid, the plasmid can be cured at 43°C.